

FROM FACTORS IN A HENRIOT GIBBAL
SOLITON MODEL WITH CONTINUOUS
SPACE DIMENSION

by

Bachel Mary Carter

A thesis submitted to the Faculty of Science,
University of the Witwatersrand, Johannesburg,
in fulfillment of the requirements for the degree of
Doctor of Philosophy.

Pretoria
November 1987

I dedicate this thesis to God, my parents
and to my husband John.

ABSTRACT

The Skyrme model [Sky61,62], in which baryons are considered to be chiral solitons in a meson field theory, has proved remarkably successful in describing low-energy phenomena. Given only the two free parameters in the Skyrme Lagrangian, a wide range of static properties has been reproduced to within 30%. Furthermore, the topological winding number of the Skyrme soliton has now been conclusively shown to be the conventional baryon number [Mit83a,b].

In contrast, one knows that high-energy nucleon scattering data displays baryon scaling [Nje88], indicating the presence of quasifree quarks. Together with the imposition of chiral symmetry, this leads naturally to the concept of a hybrid chiral model. In the present work a hybrid chiral soliton model, in which a quark bag is stabilized by a Skyrmion tail, has been studied. Continuity of the normal component of the axial vector current must then be enforced at the bag surface.

Remarkably, the baryon number of the hybrid soliton is unity for any bag radius, the soliton contribution being cancelled by that of the vacuum. In view of the importance of the baryon number, it is surprising that continuity of the baryon density has not been enforced previously. Here this continuity is applied as a constraint on the model. For a model with massless pions only, one can then predict the axial vector coupling constant g_A as a function of the bag radius, the values so obtained agreeing closely with the Goldberger-Treiman prediction $g_A = 1.83$. If one incorporates both meson masses and massive pions, one predicts the unique value $g_{\text{EM}} = 13.4$, to be compared with the experimental value of 13.5.

Given the good agreement for these and other static properties, a far more stringent test has been applied. The isoscalar charge, isovector magnetic and axial form factors have been calculated for the first time in a hybrid model. These form factors then prove to be more sensitive to the quark core. In fact, despite the appearance of surface induced diffraction minima, the overall agreement with the experimental dipole fit is better than that for the pure Skyrmin. These results therefore suggest the introduction of quarks, but with a softer bag surface.

DECLARATION

I declare that this dissertation is my own, unaided work. It is being submitted for the degree of Doctor of Philosophy in the University of the Witwatersrand, Johannesburg. It has not been submitted before for any degree or examination in any other University.

R.S. Carter

10 day of December, 1967

ACKNOWLEDGMENTS

A big word of thanks to Dr. Herb Miller whose guidance and encouragement made this thesis possible. In particular, I appreciated his optimism and willingness to share his knowledge of physics.

I would also like to thank Prof Dieter Haise for agreeing to be my co-supervisor and for his help in ensuring that everything ran smoothly at Wite. In particular, I would like to thank him for his careful reading of this thesis and his helpful suggestions.

I thank Dr Susan Martin, formerly Chief Director of NERNS, for permitting the inclusion of research work done at NERNS in my thesis.

I thank my husband and my colleagues at NERNS for their support.

I thank Anne Schuster for her careful editing of the thesis.

Finally, a big word of thanks to Lynette Lechtenborgh for typing this thesis, and the alterations, with such patience.

CONTENTS

	Page
1. INTRODUCTION	1
2. THE FIKK SKYRME MODEL	6
2.1 The baryon number	6
2.1.1 The magnetic monopole - an illustrative example	7
2.1.2 The Wess-Zumino action	10
2.1.3 Coupling the Wess-Zumino action	13
2.2 The Skyrme Lagrangian	13
2.3 The hedgehog solution	15
2.4 Quantizing the rotation of the Skyrme	18
2.5 Numerical Results	22
3. BAO MODELS	24
3.1 The MIT bag model	24
3.2 Chiral bag models	27
4. THE HYBRID CHIRAL SOLITON MODEL WITH PIONS	35
4.1 An outline of the model	36
4.2 Details of the numerical solution	40
4.3 Comparison with other models	44
APPENDICES	
4A THE EIGENVALUES AND EIGENVECTORS FOR THE QUARK GLASS PARTICLE STATES	60
4B THE CALCULATION OF THE NORMAL COMPONENT OF THE AXIAL VECTOR CURRENT	67
4C THE CALCULATION OF THE VACUUM EXPECTATION VALUES	73

6. THE HYBRID CHIRAL SOLITON MODEL WITH PIONS AND OMEGA NUCLEONS	89
6.1 The Lagrange density	89
6.2 The equations of motion	96
6.3 The boundary conditions	91
6.4 Details of the numerical solution	92
6.5 Comparison with other models	98
6. NUCLEON FORM FACTORS	105
6.1 The projection of the hybrid chiral soliton	106
6.2 Definition of the nucleon form factors	110
6.3 The nucleon form factors for the Skyrme tell	116
6.4 The nucleon form factors for the quark chiral bag	121
6.5 Numerical results	120
APPENDIX	
6A THE CALCULATION OF THE MATRIX ELEMENTS OF THE ELECTROMAGNETIC CURRENT OPERATOR FOR THE PURE SKYRMION	135
7. CONCLUDING REMARKS	138
REFERENCES	142

CONVENTIONS [1964]

Metric tensor:

$$g_{\mu\nu} = g^{\mu\nu} = \begin{bmatrix} 1 & 0 & 0 & 0 \\ 0 & -1 & 0 & 0 \\ 0 & 0 & -1 & 0 \\ 0 & 0 & 0 & -1 \end{bmatrix}$$

Vectors:

$$x^\mu = (t, \mathbf{x})$$

$$\partial_\mu = \frac{\partial}{\partial x^\mu}$$

A notation arrow denotes the three-dimensional part of the contravariant four vector, that is

$$\mathbf{Y} = (Y^i, i = 1, 2, 3)$$

Unless otherwise stated, a repeated index indicates a summation.

Inner Product:

The inner product is given as

$$Y \cdot X = Y_\mu X^\mu = -Y_0 X^0 - \mathbf{Y} \cdot \mathbf{X}$$

and, in particular,

$$Y^2 = Y_\mu Y^\mu = Y_0^2 - \mathbf{Y}^2$$

The 0th Albertson operator is

$$\alpha = \alpha_{\mu}^{\mu} = \alpha_0^2 - \psi^2.$$

and the four axioms reads

$$\psi^{\mu} = (\alpha, \vec{\gamma}).$$

Totally antisymmetric Levi-Civita tensor:

$$\epsilon^{\alpha\beta\gamma\delta} = \begin{cases} +1 & \text{if } (\alpha, \beta, \gamma, \delta) \text{ is an even permutation of } (0, 1, 2, 3) \\ -1 & \text{if it is an odd permutation of } (0, 1, 2, 3) \\ 0 & \text{otherwise.} \end{cases}$$

Three-dimensional antisymmetric tensor:

$$\epsilon^{ijk} = \epsilon_{ijk} = \begin{cases} 1 & \text{if } (i, j, k) \text{ is an even permutation of } (1, 2, 3) \\ -1 & \text{if } (i, j, k) \text{ is an odd permutation of } (1, 2, 3) \\ 0 & \text{otherwise.} \end{cases}$$

Pauli matrices:

$$\sigma^1 = \begin{bmatrix} 0 & 1 \\ 1 & 0 \end{bmatrix} \quad \sigma^2 = i \begin{bmatrix} 0 & -1 \\ 1 & 0 \end{bmatrix} \quad \sigma^3 = \begin{bmatrix} 1 & 0 \\ 0 & -1 \end{bmatrix}.$$

Dirac matrices:

$$\gamma^0 = \begin{bmatrix} 1 & 0 \\ 0 & -1 \end{bmatrix}$$

$$\vec{\gamma} = \begin{bmatrix} 0 & \vec{\sigma} \\ -\vec{\sigma} & 0 \end{bmatrix}$$

Related matrices:

$$\gamma_5 = \gamma^5 = i\gamma^0\gamma^1\gamma^2\gamma^3 = \begin{pmatrix} 0 & 1 \\ 1 & 0 \end{pmatrix}$$

$$\sigma^{\mu\nu} = \frac{1}{2} (\gamma^\mu\gamma^\nu - \gamma^\nu\gamma^\mu).$$

Conjugate Spinors:

$$\bar{u} = u^\dagger \gamma^0.$$

Physical constants:

$$M_N = 938.9 \text{ MeV}$$

$$\hbar c = 197.3268 \text{ MeV fm.}$$

1. INTRODUCTION

The underlying theory for the strong interactions is currently believed to be Quantum Chromodynamics (QCD). This Lagrangian field theory is based on the local gauge symmetry group $SU(3)_c$ and the existence of pointlike quarks, which transform as the fundamental representation of the group. The corresponding spin-1 octet of gauge bosons, needed to enforce local gauge invariance, are the gluons.

This theory is renormalizable as in the case of Quantum Electrodynamics (QED). The behaviour of the QCD running coupling constant $\alpha_s(q^2)$ is, however, quite different from that of QED because of the non-Abelian nature of the group $SU(3)_c$. Indeed, in direct contrast to QED, as the space-like component of the momentum becomes large $q^2 \rightarrow \infty$, the coupling constant $\alpha_s(q^2) \rightarrow 0$. This explains the occurrence of Bjorken scaling [Bj69] in high-energy lepton scattering, in which the leptons appear to scatter off quasifree pointlike quarks in the nucleus. In direct contrast to this asymptotic freedom, one knows that in nature quarks and gluons must be permanently bound into colour singlet states since no free quarks or gluons have yet been observed. Although it can be shown that as $q^2 \rightarrow 0$, $\alpha_s(q^2)$ becomes infinitely large, this has not as yet been shown to yield this confinement.

In most phenomenological models these two limits are included ad hoc. Confinement is enforced by either a confining potential or bag and/or soliton (Chapter 3); apart from this confinement, the quarks are regarded as at most weakly interacting.

In addition to the quantum number of colour, the quarks have a further quantum number called flavour. At present there are six such flavours, namely up, down, strange, charmed, top and bottom, the first two of which are most important in present work. In the absence of current masses for the quarks, the QCD Lagrangian possesses a chiral symmetry $SU(N_f)_L \times SU(N_f)_R$, where N_f denotes the number of flavours. Unlike the colour symmetry $SU(3)_C$, this is a global rather than a local symmetry. In the ground state this symmetry is spontaneously broken to diagonal $SU(N_f)$, giving rise to $N_f^2 - 1$ massless Goldstone bosons. In addition, there are two conserved vector currents, namely the vector and axial vector currents. For the case $N_f = 2$ (massless up and down quarks only), the three massless bosons should correspond to the pion isotriplet π^{\pm}, π^0 . The existence of a finite mass for the physical pions indicates that the chiral symmetry is not exact in nature. For this reason the idea of PCAC (partially conserved axial current) has been developed. This theory has in fact been very successful in predicting the low-energy properties of baryons, in particular the Goldberger Treiman relation [1958] and the Adler-Weisberger sum rule [Adler, S, Weisberg].

Thus one is led to the concept of a chiral bag model in which quarks are surrounded by a meson cloud. This should then interpolate between the regime of Bjorken scaling and that of low-energy pion physics (PCAC). The axial vector current conservation predicted from the chiral symmetry provides the connection between the quark and meson sector.

If one neglects the quark sector for the moment, one can show a clear link between QCD and a meson field theory. Considering the QCD Lagrangian and taking the limit of the number of colours $N_C \rightarrow \infty$, one in fact obtains a

non-linear weakly interacting meson field theory with coupling constant $g \propto \frac{1}{N_c}$. In this scenario, baryons are regarded as chiral solitons. The baryon mass divergence of the order of N_c is then simply the divergence of the soliton mass with the inverse of the coupling constant.

If one constructs a pion Lagrangian with a minimal number of derivatives, and possessing a stable soliton solution, one is led to the Skyrme Lagrangian. Although this Lagrangian has not been formally derived from large N_c QCD, it might be expected to be a good approximation to this theory (Chapter 2).

If one considers the Skyrme Lagrangian for the group $SU(3)_f$, there is an additional term called the Wess-Zumino Lagrangian, which describes the chiral anomaly. This in turn gives rise to an anomalous baryon current, from which one may calculate a baryon number for the pion field. For the pure Skyrme, this can then be seen to represent the topological winding number for the map from compactified space-time to either the group $SU(2)$ or $SU(3)$.

Since, in addition, the pure Skyrme provides good results for the nuclear and Δ static properties, there is ample justification for describing the meson tail in a hybrid model by the Skyrme Lagrangian [SU984, Pu184, HSB84]. This model, in which a quark bag is enclosed by a Skyrme soliton, is then expected to extrapolate between the low and high energy regime.

The first constraint on the model is that it be consistent. Of primary importance here is the baryon number. Fortunately, it has been shown [G283],

that the baryon number in such a hybrid model is identically unity, independently of the bag radius. The now soliton contribution from the mesons is exactly cancelled by that of the vacuum. This is particularly remarkable in light of their different origins: the vacuum contribution is simply given as the spectral asymmetry of the quark eigenpectrum, while the soliton contribution is topological in nature.

As before, one must impose the physical constraint of axial vector current continuity at the bag surface. In the present work however, a new physical constraint has been imposed, namely baryon density continuity at the bag surface. The fact that, in all hybrid chiral bag models, the integral of the baryon density is one in no way guarantees continuity of the baryon density at the bag surface.

In conventional chiral bag models [Vem83], one can never enforce such continuity because this would require the baryon number density at the bag surface to be zero (the mesons outside carry no baryon number). In the present work continuity of the baryon density has been applied as a constraint on the model. As will be demonstrated [Chapters 4 and 5], this constraint reduces the degrees of freedom in the model, and thus automatically increases its predictive power. For the model with massless pions only [Chapter 4, GMS7b,c], one now obtains not only acceptable results for the nuclear static properties, but also a new prediction for the axial vector coupling constant $g_A(R_b)$. The results so obtained show good agreement with the value of g_A predicted from the Goldberger-Treiman relation, namely $g_A = 1.33$. Remarkably, if one incorporates both massive pions and mass vacuum [Chapter 5, GMS7b,c], the model is then uniquely

specified, and one notes the definitive prediction $K_{\text{NIN}} = 12.4$, in good agreement with the experimental value of $K_{\text{NIN}} = 12.5$. Again one obtains good results for the remaining static properties of the nucleus.

Given the success of the model in reproducing nucleus static properties that was defined at the photon point ($q^2 = 0$), one is encouraged to study its properties at higher values of q^2 . Some of the first calculations of three of the form factors for the hybrid chiral soliton will be presented [Chapter 5, GMD7d]. These form factors are more sensitive to the quark core, which was introduced to explain Bjorken scaling. They are therefore expected to provide a better fit to the data than those of the pure Skyrmion [HIN04]. This indeed proves to be the case, despite the appearance of artificial diffraction minima induced by the sharp bag surface. This calculation therefore supports the introduction of quarks but suggests that its surface should be softened.

2. THE PURE SKYRME MODEL

Here we focus on the motivation and calculational details for the pure Skyrme model. Many of the formulae and arguments will then be directly applicable to the description of the Skyrmion tail in the hybrid model. Of particular interest is the baryon number, whose origin as a topological winding number is detailed in section 2.1. In section 2.2 the form for the Skyrme action is justified, while section 2.3 describes the hedgehog solution. In addition, the projection technique of Adkins, Nappi and Witten [ANW83] is discussed in section 2.4. This section is of particular relevance to the calculation of the form factors in the hybrid model, particularly in light of the existence of finite N_c corrections to the formulae displayed. Finally, numerical results for the nucleon and Δ static properties are given in section 2.5 [ANW84]. These results illustrate the success of the pure Skyrme model in reproducing low-energy phenomena.

2.1 The baryon number

The determination of the baryon number is of particular relevance in both the pure and hybrid models. In particular, we wish to illustrate the origin and the justification of the form of the baryon current. The arguments presented here are due to Witten [W83a, W83b].

Firstly, it is helpful to consider the closely related example of the magnetic monopole. The discussion parallels that for the Skyrmion, except that the problem is of lower dimensionality and is therefore more easily visualized. The more complex case of the Skyrmion then follows naturally by analogy.

2.1.1 The magnetic monopole - an illustrative example

Consider a charged point particle of mass m moving on a three-sphere. Then its action is given as

$$S = \frac{1}{2} m \int dt \sum_i \dot{x}_i^2, \quad (2.1)$$

with the corresponding equation of motion

$$m \ddot{x}_i + m x_i \left[\sum_k \dot{x}_k^2 \right] = 0 \quad (2.2)$$

and the equation of constraint

$$\sum_k x_k^2 = 1. \quad (2.3)$$

Clearly, the system respects both the symmetry operations $x_i \rightarrow -x_i$ and $t \rightarrow -t$. If one now introduces a magnetic monopole at the centre of the sphere, there is an additional Lorentz force on the particle

$$F_i = \alpha \epsilon_{ijk} \dot{x}_j B_k, \quad (2.4)$$

where B_k is the magnetic field given by

$$B_k = \frac{\hat{r}_k}{r^2} \quad (2.5)$$

and α is the product of the electric and magnetic charges.

Here one observes that the system is now only invariant under the combined symmetry operation $x_i \rightarrow -x_i$ and $t \rightarrow -t$. If one introduces a vector potential defined by

$$\mathbf{F} = \nabla \times \mathbf{X}, \quad (2.6)$$

then one may formally write the action as

$$S = \int dt \left(\frac{1}{2} m \dot{\mathbf{x}}_1^2 + e \dot{\mathbf{x}}_1 \cdot \mathbf{F} \right). \quad (2.7)$$

There is, however, no explicit expression for \mathbf{F} . Furthermore, the inherent problems in the action can be made far clearer by considering the Feynman path integral around a closed path γ , $\int_{\gamma} dx_i e^{i\mathbf{A} \cdot \mathbf{v}}$, to which the second term in the action contributes

$$\exp \left[i e \int_{\gamma} \mathbf{A}_1 \cdot d\mathbf{x}_1 \right]. \quad (2.8)$$

Using Stokes' theorem, one may rewrite this expression as

$$\exp \left[i e \int_{\gamma} \mathbf{A}_1 \cdot d\mathbf{x}_1 \right] = \exp \left[i e \int_{\mathcal{D}} \nabla_{1j} \cdot d\mathbf{x}_{1j} \right], \quad (2.9)$$

where the left-hand side is the magnetic flux through the area \mathcal{D} bounded by γ . However, γ also bounds the area \mathcal{D}' , the surface of the sphere enclosing \mathcal{D} (see Fig. 2.1). Equivalently therefore, one must be able to write

$$\exp \left[i e \int_{\gamma} \mathbf{A}_1 \cdot d\mathbf{x}_1 \right] = \exp \left[-i e \int_{\mathcal{D}'} \nabla_{1j} \cdot d\mathbf{x}_{1j} \right]. \quad (2.10)$$

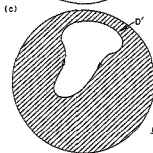
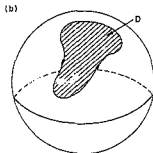
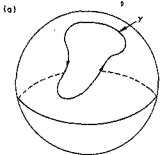


Figure 2.1 The curve y on the two sphere (a) bounds both the disc D (b) and D' (c).

For the sake of consistency one demands that these two quantities must be equal, that is

$$1 = \exp\left[ie \int_{D=0} F_{1j} dx_{1j}\right] = \exp\left[ie \int_{S_2} F_{1j} dx_{1j}\right]. \quad (2.11)$$

Since $\int_{S_2} F_{1j} dx_{1j} = 4\pi$, this equation is obeyed iff e is either integral or half integral. This argument therefore predicts Dirac's quantization condition for the product of the electric and magnetic charges.

2.1.2 The Wess-Zumino action

If one now returns to large N_c QCD, one has the chiral symmetry $SU(3)_L \times SU(3)_R$, which is spontaneously broken to diagonal $SU(3)$. To describe its low-energy behaviour one introduces the field $U(\vec{x}, t) \in SU(3)$, which transforms under the group $SU(3)_L \times SU(3)_R$ as

$$U \rightarrow LUU^{-1}, \quad (2.12)$$

where L and R are arbitrary $SU(3)$ matrices. One may write U in the general form

$$U = \exp(i\lambda_a \frac{\tau_a}{f_\pi}), \quad (2.13)$$

where λ_a denotes the Gell-Mann matrices, τ_a the eight Goldstone boson fields and c the appropriate constant. As will be shown later, the constant c can be identified using the axial vector current, as $c = f_\pi$, where f_π is the pion decay constant. One can therefore write

$$U = \exp(i\lambda_a \frac{\sigma_a}{2} \tau_a) . \quad (2.14)$$

The action can then be constructed simply by demanding chiral symmetry and a minimal number of derivatives. If one considers at most two derivatives, one obtains uniquely

$$S = \frac{1}{4} f_\pi^2 \int d^4x \operatorname{Tr} (\partial_\mu U \partial^\mu U^\dagger) . \quad (2.15)$$

This clearly possesses two symmetries, namely the naive parity operation $x \rightarrow -x$, $t \rightarrow t$, $U \rightarrow U$ and the operation which counts the number of baryons modulo 2, that is $x \rightarrow x$, $t \rightarrow t$ and $U \rightarrow U^\dagger$ ($\tau_a \rightarrow -\tau_a$). In contrast, QCD possesses only the combined symmetry $x \rightarrow -x$, $t \rightarrow t$, $U \rightarrow U^\dagger$, corresponding to the parity operation, and here one sees a clear analogy with the breaking of the symmetry by the magnetic monopole.

Fixing space-time as a very large four-dimensional sphere M , the field U then maps M into the $SU(3)$ manifold. The four-sphere in the $SU(3)$ manifold that is the image of M under U is then the boundary of two five-spheres, G and G' , just as the curve v bounds the discs D and D' . If one postulates the form for additional terms in the action, similar to that introduced by the monopole

$$I = \int_G \omega_{1jkl} dx^1 dx^j dx^k dx^l . \quad (2.16)$$

There is again an alternative form

$$r = - \int_{Q^4} \omega_{ijklm} dx_{ijklm} \quad (2.17)$$

which implies that

$$\int_S \omega_{ijklm} dx_{ijklm} = 2\pi n \quad (2.18)$$

where n is integral and S is any 5 sphere in $SU(5)$.

Here ω_{ijklm} is a five-dimensional tensor, corresponding to the field F_{ij} in the magnetic monopole, and similarly to F_{ij} , it can be expressed as a total divergence. Its specific form on the five-sphere with co-ordinates y_i is given as

$$\omega_{ijklm} dx_{ijklm} = - \frac{1}{260\pi^2} dx_{ijklm} \text{Tr} \left[U^t \frac{\partial U}{\partial y^i} U^t \frac{\partial U}{\partial y^j} U^t \frac{\partial U}{\partial y^k} U^t \frac{\partial U}{\partial y^l} U^t \frac{\partial U}{\partial y^m} \right] \quad (2.19)$$

If one normalizes U on the basic sphere correctly, one obtains the action

$$S = \frac{1}{4} r_0^2 \int d^4x \text{Tr} (g_{\mu\nu} U^\mu U^\nu) + \pi r_0^2 \quad (2.20)$$

One then applies Stokes' theorem to obtain the Nambu-Goto action, r_0 , in the form

$$r_0 = \frac{2}{16\pi^2 (2\pi)^5} \int d^4x \epsilon^{\mu\nu\alpha\beta} \text{Tr} A_\mu A_\nu A_\alpha A_\beta + \text{higher order terms} \quad (2.21)$$

where the integral runs over the surface of the five-sphere S , that is space like, and $\epsilon^{\mu\nu\alpha\beta}$ denotes the fully antisymmetric Levi-Civita tensor with $\epsilon^{0123} = 1$.

2.1.3 Gauging the Wess-Zumino action

The critical remaining question is, of course, the value of the integer n . Although it will not be shown here, if one gauges the electromagnetic subgroup, the term F_{ij} gives rise to a term describing the decay $\pi^0 \rightarrow \gamma\gamma$. Comparing this with the QED result, one obtains $n = N_c$.

Similarly, if one gauges an arbitrary subgroup of $SU(3)_L \times SU(3)_R \times U(1)$, where $U(1)$ denotes the baryon number subgroup, one can obtain the anomalous baryon current

$$j_B^\mu = \frac{1}{24\pi^2} \epsilon^{\mu\nu\alpha\beta} \text{Tr}(U^\dagger \partial_\nu U \partial_\alpha U^\dagger \partial_\beta U) . \quad (2.22)$$

The corresponding baryon number is the integral

$$B = \int d^3x B^0 = \frac{1}{24\pi^2} \int d^3x \epsilon^{0ijk} \text{Tr}(U^\dagger \partial_i U \partial_j U^\dagger \partial_k U) . \quad (2.23)$$

This can also be identified as the topological winding number of the map $U: M \rightarrow SU(3)$. This number simply denotes the number of times that the mapping U covers the $SU(3)$ manifold as x^μ ranges over M . The possible values are thus given by the homotopy class $\pi_3(SU(3)) = \mathbb{Z}$. One sees that the solutions can therefore be classified, as those with integral baryon number $B = 0, 1, 2, \dots$

2.2 The Skyrme Lagrangian

Looking at the current quark masses as a function of flavour, one observes that there are only two light quark flavours: up and down with masses $m_u = 4.8$ MeV and $m_d = 8$ MeV respectively [1087]. Since these masses are

small compared to hadron masses, they can be set to be identically zero to a good approximation. One is then working with the chiral symmetry group $SU(2)_L \times SU(2)_R$ and the field U is given as

$$U = \exp(i\vec{T} \cdot \vec{\phi}/f_\pi), \quad (2.24)$$

where \vec{T} are the Pauli matrices, $\vec{\phi}$ can be shown to denote the pion field and f_π is again the pion decay constant, which is given experimentally as $f_\pi = 93$ MeV.

Despite the fact that the Wess-Zumino term is identically zero for $SU(2)$, the anomalous baryon current is still given by equation (2.20). Furthermore, since the homotopy classes are identical, that is $\pi_3(SU(2)) = \pi_3(SU(3)) = \mathbb{Z}$, the soliton still possesses an integral baryon number.

Imposing chiral symmetry on the Lagrangian again yields the unique form with two derivatives

$$L = \frac{1}{2} f_\pi^2 \int d^3x \text{Tr}(\partial_\mu U \partial^\mu U^\dagger). \quad (2.25)$$

However, this Lagrangian supports no stable solitonic solutions, as can be seen from a simple scaling argument [HS85]. If one also permits terms incorporating four derivatives, of which at most two should be time derivatives, there is only one such possible term and the Lagrangian becomes

$$L = \frac{1}{2} f_\pi^2 \int d^3x \text{Tr}(\partial_\mu U \partial^\mu U^\dagger) + \frac{1}{4} a^2 \int d^3x \text{Tr}(L_\mu L_\mu)^2, \quad (2.25a)$$

where

$$L_\mu = (a_\mu U) U^\dagger. \quad (2.25b)$$

The restriction to two time derivatives, while not essential, does permit the use of the classical methods for quantization.

Expanding (2.23) to first order in the pion field, one obtains

$$L = + \frac{1}{2} \int d^3x \partial_\mu \pi \partial^\mu \pi . \quad (2.27)$$

This is, of course, the conventional pion kinetic energy term. Similarly, the second term in (2.24) describes π - γ interaction. The coefficient a^2 can be estimated from π - γ scattering, and this yields the following bounds [JRS1]:

$$7 \times 10^{-5} \leq a^2 \leq 5 \times 10^{-2} . \quad (2.28)$$

If desired, one can also incorporate a chiral symmetry breaking term in the Lagrange density, which gives a mass m_π to the pion [AND4a]. This has the form

$$\mathcal{L}_m = \frac{1}{4} f_\pi^2 m_\pi^2 \text{Tr}(U-1) . \quad (2.29)$$

Expanding U to the second order in the pion field

$$U = 1 + i \frac{\vec{\pi} \cdot \vec{H}}{f_\pi} - \frac{1}{2} \frac{\vec{\pi} \cdot \vec{H} \vec{\pi} \cdot \vec{H}}{f_\pi^2} , \quad (2.30)$$

this term can be shown to yield the mass term in the conventional form

$$\vec{K}_\mu = -\frac{1}{2} \vec{a}_\mu \vec{K} \cdot \vec{K} . \quad (2.31)$$

Finally, if one calculates the axial vector current to first order in the pion field, one obtains (Appendix 40)

$$\vec{K}_\mu = f_\pi \partial_\mu \vec{\pi} , \quad (2.32)$$

thus justifying the choice of $\vec{a} = \vec{e}_\mu$.

2.3 The hedgehog solution

In order to simplify the resulting Lagrange equation one normally chooses the hedgehog ansatz for $\vec{\pi}$

$$U = \exp(-i\vec{\pi} \cdot \hat{r}) . \quad (2.33)$$

A simple sketch of $\vec{\pi}$ versus \vec{r} indicates the appropriateness of the name since at each point in space the pion field points radially outward from a common origin. Although one hopes that the hedgehog configuration is in fact a minimal energy solution, there is to our knowledge no conclusive proof for this.

Furthermore, for non-zero topological baryon number B , U must cover the manifold of $SU(2)$, that is the sphere S_3 in isospin space, in a non-contractable way as $\vec{\pi}$ covers all space. Thus $\vec{\pi}$ must cover the sphere S_2 for any value of $n = (\vec{\pi} \cdot \vec{\pi})^{1/2}$. The simplest choice is then in fact $\vec{\pi} = \hat{r}$, as suggested above.

Substituting this form for U into the Lagrange density for massless pions yields

$$\mathcal{L} = -\frac{1}{2} r^2 \left(\rho'^2 + \frac{2\sin^2 \theta}{r^2} \right) - \frac{1}{2} \frac{\sin^2 \theta}{r^2} \left(\rho'^2 + \frac{1}{2} \frac{\sin^2 \theta}{r^2} \right), \quad (2.34)$$

from which one derives the Euler-Lagrange equation

$$\rho'' + \frac{2}{r} \rho' - \frac{\sin 2\theta}{r^2} + \frac{A'}{r^2} \left(\sin^2 \theta \rho'' + \frac{1}{2} \sin 2\theta (\rho'^2 - \frac{\sin^2 \theta}{r^2}) \right) = 0, \quad (2.35)$$

$$\text{where } A' = \frac{2\alpha_0^2}{r^2}.$$

Looking at the two limits $r \rightarrow 0$ and $r \rightarrow \infty$, one observes that for a finite energy solution, $E = \int d^3x \mathcal{L}$, one requires

$$\rho(0) = m \text{ and } \rho(\infty) = n, \quad (2.36)$$

where m and n are both integers. Without loss of generality, n can be taken to be zero and m is to be specified by the baryon number as shown below.

The baryon number density for the hedgehog derived from equation (2.20) is given as

$$b^0(r) = -\frac{1}{2\pi^2 r^2} \sin^2 \theta \frac{d\theta}{dr}. \quad (2.37)$$

Integrating the baryon density over all space gives the baryon number

$$B = \int_0^{\infty} dr^2 r^3 u^3(r) = \frac{1}{2} (\phi(0) - \frac{1}{2} \sin 2\phi(0)) . \quad (2.38)$$

The baryon number is clearly integral, and for a single baryon one requires

$$\phi(0) = \pi \text{ and } \phi(\infty) = 0 . \quad (2.39)$$

When the dimensionless variable $\bar{r} = r_0 r / \Lambda^{-1}$ is introduced, the equation for $\phi(\bar{r})$ is independent of the choice of κ^2 or f_{π} , and the resulting universal solution $\phi(\bar{r})$ is shown in fig. 2.2.

2.4 Quantizing the rotations of the Skyrmeion

The results of this semi-classical projection scheme were originally derived in the paper by Adkins, Nappi and Witten [ANW83]. They are, however, utilized here because of their relevance to the calculation of the form factors in the Skyrme sector of the hybrid model. The existence of finite N_c corrections to the above formulae are discussed in section 5.2.

Given a solution in the $B = 1$ sector, $U(\vec{R})$, then $\tilde{U}(\vec{R}) = AU(\vec{R})A^{-1}$ where A is any $SU(2)$ matrix is also a solution. This corresponds to the existence of zero frequency rotational modes. If one introduces time dependence in the form

$$U(t) = A(t)U(\vec{R})A^{-1}(t) , \quad (2.40)$$

one obtains the Lagrange density in the form

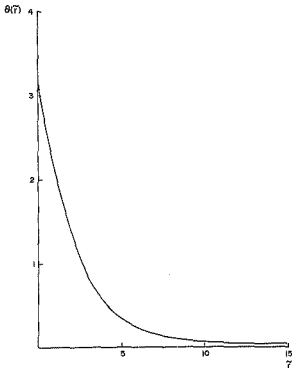


Figure 3.2 The chiral angle $\theta(r)$ for the pure Skyrme soliton versus the dimensionless radial variable r

$$z = z_0 + A \operatorname{Tr}(a_0 a_0 \rho^{-1}), \quad (2.41)$$

where

$$A = \frac{2c}{3} c_0^2 \int_0^1 dt t^2 a_0^2 b \left[1 + \frac{1}{2} A' (t^2 + \frac{a_0^2 b^2}{t^2}) \right], \quad (2.42)$$

and $A' = 16 a_0^2 / a_0^2$, as before.

Rewriting Δ as

$$\Delta = a_0 + i\mathbf{L} \cdot \mathbf{T}, \quad a_0^2 + \mathbf{T}^2 = 1, \quad (2.43)$$

one sees that the Lagrangian density

$$\mathcal{L} = \mathcal{L}_0 + 2A \sum_{l=0}^2 (a_l^2)^2, \quad (2.44)$$

is that of a free particle constrained to move on a three-sphere.

After the introduction of the spin and isospin operators

$$S_k = \frac{1}{2} i(a_0 \frac{\partial}{\partial a_k} - a_k \frac{\partial}{\partial a_0} - a_l a_m \theta_l \frac{\partial}{\partial a_m}), \quad (2.45)$$

$$I_k = \frac{1}{2} i(a_k \frac{\partial}{\partial a_0} - a_0 \frac{\partial}{\partial a_k} - a_l a_m \theta_l \frac{\partial}{\partial a_m}), \quad (2.46)$$

where $\mathbf{T}^2 = \mathbf{I}^2$,

the Hamiltonian becomes

$$H = H_0 + \frac{1}{2I} \mathbf{N}^2, \quad (2.37)$$

with eigenpectrum

$$E = H_0 + \frac{s(s+1)}{2I}, \quad (2.38)$$

where the allowed values of the spin and isospin are $s = 0, 1/2, 1, 3/2, 2, \dots$. The corresponding eigenvectors for states with spin and isospin $s = 1$ and third component a_3 and i_3 respectively are proportional to the Wigner D function.

$$|i = s, i_3, a_3\rangle = (-)^{i+i_3} \sqrt{\frac{2I+1}{(2s+1)}} D_{i_3, -i_3}^i(A), \quad (2.39)$$

Since A and $-A$ are classically indistinguishable, one must demand that

$$D_{i_3, -i_3}^i(A) = \pm D_{i_3, -i_3}^i(-A). \quad (2.40)$$

Choosing the minus sign gives the fermionic states with $i = s = \frac{1}{2}, \frac{3}{2}, \dots$

The specific form for selected nucleon and Δ states is given below:

$$\begin{aligned}
 |p_1^+\rangle &= \frac{1}{\sqrt{2}} (a_1 + ia_2) & |p_1^-\rangle &= -\frac{1}{\sqrt{2}} (a_0 - ia_3) \\
 |p_2^+\rangle &= \frac{1}{\sqrt{2}} (a_0 + ia_3) & |p_2^-\rangle &= -\frac{1}{\sqrt{2}} (a_1 - ia_2) \\
 |a_1^{++}, a_2 = \frac{3}{2}\rangle &= \frac{\sqrt{2}}{\sqrt{3}} (a_1 + ia_2)^2 \\
 |a_1^{++}, a_2 = \frac{1}{2}\rangle &= -\frac{\sqrt{2}}{\sqrt{3}} (a_1 + ia_2)(1 - 3(a_0^2 + a_3^2)) .
 \end{aligned}
 \tag{2.61}$$

2.5 Numerical Results

The results for the static properties of the nucleon and Δ obtained by Adkins and Nappi with massive pions (ANS4a) are presented in Table 2.1 as representative of the quality of the fit given by the pure Skyrme model. As indicated, f_π and a^2 have been fitted to the nucleon and Δ masses, and overall there is agreement with the experimental data to within 30%. The largest discrepancies lie in the value of f_π , here treated as a free parameter, and g_A the axial vector coupling constant. Conversely, if f_π is set to its experimental value of 93 MeV, the nucleon and Δ masses lie too high, and this remains an unsolved problem in the Skyrme model. If, however, one uses the finite M_π correction to g_A proposed in present work, namely the multiplicative factor $\frac{3}{2}$, one obtains $g_A^* = 1.09$ in far better agreement with the experimental value of 1.26. This factor will, however, then destroy the good agreement obtained for ϵ_{1100} .

Table 2.1

Nucleon and delta static properties in the pure Skyrme model with massive pions

Quantity	Prediction	Experiment
m_π (MeV)	input	138.0
m_N (MeV)	input	938
m_Δ (MeV)	input	1232
r_N (fm)	0.84	0.83
$\langle r_N^{-2} \rangle_{I=0}^{1/2}$ (fm)	0.69	0.72
$\langle r_N^{-2} \rangle_{I=1}^{1/2}$ (fm)	1.04	0.98
$\langle r_N^{-2} \rangle_{N, I=0}^{1/2}$ (fm)	0.96	0.81
$\langle r_N^{-2} \rangle_{N, I=0}^{1/2}$ (fm)	1.04	0.80
μ_D (fm)	1.97	2.70
μ_Δ (fm)	-1.24	-1.41
S_A	0.65	1.23
K_{eff}^*	11.8	13.5
$K_{\text{eff}\Delta}$	17.8	20.3
μ_{eff}	2.3	3.3

*This value does not satisfy the Goldberger-Treiman relation [64b].

3. BAG MODELS [Lehll, Cle78]

Although, in principle, the QCD equations provide a complete description of baryons, they prove intractable in practice. This has led to the development of several highly successful phenomenological models, in particular the bag models. These were developed to explain the following two experimental observations. Firstly, at short distances, or high momentum transfer, quarks appear as free pointlike objects. This corresponds to the limit of asymptotic freedom where the QCD quark coupling constant $\alpha_s(q^2) \rightarrow 0$, as $q^2 \rightarrow \infty$. Secondly, at large distances, the forces on a quark must be increasingly large, confining the quarks within the baryon. As a crude first approximation one can divide space into two regions - one inside a volume V , where the quarks may move freely, and the other outside V , which the quarks cannot penetrate.

3.1 The MIT bag model

This is the essence of the MIT bag model where the volume V_b takes the form of a spherical bag [GJ79]. Inside the bag radius, R_b , the quarks obey the free Dirac equation

$$(i\gamma_\mu \partial^\mu - m_q)\psi = 0, \quad (3.1)$$

where m_q is the current quark mass. At the surface of the sphere one demands that there be no current flow, that is

$$\vec{n} \cdot \vec{\gamma} \psi = 0, \quad (3.2)$$

where \hat{n}^r denotes the unit outward normal to the bag. This can be satisfied if

$$\psi|_{R_0} = \psi. \quad (3.2)$$

One should note that this implies that, at the bag radius, $\Psi^r|_{R_0} = 0$. In turn, one observes that $\psi^r|_{R_0} \neq 0$, that is, it is non-zero at the bag radius, although it is zero outside.

Considering the case of the nucleon that contains three massless quarks (that is, up or down), the energy is simply given as

$$E = \frac{3E_0}{V}, \quad (3.3)$$

where E_0 is the energy of the lowest lying single particle state. Applying the boundary condition (3.2), one can show this to be the $1s_{1/2}$ state with energy, $E_0 = 2.042B$. This energy is, however, clearly unstable against increases in R_0 , and to stabilize the solution a volume term of the form $\frac{4\pi B}{3} R_0^3$ must be added. Here the constant B is interpreted as the energy density necessary to form the bag from the vacuum and is customarily taken to be 140 MeV fm^{-3} . Determining R_0 to minimize the total energy, one can then calculate the static properties for the baryons in the model. (For the present work in chiral soliton models such a stabilizing term is in fact unnecessary, and unless otherwise stated, it will be omitted.)

The important successes for the MIT bag model are listed below:

- (i) Bjorken scaling is taken into account [3,60].
- (ii) The prediction of the ratio of the magnetic moments for the neutron and proton $\mu_n/\mu_p = -2/3$. Strictly speaking however, this relationship may be derived entirely from the SU(3) flavour octet symmetry and is independent of the particular form of the model. It is nonetheless closer to the experimental value -0.385 than the prediction from the pure Skyrme model $\mu_n/\mu_p = -0.75$ [485].
- (iii) The prediction for g_A , the axial vector coupling constant. This assumes the value $5/3$ for non-relativistic quarks but shrinks to the value 1.1 for massless quarks. The experimental value of 1.26 can clearly be reached with small but finite quark mass. [485]
- (iv) The following mass splitting formulae can be derived from one gluon exchange within the bag. Here m_n, m_p, m_H and m_Δ denote the masses of the pion, the nucleon, nucleus and Δ respectively. [485]

$$\frac{m_\Delta}{m_p} = \left\{ \left(\frac{3}{2} \right)^{3/4} \right. \quad \text{theory} \\ \left. 1.18 \left(\frac{3}{2} \right)^{3/4} \right\} \quad \text{experiment} \quad (3.5)$$

$$\frac{(m_n^{4/3} - m_p^{4/3})}{(m_\Delta^{4/3} - m_n^{4/3})} = \left\{ \frac{4}{3} \right\} \quad \text{theory} \\ \left. 1.187 \left(\frac{4}{3} \right) \right\} \quad \text{experiment} \quad (3.6)$$

Again, this relationship is independent of the particular bag or potential model used.

The shortcomings of the model are clearly numerous, not least of which is the lack of a precise relationship to QCD. A few of the more important failings are given below, and the discussion now will be restricted to the case of the nucleus.

- (i) *The division of space into two distinct regions:* This question has been addressed both by potential and soliton bag models. (In fact, the MIT bag model may itself be regarded as a potential model with an infinite square well potential of radius R_0). Frequently used potentials are r , r^2 and r^3 , while the potential in soliton models is to be generated self consistently by the σ field. Clearly, none of these models in fact predicts confinement, but rather redefines its precise form. In some sense therefore, the MIT model has the advantage of simplicity.
- (ii) *Centre of mass corrections:* The introduction of an origin in the description of a nucleon inevitably destroys the relativistic invariance of the system. Without a means to correctly boost the system, such corrections are impossible to calculate. They have, however, been estimated to be about 30% of the total energy. [THORN]
- (iii) *The breaking of chiral symmetry:* This is introduced by the appearance of a scalar potential, which acts like a quark mass term, in the Dirac equation. It can be clearly seen by considering a quark reflected from the bag boundary. Before collision, it has momentum \vec{p} and spin \vec{S} with helicity $h = \vec{S} \cdot \vec{p}$. After collision, the momentum is reversed, while the spin remains unchanged, corresponding to helicity $h' = \vec{S} \cdot (-\vec{p}) = -h$, that is, the helicity has been inverted.

3.2 Chiral bag models

In chiral bag models of the nucleon [WILSON, B79] chiral symmetry is restored by the introduction of an exterior pion field. Considering the Lagrange density for massless quarks

$$I = \frac{1}{2} \bar{\psi} \gamma_5 \gamma_\mu \psi, \quad (3.7)$$

one observes that it is invariant under the transformation

$$\psi \rightarrow \exp(i\bar{\alpha} \gamma_5) \psi. \quad (3.8)$$

Corresponding to this invariance is the Noether current

$$J_\mu^5 = \bar{\psi} \gamma_\mu \gamma_5 \psi. \quad (3.9)$$

commonly called the axial vector current. Using the Dirac equation for massless quarks, this current can then be shown to be exactly conserved, that is

$$\partial_\mu J_\mu^5 = 0. \quad (3.10)$$

For the MIT bag, the bag potential acts as a mass term, and the quark axial vector current is no longer conserved. If, however, one now introduces a pion field $\vec{\pi}$, it contributes an axial vector current of the form

$$J_\mu^5 = f_\pi \partial_\mu \vec{\pi}. \quad (3.11)$$

and one can demand that the total axial vector current be conserved at the bag surface, which yields

$$f_\pi \partial_\mu \vec{\pi} = - \bar{\psi} \gamma_\mu \gamma_5 \psi = i \bar{\psi} \gamma_5 \psi. \quad (3.12)$$

This boundary condition is appropriate to the linear chiral bag model since the MIT bag boundary condition (3.3) has been used. Furthermore, this condition couples the pions to the quarks, as expected.

A good consistency check on the validity of chiral bag models is the prediction of the Goldberger-Treiman relation

$$g_A = g_{\pi NN} \frac{f_\pi}{M_N} \quad (3.13)$$

where g_A is the axial vector coupling constant, $g_{\pi NN}$ is the pion-nucleon effective coupling constant and M_N is the nucleon mass. It can be derived simply by comparing the asymptotic pion field from the chiral bag model and that from a static nucleonic charge.

Turning to the chiral bag, one observes that equation (3.13) can be used to derive the source term for the pions

$$\nabla_\mu = (D + \frac{1}{2} \sigma_{\mu\nu} \nabla^\nu) \psi = \frac{1}{f_\pi} \nabla_\mu \psi + g_\pi \quad (3.14)$$

where g_π is the surface δ term. If $\vec{\Sigma}$ and $\vec{\Upsilon}$ denote the classical spin and isospin of the nucleus, one can derive the asymptotic pion field from this source as [von Sm, vSK1990]

$$\vec{\Sigma} = -\frac{1}{2\pi^2} \frac{3}{4} g_A \frac{g_\pi}{f_\pi} 2(\vec{\Sigma} \cdot \vec{r}) 2\vec{\Upsilon} \frac{\exp(-m_\pi r)}{r} \quad (3.15)$$

Here $g_A^{(q)}$ denotes the value of the axial vector coupling constant for the quark bag.

Alternatively, one can consider the equation of motion for the classical pion field

$$(\square + \frac{m_\pi^2}{M^2}) \phi = -\frac{g_{\pi NN}}{M} \psi^\dagger \alpha^i \psi \partial_i \chi, \quad (3.16)$$

where χ denotes the nucleus wave function and ψ and $\bar{\psi}$ the spin and isospin operators respectively. If one takes the nucleon to be non-relativistic, one may replace the right-hand side, representing the source term for the pions by

$$\frac{g_{\pi NN}}{M} \nabla \cdot \hat{\alpha} \psi^\dagger \psi \chi, \quad (3.17)$$

The construction of the asymptotic pion field yields

$$\phi_{\mathbf{k}}^{\pm} = -\frac{g_{\pi NN}}{M} \frac{e^{i\mathbf{k} \cdot \mathbf{r}}}{2\omega_{\mathbf{k}}} \nabla \cdot \hat{\alpha} \psi^\dagger \psi \chi, \quad (3.18)$$

Comparing the two fields, one predicts

$$\frac{3}{2} \epsilon_A^{\pm}(\mathbf{k}) = \frac{g_{\pi NN}^{\pm}(\mathbf{k})}{M}. \quad (3.19)$$

If, as can be shown, $\epsilon_A^{\pm} = 3/2 \epsilon_A^{(\pm)}$, then (3.19) becomes the Goldberger-Treiman relation (3.12).

It is interesting to note that if one considers a second nucleon, its interaction with the pion field of nucleon 1 (3.18) is given by

$$V_{\text{GPP}}(r_{12}) = -\frac{g_{\text{NN}}^2}{4\pi} \frac{1}{r_{12}} (\vec{\sigma}_1 \cdot \vec{\sigma}_2) (\vec{\tau}_1 \cdot \vec{\tau}_2) \frac{\exp(-m_\pi r_{12})}{r_{12}}, \quad (3.20)$$

which, as the nucleon separation r_{12} becomes large, tends to

$$V_{\text{GPP}}(r_{12}) \approx -\frac{g_{\text{NN}}^2}{4\pi} \frac{1}{r_{12}} (\vec{\sigma}_1 \cdot \vec{\sigma}_2) (\vec{\tau}_1 \cdot \vec{\tau}_2) \frac{\exp(-m_\pi r_{12})}{r_{12}}. \quad (3.21)$$

This can be recognized as the one-pion exchange potential for large distances, and serves to illustrate the role of mesons in nucleon-nucleon interaction.

The above derivation of the Goldberger-Treiman relation, while providing the clearest link between the traditional picture of a nucleon as a pion source and a hybrid chiral soliton model, is not applicable to the non-linear case. For the present work it is instructive to consider an alternative calculation for g_A due to Jaffe [Jaf79], in which the axial vector coupling constant is derived as the zero momentum limit of the axial vector form factor. Here one also derives the factor $3/2$ in the equation $g_A = 3/2g_1^{(A)}$. This discussion will be particularly relevant to the present work in hybrid Skyrme solitons. There are, however, some differences which will be underlined.

The total axial vector current is given, as before, by

$$\vec{A}_\mu(\vec{r}) = \frac{1}{2} g_{\text{NN}} \vec{\sigma} \cdot \vec{\tau} \delta(\vec{r}_b - \vec{r}) + \vec{r}_b \cdot \vec{\tau} \delta(\vec{r} - \vec{r}_b). \quad (3.22)$$

For the nucleon, one can define the zero momentum limit of the axial form factor as

$$\tilde{\chi}_\mu(\mathbf{q}) = \lim_{\tilde{q} \rightarrow 0} \int d^3r e^{i\tilde{q}\cdot\mathbf{r}} \langle N | \tilde{\chi}_\mu(\mathbf{r}) | N_0 \rangle, \quad (2.23)$$

where N denotes the nucleon state. Thus its non-relativistic limit is given by

$$u^\dagger (\mathbf{x}_A \cdot \vec{\sigma} + \frac{g_A}{2M_N} \sigma \cdot \vec{q}) u, \quad (2.24)$$

where u is the nucleon spinor, M_N is the nucleon mass, \mathbf{x}_A is the axial vector and g_A is the axial pseudovector coupling constant.

If one calculates $\tilde{\chi}_\mu(\mathbf{q})$ for the chiral quark bag only one obtains

$$\tilde{\chi}_\mu^A(\mathbf{q}) = [\tilde{u}(\mathbf{q}) \delta_{\mu 3} + \tilde{v}(\mathbf{q}) (3\hat{q}_\mu \hat{q}_3 - \delta_{\mu 3})] \langle \sum_a \sigma_j \frac{1}{2} \rangle, \quad (2.25)$$

where \mathbf{q} denotes $[\tilde{q}]$, the sum is over the quarks a , and the function \tilde{u} and \tilde{v} are given by

$$\tilde{u}(\mathbf{q}) = b_0^2 \int_0^{R_0} dr r^2 J_0^2(q_0 r) - \frac{1}{3} J_1^2(q_0 r) J_0(qr) \quad (2.26a)$$

$$\tilde{v}(\mathbf{q}) = \frac{2}{3} b_0^2 \int_0^{R_0} dr r^2 J_1^2(q_0 r) J_0(qr). \quad (2.26b)$$

Here R_0 and b_0 denote respectively the energy and normalization constant for the lowest energy state. Taking the limit $\tilde{q} \rightarrow 0$ only, the first integral survives, and one may write the axial form factor for the quark core as

$$A_A^{(1)}(0) = g_A^{(1)} a_A^1 \frac{r^1}{2} u. \quad (3.27)$$

Performing a similar calculation for the pion field, one can derive the total axial vector form factor in the form

$$A_A^{(1)}(q) = u^T (\hat{a}(q) a_{A1} + \hat{b}(q) (2\hat{a}_1 a - \hat{q} a_{A1})) \frac{r^1}{2} u. \quad (3.28)$$

Using the condition of conserved axial vector currents, one may derive the relationship

$$\hat{b}(q) = -2\hat{a}(q). \quad (3.29)$$

The total axial vector current may thus be written as

$$A_A^{(1)}(q) = \frac{2}{3} \hat{a}(q) u^T (a_{A1} - a - \hat{q} a_{A1}) \frac{r^1}{2} u. \quad (3.30)$$

Since the contribution to \vec{v} from the pion field can be shown to be zero, one has

$$A_A^{(1)}(0) = \frac{2}{3} g_A^{(1)} a_A^1 \frac{r^1}{2} u. \quad (3.31)$$

and thus

$$g_A = \frac{2}{3} g_A^{(1)}. \quad (3.32)$$

Critical to this discussion is of course the fact that \vec{v} is identically zero for the pion field. For hybrid Higgs models, \vec{v} is no longer zero for the

pin field and equation (3.22) no longer holds. The calculation for the chiral bag in the hybrid chiral soliton is, however, very similar to the above, but an important difference appears at this juncture.

Up to this point all the arguments have been based on nucleon states with good spin and isospin. In practice, one is forced to make the hedgehog ansatz $\vec{\psi} = s(r)\hat{r}$, which has neither good spin nor good isospin. Certainly, if one calculates the axial vector coupling constant for the hedgehog quark core, one obtains

$$g_{Aq}^H = -\frac{8}{3} g_{Aq} \quad (3.23)$$

If one can derive the total hedgehog axial constant as $g_A^H = \frac{3}{2} g_{Aq}^H$ (only possible if $s(r) \rightarrow \frac{\Lambda}{r}$ as $r \rightarrow \infty$), one might propose

$$g_A^H = -\frac{8}{3} g_A \quad (3.24)$$

This factor is of course the correction factor, as originally introduced by Jackson and Ito [JKI2] for the axial vector constant in the Skyrme model.

Finally, if one is given the asymptotic form of the field as

$$\vec{\psi} \rightarrow \hat{r} \frac{\Lambda}{r} \hat{r}, \quad r \rightarrow \infty, \quad (3.25)$$

one can define

$$g_A^H = \text{Def} g_A^H \quad (3.26)$$

Naturally, this definition must be consistent with the calculation from the axial vector current. Fortunately, this is true both for the chiral bag model [Wen82] and the hybrid chiral soliton model [DMS74].

The idea of chiral bag models can be extended by permitting the pion field to penetrate the quark bag, the so-called Cloudy Bag Model (CBM). This model in fact predicts better values for the nucleon static properties, in particular g_A . For the sake of simplicity, this model has not, however, been used in the present work.

The most important difference between the classical chiral bag models and the hybrid chiral solitons discussed in the present work is the inclusion of the vacuum contributions. Such contributions have only recently been taken into account, and will prove central to the present work.

4. THE HYBRID CHIRAL SOLITON MODEL WITH PIONS

Given the relevance and predictive power of both chiral bag models and the Skyrme soliton, it becomes eminently reasonable to consider a hybrid model. Such a model was indeed independently proposed by three different groups [BOS84, MAL84, LSH84] and is described below. In all previous work, baryon density continuity has not been enforced, and in general, this density shows a distinct discontinuity at the bag surface. The results of imposing such continuity [GMS7b,c] as a constraint on the model are presented and compared both with experiment and the results of other hybrid chiral soliton models.

4.1 An outline of the model

Firstly, in the region outside the chiral bag of radius R_b , one has the Skyrme soliton. As before, the Lagrange density for the pion field is given by

$$\mathcal{L} = \frac{1}{4} f_\pi^2 \text{Tr}(\partial_\mu U \partial^\mu U^\dagger) + \frac{1}{4} \epsilon^2 \text{Tr}[U^\dagger \partial_\mu U \partial^\mu U^\dagger U]^2, \quad (4.1)$$

with

$$U = \exp(-i\vec{T} \cdot \vec{\pi}(r)). \quad (4.2)$$

The total baryon number in this region is simply the integral of equation (2.32):

$$B_b = \frac{1}{\pi} [s(R_b) - \frac{1}{2} \sin(2s(R_b))]. \quad (4.3)$$

Secondly, inside the chiral bag one has free massless quarks with the Dirac Lagrange density

$$\mathcal{L} = \frac{1}{2} \bar{\psi} \gamma_{\mu} \partial^{\mu} \psi . \quad (4.4)$$

Such quarks obey the free Dirac equation

$$i \gamma_{\mu} \partial^{\mu} \psi = 0 , \quad (4.5)$$

together with the chiral boundary condition

$$-i \vec{\gamma} \cdot \vec{r} = \exp(-i \vec{\gamma} \cdot \vec{r} \cdot \vec{g}(R_b)) \vec{r} . \quad (4.6)$$

The quark energy eigenvalues and eigenstates may be determined straightforwardly, and details of the calculation are given in Appendix 6A. In figure 4.1 the quark eigenenergies are given as a function of $s(R_b)$; the occupied and empty levels are denoted by solid and dotted lines respectively.

At first it might seem that the baryon number of such a system is not unity since the u^s valence quarks already carry baryon number one. The missing contribution is of course the baryon number of the vacuum to be defined below.

Indeed, it is instructive to consider at this point, the general problem of finding the expectation value of the operator $(\vec{V} \cdot \vec{U})_r$ for an arbitrary single particle operator \hat{O} , between the states of the valence and vacuum quarks

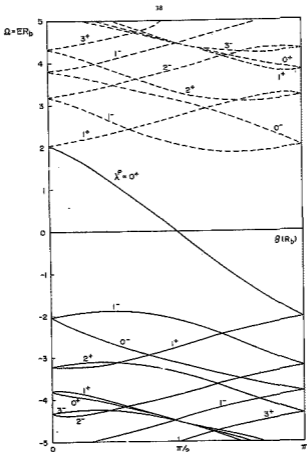


Figure 4.1 The quark single particle energies as a function of the chiral angle at the bag radius

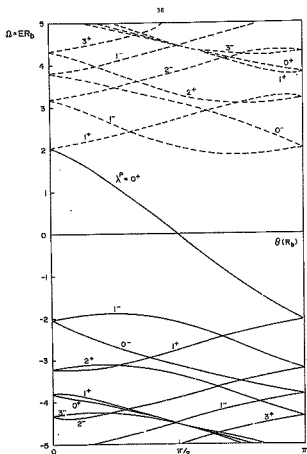


Figure 4.3 The quark single particle energies as a function of the central angle at the bag radius

since the results have a wider application. Let U_n and $r_n(x)$ denote the complete set of quark eigenvalues and eigenvectors respectively, and let D_n denote $U_n^{-1} U_n$. Then, quantizing the fermion field as

$$\psi = \sum_{U_n > 0} r_n(x) b_n + \sum_{U_n < 0} r_n(x) d_n^\dagger, \quad (4.8)$$

one observes that the symmetrized expectation value of $\frac{1}{2} \{\bar{\psi}, \not{\partial} \psi\}$ splits into two pieces:

- (i) the expectation value of normal ordered part $\frac{1}{2} \{\bar{\psi}, \not{\partial} \psi\}$, which is only non-zero for occupied particle states ($U_n > 0$) or empty hole states ($U_n < 0$). From fig. 4.1 one sees that this, the valence quark contribution, will only be non-zero for $\epsilon(U_n) \geq \frac{\pi}{2}$. For larger angles the valence quark energy becomes negative, and the valence quarks then yield no contribution to the normal ordered part.

- (ii) the vacuum expectation value

$$\theta_v = \frac{i}{2} \langle 0 | \{\bar{\psi}, \not{\partial} \psi\} | 0 \rangle = -\frac{1}{2} \sum_n \text{sign}(U_n) \theta_n = -\frac{1}{2} \sum_n \text{sign}(U_n) \theta_n, \quad (4.9)$$

where

$$\theta_n = \bar{r}_n \not{\partial} r_n, \quad (4.10)$$

and the sum runs over all positive and negative energy states.

since the results have a wider application. Let Ω_n and $\varphi_n(x)$ denote the complete set of quark eigenvalues and eigenvectors respectively, and let Ω_n denote E_{Ω_n} . Then, quantizing the fermion field as

$$\psi = \sum_{\Omega_n > 0} \varphi_n(x) b_n + \sum_{\Omega_n < 0} \varphi_n(x) d_n^\dagger, \quad (4.8)$$

one observes that the symmetrized expectation value of $\frac{1}{2} (\bar{\psi}, \bar{\psi})$ splits into two pieces:

- (i) the expectation value of normal ordered part $\frac{1}{2} :(\bar{\psi}, \bar{\psi}):$, which is only non-zero for occupied particle states ($\Omega_n > 0$) or empty hole states ($\Omega_n < 0$). From fig. 4.1 one sees that this, the valence quark contribution, will only be non-zero for $\theta(\Omega_n) \leq \frac{\pi}{2}$. For larger angles the valence quark energy becomes negative, and the valence quarks then yield no contribution to the normal ordered part.

- (ii) the vacuum expectation value

$$\langle \psi, \bar{\psi} \rangle = \frac{1}{2} \langle 0 | (\bar{\psi}, \bar{\psi}) | 0 \rangle = -\frac{1}{2} \sum_n \text{sign}(\Omega_n) \Omega_n = -\frac{1}{2} \sum_n \text{sign}(\theta_n) \Omega_n, \quad (4.9)$$

where

$$\theta_n = \frac{\pi}{2} - \theta_{\Omega_n}, \quad (4.10)$$

and the sum runs over all positive and negative energy states.

Returning to the baryon number, one observes that the baryon number of the vacuum is simply given by

$$B_v = -\frac{1}{2} \sum_n \text{sign}(R_n) \quad (4.11)$$

$$\text{since } B_v = \int d^3x \psi^{\dagger} \psi = 1.$$

Upon regularization, this becomes

$$B_v = -\frac{1}{2} \lim_{\epsilon \rightarrow 0} \sum_{R_n} \text{sign}(R_n) e^{-\epsilon |R_n|^2}. \quad (4.12)$$

This expression can be evaluated either analytically [GMS] or numerically [VMS], with the result that

$$B_v(\theta(R_0)) = -\frac{1}{2} (\theta(R_0) - \frac{1}{2} \text{sign}(\theta(R_0))) = -B_0(\theta(R_0)) \quad -\frac{\pi}{2} \leq \theta(R_0) \leq \frac{\pi}{2}. \quad (4.13)$$

Outside this range one can apply the symmetry relation

$$B_v(\theta(R_0) + \pi) = B_v(\theta(R_0)) \quad (4.14)$$

since the quark eigenpectrum is identical for the angles $\theta(R_0)$ and $\theta(R_0) + \pi$. It is now possible to verify that the baryon number, $B = B_u + B_d + B_s$, is indeed unity for all R_0 . There are two possible cases. For $0 \leq \theta(R_0) \leq \pi/2$ one can see that there is a filled valence quark state with positive energy, which carries baryon number $B_q = 1$. Furthermore, the baryon number from the

annihilated and the vacua cancel each other and thus the total baryon number is

$$B = B_V + B_C + B_B = 1, \quad (4.16)$$

as desired. For $\pi/2 \leq \phi(R_B) \leq \pi$ the valence quark level disappears into the Dirac sea, and one only has the vacuum contribution

$$B_V(\phi(R_B)) + B_C(\phi(R_B) - \pi) = 1 - \frac{1}{2}(\phi(R_B)) - \frac{1}{2} \sin 2\phi(R_B) = 1 - B_B(\phi(R_B)). \quad (4.18)$$

Again, the total baryon number is

$$B = B_B + B_V = 1. \quad (4.17)$$

The link between the quark and meson sector is, as in chiral bag models, provided by the conservation of the axial vector current, \vec{A}_μ . This current can be derived from the Lagrangian density by considering its transformation under the symmetry group $SU(2)_L \times SU(2)_R$ (Appendix 4B).

Since one wishes this current \vec{A}_μ to be conserved $\partial_\mu \vec{A}^\mu = 0$, one must enforce continuity of its normal component at the bag surface

$$\vec{r}_1^i \partial_{\alpha i} \vec{A}_\alpha = \vec{r}_2^i \partial_{\alpha i} \vec{A}_\alpha. \quad (4.18)$$

Turning to the quark sector one sees that the right-hand side requires the

calculation of the expectation value [48.7]

$$\overline{\psi \overline{\psi}} \cdot \overline{\psi \psi} = \overline{\psi \psi}^2. \quad (4.10)$$

at the bag surface. Adopting the standard approach to the calculation of such quantities, one defines the vacuum expectation value as

$$\overline{\psi \overline{\psi}}_{\text{vac}}^4 = -\frac{N_c}{2} \lim_{\eta \rightarrow 0} \sum_n \text{sign}(\epsilon_n) (\overline{\psi} \overline{\psi} \cdot \overline{\psi \psi})_n^{-1} (\epsilon_n)^2. \quad (4.11)$$

Thus, it for a single quark level (48.12)

$$\overline{\psi \overline{\psi}} \cdot \overline{\psi \psi} \Big|_{r=R_b} = \frac{1}{4\pi R_b^3} \frac{d\epsilon_n}{d\eta}. \quad (4.12)$$

one may rewrite the above expression as

$$4\pi R_b^3 \overline{\psi \overline{\psi}}_{\text{vac}}^4 = -\frac{N_c}{2} \lim_{\eta \rightarrow 0} \sum_n \text{sign}(\epsilon_n) \frac{d\epsilon_n}{d\eta} = -(\epsilon_n)^2. \quad (4.13)$$

Unfortunately, this limit as defined is divergent (see [48.13]). One can, however, apply a naive renormalization prescription in which the divergences are subtracted in such a way that one recovers the pure Skyrme model in the limit $N_c \rightarrow 0$. In the present work the results of Vazirni et al, where $\epsilon \approx \epsilon(N_c)$ (see [48.14], Appendix 4D), will be used, namely

$$4\pi R_b^3 \overline{\psi \overline{\psi}}_{\text{vac}}^4 = N_c \frac{d\epsilon_n}{d\eta}. \quad (4.14)$$

where

$$\frac{d\alpha_0(\theta)}{d\theta} = \frac{3}{4\pi} \left[2\theta + \sum_{n=1}^4 n c_n^2 \sin(2n\theta) \right] - \frac{\pi}{2} \quad \theta \leq \frac{\pi}{2}$$

and

$$\left. \frac{d\alpha_0}{d\theta} \right|_{\theta=\pi/2} = - \left. \frac{d\alpha_0}{d\theta} \right|_{\theta=0} \quad \frac{\pi}{2} \leq \theta \leq \pi. \quad (6.24)$$

with $c_1 = -0.82382$, $c_2 = -0.053623$, $c_3 = 0.0028195$ and $c_4 = -2.752-4$. If $\theta(H_0)$ is less than $\pi/2$, the contribution from the valence quark $N_0 \frac{d\alpha_0}{d\theta}$ must be added explicitly. In total therefore, in the quark sector,

$$4\pi n_0^2 r_1^2 \frac{d\alpha_0}{d\theta} \Big|_{\theta=0} = N_0 [g(\frac{\pi}{2}) - \theta(H_0)] \frac{d\alpha_0}{d\theta} + \frac{d\alpha_0}{d\theta} = N_0 \frac{d\alpha_0}{d\theta}. \quad (4.26)$$

In the meson sector one has simply (4.20)

$$6\pi n_0^2 r_1^2 \frac{d\alpha_0}{d\theta} \Big|_{r=r_0} = 4\pi (r_0 r_1)^2 \frac{r_0}{d\theta} \left[1 + \frac{16\pi^2 \sin^2 \theta}{(r_0 r_1)^2} \right] \Big|_{r=r_0}. \quad (4.27)$$

One can therefore write the boundary condition (4.21) in its final dimensionless form as

$$4\pi \frac{d\alpha_0}{d\theta} \Big|_{r=r_0} = 4\pi (r_0 r_1)^2 \frac{r_0}{d\theta} \Big|_{r=r_0} \left[1 + \frac{16\pi^2 \sin^2 \theta}{(r_0 r_1)^2} \right] \Big|_{r=r_0}. \quad (4.27)$$

Given the conservation of the axial vector current, and in view of the global $SU(2)_L \times SU(2)_R$ symmetry, one might well be interested in its partner current, namely the vector current \mathbf{V}_μ .

One can in fact show that this too is conserved at the boundary since

$$\hat{r}_i^2 \partial_\mu^2 y_{\text{eff}}^i = \hat{r}_i^2 \partial_\mu^2 y_{\text{eff}}^i / \eta^2 = 0 \quad r = R_b. \quad (4.28)$$

The other important conserved current is of course the baryon current, independently conserved in quark and meson sectors. For the Skyrme tail

$$\hat{r}_i^2 \partial^\mu \hat{b}^i = 0 \quad \forall r. \quad (4.29)$$

In the quark sector

$$\hat{r}_i^2 \partial^\mu \hat{b}^i = -\nabla^\nu \hat{r} \cdot \hat{r}. \quad (4.30)$$

Using the bag boundary condition, (4.17) one can show that

$$-\nabla^\nu \hat{r} \cdot \hat{r} |_{r=R_b} = \nabla^\nu [1 - \exp(-\hat{r}^2 / r^2) g^{\nu\alpha} (R_b)] |_{r=R_b} = 0, \quad (4.31)$$

which is in agreement with the same quantity in the Skyrme sector.

This conservation law does not however imply continuity of the baryon number density, merely that the baryon number

$$B = \int d^3x \hat{b}^0(x) \quad (4.32)$$

should be a constant of the motion. This continuity certainly does not apply in the MIT bag model for which

$$\hat{n} \cdot \nabla_{\mathbf{r}} \Big|_{r=R_0} = \nabla \cdot \hat{\mathbf{r}} \Big|_{r=R_0} = 1 \nabla \cdot \hat{\mathbf{r}} \Big|_{r=R_0} = 0. \quad (4.33)$$

Inside, the baryon density is finite; outside it is zero.

Neither is this continuity automatically satisfied in chiral soliton models. Inside the bag the baryon density, whose detailed calculation is given in Appendix 40, is given as the sum of two terms:

- (1) the baryon density for the valence quarks, $B_q^0(\mathbf{R}) = e(\frac{1}{2} - s(B_0)) \rho_0^3$ and
- (2) the baryon density for the vacuum defined as

$$B_v^0(\mathbf{R}) = -\frac{1}{2} \lim_{\epsilon \rightarrow 0} \sum_{\mathbf{n}} \text{sgn}(n_i) \rho_0^3(\mathbf{R}) \rho_0(\mathbf{R}) e^{-\epsilon(n_i)^2}. \quad (4.34)$$

One notes that, apart from an overall normalization constant $1/\rho_0^3$, the total baryon density at the bag radius is independent of the radius R_0 and depends only on $s(B_0)$. If one defines

$$B_4^{\text{eff}}(s(B_0)) = \rho_0^3 \int_{\mathbb{Z}^3} \text{dn}^2(\mathbf{R}), \quad (4.35)$$

then B_4^{eff} is a dimensionless function of $s(B_0)$ only.

In contrast, the corresponding quantity in the meson sector

$$B_3^0(s(B_0)) = -\frac{2}{3} \sin^2 \theta \Big|_{r=R_0} \quad (4.36)$$

is a function of both $s(R_0)$ and its first derivative.

If one has a solution satisfying the boundary condition (4.26) for given s^2 , one can construct a neighbouring solution for which $s(R_0)$ is identical, but $\frac{ds}{dr}|_{r=R_0}$ differs, simply by adjusting s^2 . If the first satisfies baryon density continuity, then the second cannot. Clearly then, baryon density continuity is not guaranteed.

In the present work this constraint has been imposed, that is

$$D_3^{*uv}(s(R_0)) = -\frac{2}{3} \sin^2 \theta \left. r \frac{ds}{dr} \right|_{r=R_0} \quad (4.27)$$

For any given radius R_0 the model is then uniquely specified and can be used to predict the static properties of the nucleus.

4.2 Details of the numerical solution

In the Skyrme sector, the chiral angle θ obeys the Euler-Lagrange equation (2.25). Introducing the dimensionless variable $\tau = \ln r/r_0$, where r_0 is an arbitrary distance (taken to be 1 fm in the present work) this equation becomes

$$\ddot{\theta} (1 + \lambda_0 e^{-2\tau} \sin^2 \theta) + \dot{\theta} (1 - \lambda_0 e^{-2\tau} \sin^2 \theta) - \alpha \sin 2\theta (1 - \frac{1}{2} \lambda_0 e^{-2\tau} (\dot{\theta}^2 - \sin^2 \theta)) = 0, \quad (4.28)$$

$$\text{where } \lambda_0 = \frac{3\alpha^2}{(f_\pi^2 r_0)^2}.$$

From its long-range behaviour one may deduce

$$\phi(r) \sim \alpha e^{-2r} \quad \text{as } r \rightarrow \infty. \quad (4.39)$$

One can then determine α and α^2 by integrating ϕ in from infinity to $\phi(R_b)$ and demanding that all two boundary conditions (4.27) and (4.28) be satisfied. In terms of the new variables these become

$$R_b \frac{d\phi}{ds} = \alpha_0 (r_0^2 \alpha^2 e^{2r} \frac{ds}{dr} [1 + 4_0 e^{-2r} \sin^2 s]), \quad r = r_0 \frac{R_b}{r_0} \quad (4.40)$$

given by the conservation of the axial vector current, and

$$\int_0^{\pi/2} \phi(s(R_b)) ds = -\frac{2}{\pi} \sin^2(s(R_b)) \frac{ds}{dr} \Big|_{r=R_b(R_b/r_0)} \quad (4.41)$$

given by the continuity of the baryon density.

The resulting values for α and α^2 are then given as a function of R_b in Table 4.1. In addition, the corresponding profile for ϕ as a function of the radial variable, r , is displayed in fig. 4.2, together with the results from the work of Brown et al [BDMW].

For bag radii larger than $R_b = 0.475$ the insistence on both boundary conditions leads to a negative value for α^2 . Either then relax either of the constraints the model has simply been restricted to smaller radii.

Table 4.1

The values of the asymptotic constant a , the axial vector coupling constant g_A , the coefficient for the stabilizing term a^2 , the total energy E (MeV), the isoscalar radius $\langle r^2 \rangle_{I=0}^{1/2}$ (fm) and the isovector magnetic moment μ_{2N} (nm) as a function of R_0 , the bag radius.

Bag radius R_0 (fm)	Asymptotic const a	g_A	a^2	E (MeV)	$\langle r^2 \rangle_{I=0}^{1/2}$ (fm)	μ_{2N} (nm)
0.275	0.405	1.257	0.6095	1232	0.43	2.27
0.3	0.415	1.287	0.6234	1223	0.49	2.31
0.325	0.425	1.319	0.6382	1213	0.56	2.34
0.35	0.436	1.353	0.6530	1203	0.61	2.37
0.375	0.448	1.389	0.6677	1193	0.63	2.40
0.4	0.460	1.428	0.6825	1183	0.65	2.44
0.425	0.474	1.469	0.6972	1173	0.58	2.47
0.45	0.488	1.512	0.7119	1163	0.65	2.50

The total energy is then given as the sum of three terms. The first is the energy of the Skyrmin tail, simply given as

$$\begin{aligned}
 E_0 &= - \int_{R_0}^{\infty} dr 4\pi r^2 \mathcal{E}(r) \\
 &= 2\pi E_{\text{SK}}^2 R_0^3 \left[\int dr r^2 (\dot{\phi}^2 + 2\sin^2\theta) + 4_0 e^{-\gamma} \sin^2\theta (\phi^2 + \frac{1}{2} \sin^2\theta) \right]. \quad (4.42)
 \end{aligned}$$

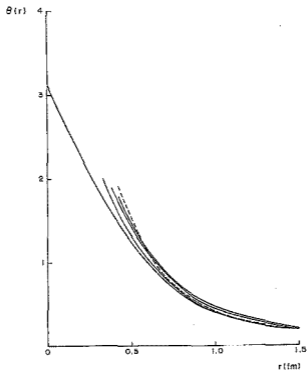


Figure 4.1 The chiral angle $\theta(r)$ as a function of the radial variable r (fm). The solid curves shown are for the pure Skyrme with $g_A = 1.31$ and for the present model with $F_0 = 0.325, 0.375$ and 0.425 fm. The dashed curve is for the model of Brown et al [BJ79BA]

The second is the energy of the valence quarks, $N_q \bar{m}_q$, only added if $v(R_b) < w/2$. The third is the bag vacuum energy for which the explicit details of calculation are given in appendix 4C where the following expression is obtained

$$E_v = N_b \frac{R_b v(R_b)}{b} , \quad (4.43)$$

with

$$v_b(s) = \frac{3}{4\pi} (s^2 + \sum_{n=1}^4 f_n \alpha_n^2 s^n) ,$$

with $f_1 = -0.80320$, $f_2 = -0.082803$, $f_3 = 0.046895$ and $f_4 = -2.732 \cdot 10^{-4}$. The total energy so calculated is given in Table 4.1.

A volume energy of the form $\frac{4\pi}{3} R_b^3$ has not been added. Although the energy shown might appear unstable with increasing R_b , one should bear in mind two points. Firstly, this variation is small, and secondly one can, if desired, introduce a minimum simply by setting $\alpha^2 = 0$ for larger radii and neglecting baryon density continuity. For the sake of completeness it can be noted that such a term, if included, would contribute less than about 50 MeV or 5% of the total energy for the radii considered.

Turning to the long-range behaviour, one observes that

$$v(r) \sim \frac{\pi r_0^2}{r} \quad \text{as } r \rightarrow \infty . \quad (4.44)$$

Comparing this with the corresponding behaviour in the chiral bag model (3.34 - 3.36), one obtains

$$g_A = \frac{5}{2} \frac{\text{Str}^2 \rho_0^2}{\rho_0^2} . \quad (4.65)$$

One should note this expression differs by a factor of $\frac{N_c+2}{N_c} = \frac{5}{3}$ from that applicable to the pure Skyrme model [APW85]. As with other calculated quantities, the dependence of g_A on ρ_0 (see Table 4.1) is rather weak. This independence is in essence the Cheshire cat assumption. What is more remarkable is its agreement with the theoretical value $g_A = 1.33$ calculated from the Goldberger-Treiman relation. A further discussion of the factor 5/3, included to obtain this agreement, is given in Chapter 8 where projection techniques are discussed. At present, one should merely note that the model supports such a factor.

The isoscalar radius is simply given as the integral

$$\langle r^2 \rangle_{I=0} = \int d^3r r^2 \mathbb{B}^0(r) , \quad (4.66)$$

where $\mathbb{B}^0(r)$ is the baryon density. As a consistency check on the numerical calculation, one should note that the contribution from the vacuum can be calculated in two independent ways. Either one constructs $\mathbb{B}_V^0(r)$ and then integrates, or one calculates

$$\langle r^2 \rangle_{I=0}^V = \int_{q_0} d^3r r^2 \psi_n^* \psi_n , \quad (4.67)$$

for each eigenstate, n , and constructs the limit

$$\langle r^2 \rangle_{I=0}^V = -\frac{1}{2} \lim_{q \rightarrow 0} \sum_n \text{sign}(E_n) \langle r^2 \rangle_{I=0}^n e^{-i(m_n)q} . \quad (4.68)$$

This corresponds to the interchange of the limit of the sum with the integration.

Finally, the isovector magnetic moment is calculated. The results for the hedgehog configuration are presented first. In the Skyrme sector one uses the results from the paper of Adkins, Nappi and Witten [ANW83]

$$\mu_{I=1,0}^H = -\frac{6\pi}{5} f_\pi^2 \int_{R_0}^{\infty} dr r^2 \sin^2 \theta \left[1 + \frac{3k}{2} \left[\left(\frac{d\theta}{dr} \right)^2 + \frac{\sin^2 \theta}{r^2} \right] \right] . \quad (4.49)$$

In the quark sector the isovector magnetic moment for a single quark state is given as

$$\mu_{I=1,0}^H = \frac{1}{3} \int d^3x \bar{\psi}_n(\vec{x}) \vec{\sigma} \psi_n . \quad (4.50)$$

To obtain the vacuum contribution one must correctly calculate and renormalize the infinite sum [WZ88, Appendix 4C]

$$\mu_{I=1}^H = -\frac{N_c}{2} \lim_{\sigma \rightarrow 0} \sum_n \text{sign}(n_0) \mu_{I=1,0}^H \sigma^{-\epsilon(n_0)} . \quad (4.51)$$

Constructing the isovector magnetic moment for the nucleon, one obtains

$$\mu_{I=1} = \mu_{I=1}^H / f_{1h} , \quad (4.52)$$

where f_{1h} is the coupling factor originally introduced for the axial vector current, namely

$$a_A^H = r_{ch} \epsilon_A \quad (4.52)$$

Again, the value of -0.5 is used in the present work. The ratio $\epsilon_A/\mu_{[1]}$ is, however, independent of this factor, and ranges from 0.55 to 0.61 in the present work. This is in close agreement with the expected value of $1.32/2.35 = 0.57$.

Lastly, a table is presented comparing experiment with the results for $R_0 = 0.395$ fm, which has been selected for its value of $\epsilon_A = 1.32$. The agreement is of course particularly good for r_A (by selection), but is also good for $\mu_{[1]}$. The energy is somewhat higher than the nuclear average mass, but this discrepancy may, at least in part, be due to center of mass excitation. The greatest difference is in the isoscalar radius. It has, however, been argued that in the pure Skyrme model there could be a correction factor of $6/\mu_0^2$ to its square [ANDERSON, NEWBERRY]. This factor arises from a possible additional term in the baryon current from the ω meson and the assumption of vector meson dominance. We have not included this term in the density and therefore its use here is strictly ad hoc. The inclusion of this factor yields $C_{I=0}^{R_0, 1/2} = 0.72$ fm, which is in much better agreement with experiment. Although the results have been presented for one particular radius, it should be stressed that overall, there is little sensitivity to R_0 . As R_0 is essentially arbitrary, this should be welcomed.

Table 4.2

The predictions of the present model at $R_b = 0.226$, compared with their experimental values.

Quantity	Prediction	Experiment
$B(\text{MeV})$	1213	1086
g_A	1.22	1.25
μ_{NM}	13.3	13.5
$\langle r^2 \rangle_{1/2}^{1/2}(\text{fm})$	0.60	0.72
$\mu_{\text{Tr}}(\text{nm})$	2.34	2.36

4.3 Comparison with Other Models

The basic difference in hybrid chiral soliton models lies in the determination of the parameters a , or equivalently g_A , and the fourth order coupling constant a^2 (f_π is usually taken at its experimental value of $f_\pi = 93 \text{ MeV}$). In fact, only one parameter need be specified since the condition of axial vector continuity then uniquely determines the other one.

In the present work this freedom has been used to enforce baryon density continuity at the surface, thus automatically specifying both g_A and a^2 for all R_b . This is in contrast with the two alternative approaches discussed below, where either g_A [BJW84] or a^2 is fixed [WJ86, WJS6] for all bag radii. In such models, the baryon density is, in general, discontinuous at the bag radius. One therefore has the physically unappealing picture of a baryon density discontinuity that moves with the arbitrary bag radius R_b . This is not particularly desirable and provides the principal motivation for the present model.

The first detailed comparison is to the work of Brown et al [23904] in which g_A has been explicitly set to the value predicted by the Goldberger-Treiman relation, that is $g_A = 1.31$, μ^2 is then regarded as a free parameter to be determined to satisfy axial vector continuity. The model is clearly closely related with the present work, and indeed, at $\mu_0 = 0.325$ fm where one now predicts $g_A = 1.32$, they are practically co-incident. The most obvious distinguishing feature between these two models is the baryon density, which is given for both models in figures 4.3 and 4.4 for $\mu_0 = 0.325$ fm and $\mu_0 = 0.425$ fm respectively. As expected, the densities in fig. 4.3 coincide and are continuous. In figure 4.4 the density in the present work is continuous (by construction), while the second shows a distinct discontinuity. This discontinuity is not, however, reflected as a correspondingly large difference for the prediction of the other static properties of the nucleon, a result that might be expected from the behaviour of $\epsilon(r)$ versus r for the two models (fig. 4.2). One can therefore, as in the present work, improve the model by enforcing baryon density continuity, without destroying the results for the static properties and providing a distinct new prediction for $g_A(R_N)$. What the values so obtained are so close to the desired one $g_A = 1.32$ is truly remarkable and is an excellent consistency check on the model as now proposed.

One can also see here the importance of the vacuum effects. Traditional hybrid chiral bag and soliton models, including only valence quark contributions, invariably predict a value of g_A approximately 50% too high [23905, 23906, 23907]. Admittedly however, if one omitted the factor $\frac{2}{3}$ for these models, as has been suggested by Pasquier [23908], they then show good agreement with the experimental value.

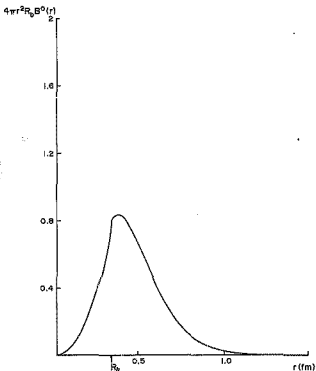


Figure 4.3 The product of the radius r_0 with the baryon density in a spherical shell $4\pi r^2 R_0 B^0(r)$ as a function of the radial variable r (fm). The results are given for the present model (Q87b,c) with $R_0 = 0.325$ fm

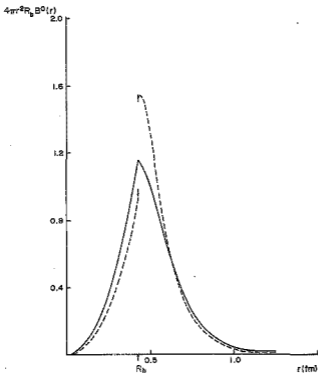


Figure 4.4 The product of the radius R_0 with the baryon density in a spherical shell $(4\pi r^2 R_0 B^0(r))$ as a function of the radial variable $r(\text{fm})$ for $R_0 = 0.425 \text{ fm}$. The solid curve indicates the result in present work [O-87b,c] while the dashed curve shows the results for the model of Brown et al. [81PWS6].

In both of the cases discussed above the constant κ^2 has been regarded merely as the coefficient of a fourth order stabilizing term. As such, it should admit the Dirac pressure of the quark bag now included explicitly. In some sense therefore the appearance of the quark bag should "turn off" the pion interaction, resulting in the closure of κ^2 falling to zero as R_b increases.

This is in direct contrast with the approach in the second class of models for comparison, namely those in which κ^2 is fixed [MUSCO, WYSE, JUVV987]. Here κ^2 is regarded as intrinsic to the pion Skyrme Lagrangian and g_A is to be determined from axial vector continuity. In the later work of the Stoy-Brack group [MIVUS, JUVV987] κ^2 has been selected to give the correct value of g_A , that is $g_A = 1.22$ at $R_b = 0$, that is for the pure Skyrme. Several criticisms can be levelled at this approach. Firstly, as expected, the baryon density is discontinuous. Secondly, unlike in present work g_A never attains the correct value for $R_b \neq 0$ (see Table 4.5). Thirdly, since within the model, $R_b > 0$, there is no reason to require g_A to attain the Goldberger-Treiman value at $R_b = 0$.

Table 4.3

The predictions for $g_A^2(R_b)$, the axial vector coupling constant, as a function of R_b , the bag radius.

R_b	$g_A^{(a)}$	$g_A^{(b)}$
0.325	1.210	1.407
0.375	1.303	1.490
0.425	1.400	1.582

(a) calculated in present work (QMBTs)

(b) calculated for $\kappa^2 = 0.0662$, that is $g_A(0) = 1.32$.

This approach also features in the work of Hoesl and Toki [2156]. There the constant κ^2 has been fixed by demanding that the equation for axial vector continuity be subject to a higher order continuity constraint as $R_b \rightarrow 0$. Now not only must one satisfy the previous equation given below

$$R_b \frac{d^2 g_A^{(a)}}{dR_b^2} \Big|_{R_b} = 4\pi (C_{\pi} r)^2 \frac{d\sigma}{dR_b} \left[1 + \frac{16\pi^2}{C_{\pi}^2} \sin^2 \theta \right] \Big|_{r=R_b}, \quad (4.54)$$

in the limit $R_b \rightarrow 0$, but one demands also that the equation

$$R_b \frac{d^2 g_A^{(a)}}{dR_b^2} \Big|_{R_b} = 24\pi 16\pi^2 \cos^2 \theta \Big|_{r=R_b}, \quad (4.55)$$

be satisfied in the limit $R_b \rightarrow 0$. This seems an unnecessarily strict requirement since insistence on equation (4.54) already removes any divergences in $\frac{d^2 g_A^{(a)}}{dR_b^2}$ for all values of κ^2 (Appendix 4C).

APPENDIX 4A THE EIGENVALUES AND EIGENFUNCTIONS FOR THE QUARK SPINOR
PAULI DIRAC EQUATION

In this appendix, the method used for obtaining the eigenvalues and eigenstates for the Dirac equation in a chiral bag

$$1 + \hat{\mu} \hat{\gamma}_3 \hat{\gamma} = 0, \quad (4A.1)$$

subject to the boundary condition

$$-(\hat{\gamma} \cdot \hat{r}) \psi = \exp(-i\hat{\gamma} \cdot \hat{r} \gamma_5) \psi, \quad (4A.2)$$

is utilized.

From the second equation one sees that the eigenstates have neither good spin \hat{S} nor good isospin \hat{T} , but rather good grand spin $\hat{J} = \hat{S} + \hat{T}$. In addition, the parity P is conserved by the boundary condition. One can therefore classify the eigenstates by the eigenvalues of the grand spin λ , its third component λ_3 and the quantum number $\kappa = P(-)^{\lambda}$.

One may therefore write the general solution to the time-independent Dirac equation as

$$\psi = \begin{Bmatrix} \chi_{\lambda, \lambda_3} \\ f_{\lambda, \lambda_3} \sigma \cdot \hat{r} \chi_{(\lambda, 2\lambda - \lambda_3)} \end{Bmatrix}, \quad (4A.3)$$

where χ and f denote the orbital and total angular momentum respectively. The corresponding radial equations [1280] are

$$M_{e,j} = -\frac{d^2 f_{e,j}}{dr^2} + \frac{k+1}{r} f_{e,j} \quad (4A.6)$$

$$N_{e,j} = \frac{d^2 f_{e,j}}{dr^2} + \frac{k+1}{r} f_{e,j}, \quad (4A.5)$$

where

$$k = \mp (j+1/2) \quad \text{for } j = 0, 1, 2, \dots \quad (4A.6)$$

and E denotes the energy. Eliminating $f_{e,j}$ from the above equations yields

$$\frac{d^2 \chi_{e,j}}{dr^2} + \frac{2}{r} \frac{d\chi_{e,j}}{dr} + \left[\epsilon^2 - \frac{2(k+1)}{r^2} \right] \chi_{e,j} = 0. \quad (4A.7)$$

This can then be recognized as the spherical Bessel equation with solution

$$\chi_{e,j} = J_e(kr), \quad (4A.8)$$

The lower component is then given by equation (4A.5) as

$$f_{e,j} = \left[\frac{d}{dr(kr)} + \frac{k+1}{kr} \right] J_e(kr). \quad (4A.9)$$

For given λ and m_λ there are thus four independent solutions to the Dirac equation:

$$\psi_1^{m_\lambda} = \psi_2^{m_\lambda} \begin{bmatrix} J_{j_\lambda} \left(\frac{1}{2} \lambda r \right) \lambda^{-\frac{1}{2}} \alpha_{m_\lambda} \\ -J_{j_{\lambda+1}} \left(\frac{1}{2} \lambda r \right) \lambda^{-\frac{1}{2}} \alpha_{m_\lambda} \end{bmatrix} \quad (4A.10)$$

$$\psi_3^{m_\lambda} = \psi_4^{m_\lambda} \begin{bmatrix} J_{j_\lambda} \left(\frac{1}{2} \lambda r \right) \lambda^{-\frac{1}{2}} \alpha_{m_\lambda} \\ J_{j_{\lambda-1}} \left(\frac{1}{2} \lambda r \right) \lambda^{-\frac{1}{2}} \alpha_{m_\lambda} \end{bmatrix}, \quad (4A.11)$$

both with $x = P(-)^{\lambda} = +1$, and

$$\psi_1^+ = N_1^{-1} \left[\begin{matrix} -\frac{1}{2} \lambda + 1 \\ \frac{1}{2} \lambda + 1 \end{matrix} \right] \lambda \frac{1}{2} \lambda m_{\lambda} \rangle \quad (4A.12)$$

$$\psi_2^+ = N_2^{-1} \left[\begin{matrix} -\frac{1}{2} \lambda - 1 \\ \frac{1}{2} \lambda - 1 \end{matrix} \right] \lambda \frac{1}{2} \lambda m_{\lambda} \rangle, \quad (4A.13)$$

both with $x = P(-)^{\lambda} = -1$.

Here N_1^{NR} and N_2^{NR} represent the normalization constants for a bag of radius R_0 and are given explicitly as

$$\langle \psi_1^{NR} | \psi_1^{NR} \rangle^2 = N_1^{-2} (J_{\lambda}^2(\alpha) + J_{\lambda+1}^2(\alpha) - 2 \frac{\alpha+1}{\alpha} J_{\lambda}(\alpha) J_{\lambda+1}(\alpha))^{-1} \quad (4A.14)$$

$$\langle \psi_2^{NR} | \psi_2^{NR} \rangle^2 = N_2^{-2} (J_{\lambda}^2(\alpha) + J_{\lambda-1}^2(\alpha) - 2 \frac{\alpha-1}{\alpha} J_{\lambda}(\alpha) J_{\lambda-1}(\alpha))^{-1}, \quad (4A.15)$$

where $\alpha = ER_0$.

To apply the boundary condition (4A.2) one needs to know the matrix element of $\sigma \cdot \hat{r}$ and $\hat{r} \cdot \sigma$ between the above states. These may be calculated using the standard techniques of rotation algebra [Ed76] and are specified by the following relations:

$$\sigma \cdot \hat{r} \left| \left(\frac{1}{2} \lambda \right) J \lambda m_{\lambda} \right\rangle = \left[\left(\frac{1}{2} \lambda \right) 2J - \lambda \right] \left| \left(\frac{1}{2} \lambda \right) J \lambda m_{\lambda} \right\rangle \quad (4A.16)$$

$$\hat{r} \cdot \sigma \left| \left(\frac{1}{2} \lambda \right) \lambda \frac{1}{2} \lambda m_{\lambda} \right\rangle = \frac{1}{2\lambda+1} \left[\left(\frac{1}{2} \lambda \right) \lambda \right] \lambda \frac{1}{2} \lambda m_{\lambda} \rangle$$

$$-\frac{1}{2\pi\sqrt{1-\lambda^2}} \operatorname{Re}(i\lambda^2) \left| \left(\frac{1}{2}\lambda\right) \lambda^{-\frac{1}{2}} \Lambda_n \right\rangle \quad (6A.17)$$

$$\begin{aligned} \nabla \cdot \nabla \left| \left(\frac{1}{2}\lambda\right) \Lambda_n \right\rangle \Lambda_n^{\frac{1}{2}} \Lambda_n \rangle &= \nabla \frac{1}{2\pi\sqrt{1-\lambda^2}} \left| \left(\frac{1}{2}\lambda\right) \lambda^{-\frac{1}{2}} \Lambda_n \right\rangle \\ &= -\frac{1}{2\pi\sqrt{1-\lambda^2}} \operatorname{Re}(i\lambda^2) \left| \left(\frac{1}{2}\lambda\right) \lambda^{-\frac{1}{2}} \Lambda_n \right\rangle . \end{aligned} \quad (6A.18)$$

When the solution is written in the form

$$\psi^{AK} = C_1 \psi_1^{AK} + C_2 \psi_2^{AK} , \quad (6A.19)$$

the boundary condition

$$-i \begin{bmatrix} 0 & \sigma \cdot \hat{r} \\ -\sigma \cdot \hat{r} & 0 \end{bmatrix} \psi^{AK} = \cos \theta \psi^{AK} - \sin \theta \begin{bmatrix} 0 & \nabla \cdot \nabla \\ \nabla \cdot \nabla & 0 \end{bmatrix} \psi^{AK} \quad (6A.20)$$

yields the following equation

$$\begin{aligned} C_1^{AK} \Lambda_n^{AK} \left\{ \left[J_n - \cos \theta J_{n+1} - \frac{\pi}{2\pi\sqrt{1-\lambda^2}} \sin \theta J_n \right] \left| \left(\frac{1}{2}\lambda\right) \lambda^{-\frac{1}{2}} \Lambda_n \right\rangle \right. \\ \left. - \frac{\operatorname{Re}(\lambda(\lambda+1))^{1/2}}{2\pi\lambda} \sin \theta J_n \left| \left(\frac{1}{2}\lambda\right) \lambda^{-\frac{1}{2}} \Lambda_n \right\rangle \right\} \\ + C_2^{AK} \Lambda_n^{AK} \left\{ \left[J_n + \cos \theta J_{n-1} + \frac{\pi}{2\pi\sqrt{1-\lambda^2}} \sin \theta J_n \right] \left| \left(\frac{1}{2}\lambda\right) \lambda^{-\frac{1}{2}} \Lambda_n \right\rangle \right. \\ \left. - \frac{\operatorname{Re}(\lambda(\lambda+1))^{1/2}}{2\pi\lambda} \sin \theta J_n \left| \left(\frac{1}{2}\lambda\right) \lambda^{-\frac{1}{2}} \Lambda_n \right\rangle \right\} = 0 . \end{aligned} \quad (6A.21)$$

For the sake of convenience the basis is now changed to the one given below:

$$\begin{aligned}
 \left| \lambda \left(\frac{\lambda-1}{2} \right) \right| \lambda m_\lambda > &= \left[\frac{\lambda+1}{2(\lambda+1)} \right]^{1/2} \left| \left(\frac{\lambda}{2} \right) \lambda + \frac{1}{2} \lambda m_\lambda \right> + \left[\frac{\lambda}{2(\lambda+1)} \right]^{1/2} \left| \left(\frac{\lambda}{2} \right) \lambda - \frac{1}{2} \lambda m_\lambda \right> \\
 \left| \lambda \left(\frac{\lambda+1}{2} \right) \right| \lambda m_\lambda &= \left[\frac{\lambda}{2(\lambda+1)} \right]^{1/2} \left| \left(\frac{\lambda}{2} \right) \lambda + \frac{1}{2} \lambda m_\lambda \right> - \left[\frac{\lambda+1}{2(\lambda+1)} \right]^{1/2} \left| \left(\frac{\lambda}{2} \right) \lambda - \frac{1}{2} \lambda m_\lambda \right> \\
 & \hspace{15em} (44.22) \\
 \left| \lambda + 1 \left(\frac{\lambda}{2} \right) \right| \lambda m_\lambda &> = - \left| \left(\frac{\lambda}{2} \right) \lambda + 1 \right| \lambda + \frac{1}{2} \lambda m_\lambda > \\
 \left| \lambda - 1 \left(\frac{\lambda}{2} \right) \right| \lambda m_\lambda &> = \left| \left(\frac{\lambda}{2} \right) \lambda - 1 \right| \lambda - \frac{1}{2} \lambda m_\lambda > .
 \end{aligned}$$

The above equations then become

$$\begin{aligned}
 & \left\{ \left[\frac{\lambda+1}{2(\lambda+1)} \right]^{1/2} \left[J_\lambda(1-\cos\theta) - \kappa J_{\lambda+1}(\cos\theta) \right] c_1^{\lambda\kappa} d_1^{\lambda\kappa} \right. \\
 & + \left. \left[\frac{\lambda}{2(\lambda+1)} \right]^{1/2} \left[J_\lambda(1+\cos\theta) + \kappa J_{\lambda-1}(\cos\theta) \right] c_2^{\lambda\kappa} d_2^{\lambda\kappa} \right\} \left| \lambda \left(\frac{\lambda}{2} \right) \right| \lambda m_\lambda > \\
 & + \left\{ \left[\frac{\lambda}{2(\lambda+1)} \right]^{1/2} \left[J_\lambda(1+\cos\theta) - \kappa J_{\lambda+1}(\cos\theta) \right] c_1^{\lambda\kappa} d_1^{\lambda\kappa} \right. \\
 & - \left. \left[\frac{\lambda+1}{2(\lambda+1)} \right]^{1/2} \left[J_\lambda(1-\cos\theta) + \kappa J_{\lambda-1}(\cos\theta) \right] c_2^{\lambda\kappa} d_2^{\lambda\kappa} \right\} \left| \lambda \left(\frac{\lambda}{2} \right) \right| \lambda m_\lambda > = 0 . \\
 & \hspace{15em} (44.23)
 \end{aligned}$$

Since the above is a form an orthonormal set with regard to angular integration, one obtains two simultaneous linear equations for $c_1^{\lambda\kappa}$ and $c_2^{\lambda\kappa}$, one of which is given by

$$\begin{aligned} & \left[\frac{\lambda}{2(\lambda+1)} \right]^{1/2} \left\{ J_{\lambda}(1+\epsilon \sin \theta) - \epsilon J_{\lambda+1} \cos \theta \right\} c_1^{\lambda} a_1^{\lambda} \\ & = \left[\frac{\lambda-1}{2(\lambda-1)} \right]^{1/2} \left\{ J_{\lambda}(1+\epsilon \sin \theta) + \epsilon J_{\lambda-1} \cos \theta \right\} c_2^{\lambda} a_2^{\lambda}, \end{aligned} \quad (4A.24)$$

or equivalently,

$$\frac{c_1^{\lambda}}{c_2^{\lambda}} = \frac{N^{\lambda}}{M^{\lambda}} \left[\frac{\lambda+1}{\lambda} \right]^{1/2} \left[\frac{J_{\lambda} \cos \theta - J_{\lambda-1} (\sin \theta - \epsilon)}{J_{\lambda} \cos \theta + J_{\lambda+1} (\sin \theta - \epsilon)} \right] = 0^{\lambda} \quad (4A.25)$$

The final state must be normalized within the bag, which implies that

$$c_1^{\lambda} a_1^{\lambda 2} + c_2^{\lambda} a_2^{\lambda 2} = 1, \quad (4A.26)$$

and finally, that

$$\psi^{\lambda} = \frac{c_1^{\lambda}}{(1+c_1^{\lambda})^{1/2}} \psi_1^{\lambda} + \frac{c_2^{\lambda}}{(1+c_2^{\lambda})^{1/2}} \psi_2^{\lambda} \quad (4A.27)$$

Solution of the set of simultaneous linear equations derived from (4A.25) is only possible if

$$\begin{aligned} & \left[\frac{\lambda+1}{2(\lambda+1)} \right]^{1/2} \left[J_{\lambda}(1-\epsilon \sin \theta) - \epsilon J_{\lambda+1} \cos \theta \right] - \left[\frac{\lambda}{2(\lambda+1)} \right]^{1/2} \left[J_{\lambda}(1-\epsilon \sin \theta) + \epsilon J_{\lambda-1} \cos \theta \right] \\ & \left[\frac{\lambda}{2(\lambda+1)} \right]^{1/2} \left[J_{\lambda}(1+\epsilon \sin \theta) - \epsilon J_{\lambda+1} \cos \theta \right] - \left[\frac{\lambda-1}{2(\lambda+1)} \right]^{1/2} \left[J_{\lambda}(1+\epsilon \sin \theta) + \epsilon J_{\lambda-1} \cos \theta \right] \\ & = 0, \end{aligned} \quad (4A.28)$$

which implies the eigenvalue equation

$$\cos \alpha \{ J_{k+1}(\alpha) J_{k-1}(\alpha) - J_k^2(\alpha) \} + \kappa J_k(\alpha) \{ J_{k+2}(\alpha) - J_{k-2}(\alpha) \} + \text{also } \frac{J_k^2(\alpha)}{\alpha} = 0. \quad (4A.28)$$

However, $\alpha = 0$ is an exception to the above discussion since only the state $\psi_1^{k\alpha}$ exists. For this case

$$\psi_1^{k\alpha} = \kappa \frac{\partial \kappa}{\partial \alpha} \psi_1^{k\alpha}, \quad (4A.29)$$

and the eigenvalue equation is given by

$$J_0(\alpha) \{ 1 - \cos \alpha \} - \kappa J_1(\alpha) \cos \alpha = 0, \quad (4A.31)$$

or equivalently,

$$\frac{J_1(\alpha_0)}{J_0(\alpha_0)} = \kappa \frac{1 - \cos \alpha}{\cos \alpha} = \frac{\kappa \sin \alpha}{1 + \cos \alpha}. \quad (4A.32)$$

The above formulae are identical to those derived in the work of Wentz and the (TRB4), except for the omission of a factor (- κ) in the formula for $J_0^{k\alpha}$. This is then cancelled by the appearance of an additional relative sign in the different definitions of $\psi_1^{k\alpha}$ and $\psi_0^{k\alpha}$.

APPENDIX 4B THE CALCULATION OF THE NORMAL COMPONENT OF THE AXIAL VECTOR CURRENT

(1) Quark sector

The Lagrange density is given by

$$\mathcal{L}_q = \frac{1}{2} \bar{\psi} \gamma_\mu \partial^\mu \psi. \quad (4B.1)$$

Under infinitesimal left and right transformations, specified by \bar{U}_L and \bar{U}_R respectively, the quark field transforms as

$$\psi \rightarrow \left[1 + \bar{U}_L \gamma \left[\frac{1+\gamma_5}{2} \right] + \bar{U}_R \gamma \left[\frac{1-\gamma_5}{2} \right] \right] \psi. \quad (4B.2)$$

The corresponding change in the Lagrange density is

$$\delta \mathcal{L}_q = -\bar{\psi} \gamma_\mu \partial_\nu \bar{U}_L \gamma \left[\frac{1-\gamma_5}{2} \right] \psi - \bar{\psi} \gamma_\mu \partial_\nu \bar{U}_R \gamma \left[\frac{1+\gamma_5}{2} \right] \psi + \dots \quad (4B.3)$$

The left- and right-handed currents are given by

$$j_\mu^L = -\frac{\delta \mathcal{L}_q}{\delta \partial_\mu \bar{U}_L} = \bar{\psi} \gamma_\mu \gamma \left[\frac{1-\gamma_5}{2} \right] \psi, \quad (4B.4)$$

and

$$j_\mu^R = -\frac{\delta \mathcal{L}_q}{\delta \partial_\mu \bar{U}_R} = \bar{\psi} \gamma_\mu \gamma \left[\frac{1+\gamma_5}{2} \right] \psi. \quad (4B.5)$$

The axial vector current is then given by

$$\begin{aligned} X_{\mu} &= \frac{1}{2} (\hat{p}_{\mu}^2 - \hat{p}_{\mu}^2) \\ &= \nabla_{\mu} \hat{r} \cdot \hat{r} \cdot \nabla_{\mu} \end{aligned} \quad (48.6)$$

with normal component

$$\hat{r} \cdot \nabla_{\mu} \hat{r} \cdot \hat{r} = \frac{1}{2} \nabla_{\mu} \hat{r} \cdot \hat{r} \cdot \nabla_{\mu} \hat{r} \cdot \hat{r} \end{aligned} \quad (48.7)$$

For any quark state, ψ_{μ} , this can then be expressed in terms of the derivative of the energy using the argument given below.

Consider the scalar

$$\hat{r} \cdot \nabla_{\mu} \exp(-i\hat{p} \cdot \hat{r} \cdot \nabla_{\mu}) \psi_{\mu} \Big|_{\text{rot } \hat{r}} \end{aligned} \quad (48.8)$$

Then its partial derivative is given by

$$\begin{aligned} \frac{\partial}{\partial \hat{r}} \left[\hat{r} \cdot \nabla_{\mu} \exp(-i\hat{p} \cdot \hat{r} \cdot \nabla_{\mu}) \psi_{\mu} \right] \Big|_{\text{rot } \hat{r}} \\ = -i \hat{p} \cdot \hat{r} \cdot \nabla_{\mu} \exp(-i\hat{p} \cdot \hat{r} \cdot \nabla_{\mu}) \psi_{\mu} \Big|_{\text{rot } \hat{r}} \end{aligned} \quad (48.9)$$

Using the boundary condition

$$-i \hat{p} \cdot \hat{r} \cdot \nabla_{\mu} = \exp(-i\hat{p} \cdot \hat{r} \cdot \nabla_{\mu}) \psi_{\mu} \end{aligned} \quad (48.10)$$

the above expression becomes

$$\nabla_n \nabla \cdot \hat{r} \times \nabla_B \nabla \cdot \hat{r} \times \nabla_n \Big|_{r=0} \quad (48.11)$$

which is simply twice the normal component of the axial vector current (48.7). The integral of (48.8) over the bag surface is

$$\int d^3x \nabla_n \exp(-i\hat{r} \cdot \hat{r} \times \nabla_B) \nabla_n \quad (48.12)$$

which, again using (48.10), becomes

$$-i \int d^3x \hat{r} \cdot \nabla_n \nabla \nabla_n \quad (48.13)$$

Using Stokes's theorem, this becomes

$$-i \int_{\partial V} d^2x \hat{x} \cdot \nabla_n \nabla \nabla_n \quad (48.14)$$

which can be reduced, using the Dirac equation,

$$-i \nabla \cdot \nabla \nabla_n = F_n^{\alpha\beta} \gamma^{\alpha\beta} \nabla_n \quad (48.15)$$

so

$$2i \int_{\partial V} d^2x \nabla_n^{\alpha\beta} \nabla_n = 2\mathcal{M}_n \quad (48.16)$$

Combining (48.8) and (48.16) yields

$$\frac{d\mathcal{M}_n}{dt} = \frac{1}{2} \int d^3x \nabla_n \nabla \cdot \hat{r} \times \nabla_B \nabla \cdot \hat{r} \times \nabla_n \quad (48.17)$$

or in its final form

$$\begin{aligned} \bar{K}_\mu &= \frac{1}{4} e^2 \text{Tr}(\bar{\psi}(0, \mathbf{0}_\mu \psi^T)) \\ &= -e^2 (\hat{c}^2 \mathbf{0}_\mu \rho + \sin^2 \theta (\hat{c} \mathbf{0}_\mu \rho^2)) . \end{aligned} \quad (48.26)$$

with normal component

$$\partial_\mu^2 \bar{K}_\mu^1 = e^2 \frac{\partial \rho}{\partial t} . \quad (48.26)$$

(b) Interaction terms

(1) Model with pions only

$$\bar{K}_{\pi-\pi} = \frac{1}{4} e^2 \text{Tr}((a_\mu U) U^\dagger, (a_\nu U) U^\dagger)^2 \quad (48.27)$$

Under transformation

$$\begin{aligned} \bar{K}_{\pi-\pi} &= 16e^2 (a_\mu \bar{U}_\mu \cdot \text{Tr}[\partial^\mu U_\nu U^\dagger a_\nu U_\mu U^\dagger + \nabla U_\mu U^\dagger a_\nu U_\mu U^\dagger \\ &+ U_\mu U^\dagger a_\nu U^\dagger]) + a_\mu \bar{U}_\mu \cdot \text{Tr}[\partial^\mu U^\dagger a_\nu U_\mu U^\dagger a_\nu U + \nabla U^\dagger a_\nu U_\mu U^\dagger \\ &a_\nu U + \nabla U^\dagger a_\nu U_\mu U^\dagger a_\nu U]) . \end{aligned} \quad (48.28)$$

As before, the normal component of the axial vector current may be calculated as

$$\partial_\mu^2 \bar{K}_\mu^1 = 16e^2 \frac{\sin^2 \theta}{\rho^2} \frac{d\rho}{dt} . \quad (48.29)$$

In total therefore, for the model with pions only,

$$\hat{C}_{\alpha}^{-1} \hat{C}_{\alpha}^{-1} = r_{\alpha}^2 \frac{d\alpha}{dt} + 10\alpha^2 \frac{\sin^2 \alpha}{r^2} \frac{d\alpha}{dt}. \quad (48.30)$$

(11) Omega masses

$$\hat{C}_{\omega\omega} = \Delta \omega^2. \quad (48.31)$$

where

$$\Delta = \frac{1}{24r^2} \epsilon^{ijkl} \text{Tr}(U^i_{\alpha} U^j_{\beta} U^k_{\gamma} U^l_{\delta}). \quad (48.32)$$

Then

$$\begin{aligned} \Delta \hat{C}_{\omega\omega} &= -\frac{10\alpha}{24r^2} \epsilon^{ijkl} \text{Tr}(\partial_{\mu} U^i_{\alpha} \partial^{\mu} U^j_{\beta} \partial_{\nu} U^k_{\gamma} \partial^{\nu} U^l_{\delta}) \\ &- \frac{10\alpha}{24r^2} \epsilon^{ijkl} \text{Tr}(\partial_{\mu} U^i_{\alpha} \partial^{\mu} U^j_{\beta} \partial_{\nu} U^k_{\gamma} \partial^{\nu} U^l_{\delta}) + \dots \end{aligned} \quad (48.33)$$

from which one obtains

$$\hat{C}_{\omega} = \frac{10\alpha}{10r^2} \epsilon^{ijkl} \text{Tr}(\partial_{\mu} U^i_{\alpha} \partial^{\mu} U^j_{\beta} U^k_{\gamma} U^l_{\delta}). \quad (48.34)$$

with normal component

$$\hat{C}_{\alpha}^{-1} \hat{C}_{\alpha}^{-1} = \frac{10\alpha}{24r^2} \frac{\sin^2 \alpha}{r^2}. \quad (48.35)$$

In total therefore, for the model stabilized by omega masses,

$$\hat{C}_{\alpha}^{-1} \hat{C}_{\alpha}^{-1} = r_{\alpha}^2 \frac{d\alpha}{dt} + \frac{10\alpha}{24r^2} \frac{\sin^2 \alpha}{r^2}. \quad (48.36)$$

APPENDIX 4C THE CALCULATION OF THE VACUUM EXPECTATION VALUES

Given an arbitrary single-particle operator \hat{O} , the vacuum expectation value of the operator $[\mathcal{F}, \hat{O} \mathcal{F}]$ is given formally as

$$O_v(\epsilon) = -\frac{1}{\epsilon} \lim_{\epsilon \rightarrow 0} \sum_n \text{sign}(\epsilon_n) \epsilon_n e^{-(\epsilon \epsilon_n)^2} = \lim_{\epsilon \rightarrow 0} O_v(\epsilon, \epsilon), \quad (40.1)$$

where $O_v(\epsilon, \epsilon)$ has been defined as

$$O_v(\epsilon, \epsilon) = -\frac{1}{\epsilon} \sum_n \text{sign}(\epsilon_n) \epsilon_n e^{-(\epsilon \epsilon_n)^2}, \quad (40.2)$$

and ϵ denotes $\epsilon(R_n)$. The sum here runs over all eigenstates ϵ_n with eigenvalues in units of R_b , $\epsilon_n = \epsilon_n R_b$, and ϵ_n denotes

$$\epsilon_n = \mathcal{F}_n \hat{O} \mathcal{F}_n. \quad (40.3)$$

This definition proves perfectly adequate for the calculation of the baryon number given as

$$B_v = -\frac{1}{\epsilon} \lim_{\epsilon \rightarrow 0} \sum_n \text{sign}(\epsilon_n) \epsilon_n e^{-(\epsilon \epsilon_n)^2}, \quad (40.4)$$

and the baryon density given as

$$K_b^0(\tau) = -\frac{1}{2} \lim_{\eta \rightarrow 0} \sum_n \alpha \operatorname{sgn}(\alpha_n) v_n^4 \tau_n^{-1} e^{-i\alpha_n \tau} \quad (40.5)$$

In the present work, the related quantity, to be referred to as the dimensionless baryon density in a spherical shell,

$$B_b^0\left(\frac{r}{b}, \sigma\right) = -\frac{1}{2} K_b^0\left(\frac{r}{b}\right)^2 \lim_{\eta \rightarrow 0} \sum_n \alpha \operatorname{sgn}(\alpha_n) \left[\int_0^{\sigma} \alpha v_n^4 \tau_n^{-1} e^{-i\alpha_n \tau} d\tau \right] \quad (40.6)$$

has been calculated.

For both these cases one can calculate the values of $B_b^0(r, \sigma)$ and $B_b^0(r, \sigma)$ for a range of values of σ , in the present work $\sigma = 0.1$ to 0.2 in increments of 0.01 . These values can then be fitted as polynomials in σ , for example

$$B_b^0(r, \sigma) = \sum_{p=0}^n a_p \sigma^p \quad (40.7)$$

and the limit $\eta = 0$ that takes, that is $B_b^0(\sigma) = a_0$. As expected, the relation

$$B_b^0(\sigma) = -\frac{1}{2} \left[\sigma - \frac{1}{2} \sin 2\sigma \right] \quad 0 \leq \sigma \leq \pi/2 \quad (40.8)$$

$$B_b^0(\sigma) = 1 - \frac{1}{2} \left[\pi - \frac{1}{2} \sin 2\sigma \right] \quad \pi/2 < \sigma \leq \pi$$

is fulfilled to five significant figures. The values for $B_b^0(\sigma) = B_b^0(r, \sigma)$, ($\frac{\pi}{2} < \sigma \leq \pi$), needed to specify baryon density continuity, are displayed in figure 40.1.

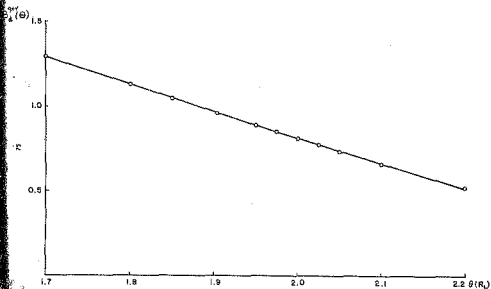


Figure 40.1 The dimensionless baryon density in a spherical shell at the bag surface, $\rho_2^{(b)}(\theta)$, as a function of the chiral angle at the bag radius $\theta(R_0)$.

Given the function $H_n^2(y, \epsilon)$, one can calculate the isoscalar radius for the nucleus

$$\langle r^2 \rangle_n^{I=0} = \frac{1}{R_0} \int_0^{R_0} dr r^2 \rho_n^2 \left(\frac{r}{R_0}, \epsilon \right). \quad (60.8)$$

Alternatively, this radius can be given as

$$\langle r^2 \rangle_n^{I=0} = -\frac{1}{2} \lim_{\eta \rightarrow 0} \sum_n a_j \rho_n(\eta_0) \langle r^2 \rangle_n^{I=0} e^{-\langle \rho_n \rangle^2}, \quad (60.10)$$

where

$$\langle r^2 \rangle_n^{I=0} = \langle r^2 \rangle_{\lambda\lambda}^{I=0} = \langle \rho_{\lambda-1}^2 \rangle_{\lambda-1}^2 \langle r_{\lambda-1}^2 \rangle_{\lambda-1}^2 + \langle \rho_{\lambda}^2 \rangle_{\lambda}^2 \langle r_{\lambda}^2 \rangle_{\lambda}^2 \quad (60.11)$$

and

$$r_{\lambda\lambda}^2 = \int_0^{R_0} dr r^4 \rho_{\lambda\lambda}^2(r). \quad (60.12)$$

This integral can be given analytically [Wat44] as

$$\begin{aligned} r_{\lambda\lambda}^2 &= \frac{1}{8} \frac{R_0^6}{\alpha^2} \left[(\alpha^2 + \lambda^2 + \lambda + \frac{1}{2}) J_{\lambda}^2(\alpha) + \alpha J_{\lambda}(\alpha) (J_{\lambda+1}(\alpha) - J_{\lambda-1}(\alpha)) \right. \\ &\quad \left. + \frac{1}{4} \alpha^2 (J_{\lambda+1}^2(\alpha) + J_{\lambda-1}^2(\alpha)) - (2\lambda^2 + 2\lambda - \frac{3}{2} + \frac{1}{2} \alpha^2) J_{\lambda+1}(\alpha) J_{\lambda-1}(\alpha) \right]. \end{aligned} \quad (60.13)$$

As stated before, $\langle r^2 \rangle_n^{I=0}$ can then be calculated in two independent ways corresponding to the interchange of the integral $\int_0^{R_0} dr$ and the limit $\lim_{\eta \rightarrow 0} \sum_n$. Again, there is numerical agreement to five significant figures.

Turning to the Casimir energy, one should note that the symmetry relations for the quark energy eigenvalues are reflected as symmetries of the vacuum Casimir energy, that is

$$\alpha_V(-\epsilon) = \alpha_V(\epsilon) , \quad (40.14)$$

and

$$\alpha_V(\pi+\epsilon) = \alpha_V(\epsilon) . \quad (40.15)$$

One need therefore only calculate $\alpha_V(\epsilon)$ for $0 \leq \epsilon \leq \pi/2$ since values outside this range can be given by the symmetry relations above.

Unfortunately however, in the corresponding definition for the Casimir energy,

$$\alpha_V(\epsilon) = \lim_{\sigma \rightarrow 0} \alpha_V(\epsilon, \sigma) = -\frac{1}{2} \lim_{\sigma \rightarrow 0} \sum_n \text{sign}(\epsilon_n) \epsilon_n e^{-\sigma \epsilon_n^2} , \quad (40.16)$$

the limit $\sigma \rightarrow 0$ is infinite.

Looking at the case $\epsilon(\epsilon_n) = 0$, corresponding to the MIT bag, one notes that

$$\alpha_V(0) = \lim_{\sigma \rightarrow 0} \alpha_V(0, \sigma) \quad (40.17)$$

is not only non-zero but infinite. Since one would like the hybrid model to approach the MIT bag model as $\epsilon_n \rightarrow \epsilon(\epsilon_n) \rightarrow 0$, one might guess that an appropriate definition might be

$$a_v(\theta) = \lim_{\eta \rightarrow 0} [a_v(\theta, \eta) - a_v(0, \eta)] . \quad (40.18)$$

Unfortunately, this limit also proves to be logarithmically divergent.

At this stage the Stony Brook group [VJ96] suggested that the model should reduce to the pure Skyrme model as $R_0 \rightarrow 0$. This corresponds to the limit $\epsilon(R_0) \rightarrow \pi$. Since $a_v(\pi-\theta) = a_v(\theta)$, one can consider the related limit $\epsilon(R_0) \rightarrow 0$. Since $a_v(\epsilon) = a_v(-\epsilon)$, one can write the expansion for small ϵ as an even polynomial in ϵ , namely

$$a_v(\theta) = a_1 + a_2 \epsilon^2 + a_3 \epsilon^4 . \quad (40.19)$$

Using the subtraction given in equation (40.18), one has ensured that $a_v(0) = 0$, which in turn implies that $a_1 = 0$. Looking at the second term in the RHS of equation (4.21), one observes that

$$\frac{d}{d\theta} \left. \frac{R_0}{\epsilon^2} \right|_{\epsilon=R_0} \sim 16 \epsilon^2 \sin^2 \theta \quad (40.20)$$

is proportional to

$$(\pi-\theta) \sin^2 \theta \quad (40.21)$$

in the limit $R_0 \rightarrow 0$.

If one requires (4.21) to be satisfied in the limit $R_0 \rightarrow 0$, one therefore requires that

$$a_2 = 0 , \quad \text{that is} \quad \left. \frac{d^2 R_0}{d\theta^2} \right|_{\epsilon=0} = 0 . \quad (40.22)$$

which can be satisfied if one takes [VGB6]

$$a_\nu(s) = \lim_{\eta \rightarrow 0} \left[a_\nu(s, \eta) - a_\nu(0, \eta) - \frac{1}{2} \sin^2 \eta \frac{d^2 a_\nu}{ds^2}(s, \eta) \Big|_{s=0} \right]. \quad (40.23)$$

This limit can be obtained in much the same way as that for the baryon number and baryon density, except that the values of η used for extrapolation must be smaller because the divergences prove more severe [VGB6]. This automatically increases the number of algorithms needed in the sum before convergence occurs for each value of η . In the present work the fit obtained by Veiztes et al [VGB6] has been used, namely

$$a_\nu(s) = \frac{3}{25} \left[s^2 + \sum_{n=1}^4 f_n \sin^2(ns) \right], \quad (40.24)$$

with $f_1 = -0.80382$, $f_2 = -0.063823$, $f_3 = 0.9036196$ and $f_4 = -2.73814$.

The constraint $\frac{d^2 a_\nu}{ds^2} = 0$ implies that

$$\sum_{n=1}^4 n^2 f_n = -1. \quad (40.25)$$

Here

$$\sum_{n=1}^4 n^2 f_n = -1 + .5 \times 10^{-6}. \quad (40.26)$$

One should note that this renormalization procedure is also appropriate for the omega stabilized case since

$$dv \left(\frac{v}{c} \right)^2 \frac{d}{dt} \sin^2 \theta \quad (40.27)$$

is also proportional to

$$(v-s)\sin^2 \theta \quad (40.28)$$

in the limit $v_0 \rightarrow 0$.

The derivative of the Ginzburg energy is then given as

$$\frac{dG}{d\theta} = \frac{3}{2\pi} \left[2s + \sum_{n=1}^4 n^2 \sin(2n\theta) \right] \quad 0 \leq \theta \leq \pi/2, \quad (40.29)$$

with $f_1 = -0.80392$, $f_2 = -0.06822$, $f_3 = 0.0125196$ and $f_4 = -2.73 \times 10^{-4}$.

Outside this range the symmetry relation gives

$$\left. \frac{dG}{d\theta} \right|_{\theta} = - \left. \frac{dG}{d\theta} \right|_{\theta=\pi-\theta} \quad \pi/2 \leq \theta \leq \pi. \quad (40.30)$$

In order to reduce the order of the mode sums required to evaluate $G_0(\theta)$ to a more manageable number, an alternative means of calculating these renormalized quantities has been suggested by Whit et al [W4306]. Turning again to the original unregularized sum for the Ginzburg energy

$$- \frac{1}{2} \sum \text{sign}(n_s) n_s, \quad (40.31)$$

one observes that it can be written in integral form as

$$-\frac{1}{2} \sum_n \alpha_n g(\alpha_n) \int_{-\infty}^{\infty} dx \delta(x - \alpha_n) . \quad (40.32)$$

The integral will then be identical if one replaces $\delta(x - \alpha_n)$ by

$$g(x, \alpha_n) = \frac{1}{\pi \nu} \exp[-(x - \alpha_n)^2 / \nu^2] , \quad (40.33)$$

where ν must be determined. Interchanging the order of summation and integration yields

$$\int_{-\infty}^{\infty} dx \rho_\nu(x, t) , \quad (40.34)$$

where

$$\rho_\nu(x, t) = -\frac{1}{2} \sum_n \alpha_n g(\alpha_n) g(x, \alpha_n) . \quad (40.35)$$

As before, this must be renormalized to obtain

$$Q_\nu(x, t) = \rho_\nu(x, t) - \rho_\nu(x, 0) - \frac{1}{2} \alpha_0 \nu^2 \left. \frac{\partial^2 \rho_\nu}{\partial x^2} \right|_{x=0} . \quad (40.36)$$

Finally therefore,

$$Q_\nu(t) = \int_{-\infty}^{\infty} dx Q_\nu(x, t) . \quad (40.37)$$

The choice $\nu = 2.5$ suggested by Met et al [WJ82] was used in the present work, and the integral range was restricted to $[-\alpha_0, \alpha_0]$, where α_0 can be

selected so that better than 1% agreement with the previous values is obtained.

Turning to the baryon number, one observes that

$$B_V(\rho) = \int_{-\infty}^{\infty} dx \rho_V(x), \quad (40.38)$$

or equivalently,

$$B_V(\rho) = \int_{-\infty}^{\infty} dx \rho_p(x), \quad (40.39)$$

since

$$\rho_p(x, 0) = -\rho_n(-x, 0), \quad (40.40)$$

and

$$\left. \frac{d^2 \rho_V}{dx^2}(x, 0) \right|_{x=0} = - \left. \frac{d^2 \rho_p}{dx^2}(-x, 0) \right|_{x=0}. \quad (40.41)$$

Similarly, the modified baryon number density is given by

$$B_V^0(x, \rho) = \int_{-\infty}^{\infty} dx \rho_V^0(x, \rho), \quad (40.42)$$

where

$$\rho_V^0(x, \rho) = -\frac{1}{2} \frac{\rho^2}{\rho_0^2} \sum_p \text{sign}(p_n) \int dx \tau_n^1 \tau_n \rho^{-\frac{1}{2}(x-\tau_n)^2 / \tau_n^2}, \quad (40.43)$$

The values calculated in this manner can be compared with those previously obtained, and they agree to within 1% (see Table 40.1).

Table 4C.1

The dimensionless baryon density in a spherical shell at the bag radius calculated using two alternative reconstruction methods.

$\bar{\rho}_b$	$s(\bar{\rho}_b)$	$\bar{\rho}_d^{[a]}(1, \bar{\rho})$	$\bar{\rho}_d^{[b]}(1, \bar{\rho})$	% difference
0.325	2.00269	0.8095	0.8071	0.07
0.375	1.80603	0.8911	0.9012	0.81
0.425	1.78220	1.1504	1.1628	0.95

[a] calculated using a polynomial fit in ρ to $\bar{\rho}_d(\eta, 1, \bar{\rho})$ [WJ04, GW70, b, c]

[b] calculated in the present work using the density restoring factor method of WJ01, Vogstad and Jaudon [WJ05]

The can also be compared with the results with the approximate fit of Vogstad et al (see Table 4C.2) [WJ05]. The integral of the baryon density, which should give the baryon number, is also given.

Table 4C.2

The total baryon number and the dimensionless baryon density in a spherical shell at the bag radius.

$\bar{\rho}_b$	$s(\bar{\rho}_b)$	$\bar{\rho}_d^{[b]}(1)$	$\bar{\rho}_d^{[c]}(1)$	% diff	$\bar{\rho}_d^{[a]}$ TOT	$\bar{\rho}_d^{[b]}$ TOT	% error	$\bar{\rho}_d^{[c]}$ TOT	% error
0.325	2.00269	0.807	0.797	?	0.24104	0.24128	0.00	0.23430	?
0.375	1.80603	0.891	0.828	6	0.30534	0.30652	0.40	0.29518	6
0.425	1.78220	1.150	1.121	3	0.36720	0.36749	0.04	0.35004	3

[a] exact result

[b] calculated in the present work [QW70, b and c]

[c] calculated using the fit of L. Vogstad et al [WJ05]

The isoscalar radius for both calculations is given in Table 40.3. One notes here that the results obtained for the isoscalar radius in the present work agree with those of Vepstein et al [K85] and not with those of Heller et al [K83B].

Table 40.3

The vacuum isoscalar radius for several values of R_0 .

R_0	$\theta(R_0)$	$\langle r \rangle_{\text{is}}^{[b]} \text{ fm}^{-1}$	$\langle r \rangle_{\text{is}}^{[a]} \text{ fm}^{-1}$	$\kappa \text{ fm}^{-1}$
0.325	2.60359	0.015836	0.015836	7
0.375	1.80683	0.026133	0.026133	5
0.425	1.75228	0.038822	0.038822	3

(b) calculated in the present work (M87a, b and c)

(a) calculated using the fit of L. Vepstein et al [K85]

Similarly, one can construct the magnetic moment and the magnetic moment density. Here the magnetic moment is given by

$$\mu_p(\kappa) = \int_{-1}^1 dx M_p(x, \theta) \quad (40.44)$$

where $M_p(x, \theta)$ is the renormalized density

$$M_p(x, \theta) = n_p(x, \theta) - \frac{1}{2} \sin^2 \theta \frac{d^2 n_p(x, \theta)}{dx^2} \Big|_{\theta=0} \quad (40.45)$$

$$(n_p(x, \theta) = 0) \quad (40.46)$$

and

$$n_p(x, \theta) = -\frac{1}{2} \sum_n \text{sign}(a_n) n_p^n(x, \theta) \quad (40.47)$$

where

$$m_0 = \frac{1}{2} \int_{V_0} d^3r \bar{\Psi}_0(\mathbf{r}, \mathbf{0}) \frac{\gamma_0}{2} \Psi_0. \quad (40.48)$$

The expression for density is identical, save that m_0 is replaced by the density

$$m_0(\mathbf{r}) = \frac{1}{2} \bar{\Psi}_0(\mathbf{r}, \mathbf{0}) \frac{\gamma_0}{2} \Psi_0. \quad (40.49)$$

Turning to the calculation of the axial vector current density, one observes that twice its integral is given by

$$\int d^3r a_\nu(\mathbf{r}) = \frac{2}{3} \frac{\partial \eta_\nu}{\partial t}. \quad (40.50)$$

The renormalization procedure for the density therefore should be that adopted for $\frac{\partial \eta_\nu}{\partial t}$. Since

$$a_\nu(\theta) = \lim_{\eta \rightarrow 0} \left[a_\nu(\theta, \eta) - a_\nu(0, \eta) - \frac{1}{2} \sin^2 \theta \frac{d^2 a_\nu}{d\theta^2} \Big|_{\theta=0} \right], \quad (40.51)$$

we may write

$$\frac{\partial a_\nu}{\partial t} = \lim_{\eta \rightarrow 0} \left[\frac{d}{dt} a_\nu(\theta, \eta) - \frac{1}{2} \sin 2\theta \frac{d^2 a_\nu}{d\theta^2} \Big|_{\theta=0} \right]. \quad (40.52)$$

Interchanging the sum and the differentiation yields

$$\frac{d}{dt} a_\nu(\theta, \eta) = -\frac{1}{2} \sum_n \sin(n\theta) \frac{dn}{dt} = -(\eta \dot{\eta})^2 + \eta^2 \dots \quad (40.53)$$

$$\frac{d^2 n_x}{dt^2}(\theta, \theta) = -\frac{1}{2} \frac{d}{dt} \sum_n \text{sign}(n_x) \frac{dn_x}{dt} \frac{-\langle n_x \rangle^2}{c} - \theta^2 \dots \quad (40.54)$$

Finally therefore,

$$\frac{dn_x}{dt} = \lim_{\theta \rightarrow 0} \left[\frac{dn_x}{dt}(\theta, 0) - \frac{1}{2} \sin 2\theta \frac{d^2 n_x}{dt^2}(\theta, \theta) \right]_{\theta=0} \quad (40.55)$$

where

$$\frac{dn_x}{dt}(\theta, \theta) = -\frac{1}{2} \sum_n \text{sign}(n_x) \frac{dn_x}{dt} \frac{-\langle n_x \rangle^2}{c} \quad (40.56)$$

Introducing the smeared direction as before yields

$$\frac{dn_x}{dt} = \int dx \alpha'_x(s, \theta) \quad (40.57)$$

where

$$\alpha'_x(s, \theta) = \alpha'_x(s, \theta) - \frac{1}{2} \sin 2\theta \frac{d\alpha'_x}{ds}(s, \theta) \Big|_{s=0} \quad (40.58)$$

and

$$\alpha'_x(s, \theta) = -\frac{1}{2} \sum_n \text{sign}(n_x) \frac{dn_x}{dt} g(s, n_x) \quad (40.59)$$

The identical formulae apply to the axial vector current density, but with $\alpha'_x(s, \theta)$ replaced by

$$\alpha'_y(s, \theta, r) = -\frac{1}{2} \sum_n \text{sign}(n_x) \alpha'_y(r) g(s, n_x) \quad (40.60)$$

where $\mathbf{a}_v(r)$ is twice the axial vector current density given as

$$\mathbf{a}_v(r) = \frac{1}{2} \nabla_{\perp}^2 \mathbf{r} + \delta_{\perp}^2 \mathbf{r}. \quad (40.61)$$

As a check on the numerical coding, the integral $\int d^3r \mathbf{a}_v(r)$ can be calculated and compared with the formula $\frac{2}{3} \frac{dR_v}{dt}$, which can be calculated using the results of Vepstas et al [V3004]. The results are displayed in Table 40.4 where it is seen that there is agreement to within 1%.

Table 40.4

The integral of twice the axial vector current density, compared with the value $\frac{2}{3} \frac{dR_v}{dt}$.

R_b	$\theta(R_b)$	$\int d^3r \mathbf{a}_v(r) [a]$	$\frac{2}{3} \frac{dR_v}{dt} [b]$	% diff
0.325	2.60320	-0.28235	-0.28231	0.6
0.375	1.88663	-0.34281	-0.34148	0.4
0.425	1.70229	-0.23618	-0.23458	0.6

[a] calculated in the present work using the method of Miat, Vepstas and Jackson [WJ385]

[b] calculated from the fit of Vepstas, Jackson and Goldhaber [V3004]

There are two supporting pieces of evidence for the renormalization scheme adopted here for $R_v(t)$. The first is the agreement between the results of the work of Vepstas et al [V3004] and those of Miat et al [WJ386]. The second is a recent calculation by Jackson and Miao [JM88] in which they assumed the strict Oshirore cut picture. There σ_A and α^2 can be assumed to be independent of R_b . The values of $\frac{dR_v}{dt}$ then calculated from axial vector continuity agree with those of Vepstas et al [V3004] at the 10% level.

5. THE HYBRID CHIRAL SOLITON MODEL WITH PIONS AND OMEGA MESONS

In the nuclear-nucleon interaction it is well known that the omega meson is responsible for short-range repulsion. It is therefore appealing to replace the stabilizing fourth order Skyrme term by a coupling term coupling the baryon density to the omega field. This was first proposed by Adkins and Kaplan [AK84], with a resulting improvement in the static nucleon and Δ properties. It is, however, incorrect to associate the new field $w(r)$, introduced in that work, with the physical omega meson field [Sis87]. Since the field $w(r)$ is the zeroth component of the field w_μ , the kinetic energy terms appear with the opposite sign to those for the physical meson. This field should rather be regarded simply as an auxiliary field that stabilizes the soliton [AK84]. In fact, the field $w(r)$ can be eliminated from the equations of motion by re-expressing it in terms of the chiral angle. Thus, in the limit $m_\omega \rightarrow \infty$, $\frac{d}{dt} = \frac{d}{dr}$ fields, where β and m_ω represent the omega coupling constant and mass respectively, the model reduces to that of Jackson et al [JJG85]. This model involves pions only, but with a sixth order stabilizing term $\frac{1}{8} \text{Tr}[R_\mu R^\mu]$, where R^μ is the baryon current, this being the lowest order term, after the fourth order term, with the correct symmetries [JJG85].

The first reason to introduce omega stabilization in the hybrid model is to determine whether one obtains, as in the case of the pure Skyrme, an improvement in the static properties. Secondly, and far more importantly, one has now introduced an additional degree of freedom, namely one can now select $w'(R_\mu)$ such that baryon density continuity is satisfied [GM97a]. This freedom, which is not present in the pure Skyrme model ($w'(C)$ must be zero if the equations are to remain non-singular) gives rise to a new and different structure, the calculational details and results of which are

outlined in the successive sections.

5.1 The Lagrange density

In the Skyrme sector the Lagrange density is given as the sum of three terms (A004b) namely

$$\mathcal{L} = \mathcal{L}_\pi + \mathcal{L}_\omega + \mathcal{L}_{\omega-\pi\pi}, \quad (5.1)$$

where \mathcal{L}_π is the pion Lagrange density

$$\mathcal{L}_\pi = \frac{1}{4} f_\pi^2 (\partial_\mu U^\dagger \partial^\mu U) + \frac{1}{2} f_\pi^2 \frac{m_\pi^2}{m_\pi^2} \tau \cdot \tau (U-1), \quad (5.2)$$

with the pion decay constant $f_\pi = 93$ MeV and the pion mass $m_\pi = 138$ MeV, \mathcal{L}_ω is the omega meson Lagrange density

$$\mathcal{L}_\omega = -\frac{1}{4} (\partial_\mu \omega_\nu - \partial_\nu \omega_\mu) (\partial^\mu \omega^\nu - \partial^\nu \omega^\mu) + \frac{1}{2} m_\omega^2 \omega_\mu \omega^\mu, \quad (5.3)$$

with the omega mass $m_\omega = 782.4$ MeV and $\mathcal{L}_{\omega-\pi\pi}$ is the interaction term describing the decay ($\omega \rightarrow \pi\pi$)

$$\mathcal{L}_{\omega-\pi\pi} = A \omega_\mu \pi^\mu \pi^\nu. \quad (5.4)$$

In the quark sector one again has the free Dirac Lagrange density

$$\mathcal{L}_q = \frac{1}{2} \bar{\psi} \gamma_\mu \partial^\mu \psi. \quad (5.5)$$

5.2 The equations of motion

Since $\Omega^1 = 0$, there is no source term for u_1 and therefore u_1 is assumed to

be zero for all r (ANSatz). Thus one may write

$$\psi^{\mu} = (u, 0) \quad (5.6)$$

If, in addition, one assumes the hedgehog ansatz, then the equations of motion are simply the Euler-Lagrange equations for the above density.

In the meson sector these equations are

$$s'' + \frac{2s'}{r} - \frac{\sin 2\theta}{r^2} - \kappa_0^2 \sin \theta + \frac{\rho}{2\pi^2 f_\pi^2} \frac{\sin^2 \theta}{r^2} u' = 0 \quad r \geq R_0 \quad (5.7)$$

$$u'' + \frac{2u'}{r} - \kappa_0^2 u + \frac{\rho}{2\pi^2} \frac{\sin^2 \theta}{r^2} s' = 0.$$

After introduction of the dimensionless variables

$$z = \kappa_0 r, \quad \tilde{u} = \frac{u}{f_\pi} \quad \text{and} \quad \tilde{\theta} = \frac{\rho \kappa_0}{2\pi^2 f_\pi} \theta, \quad (5.8)$$

the above equations become

$$\tilde{\theta}'' + \frac{2}{z} \tilde{\theta}' - \frac{\sin 2\tilde{\theta}}{z^2} - \left(\frac{z}{R_0}\right)^2 \sin \tilde{\theta} + \tilde{\theta} \frac{\sin^2 \tilde{\theta}}{z^2} \tilde{u}' = 0 \quad z \geq \kappa_0 R_0 \quad (5.9)$$

$$\tilde{u}'' + \frac{2}{z} \tilde{u}' - \tilde{u} + \tilde{\theta} \frac{\sin^2 \tilde{\theta}}{z^2} \tilde{\theta}' = 0.$$

In the quark sector one has the Dirac equation

$$i\gamma_\mu \partial^\mu \psi = 0 \quad r \leq R_0 \quad (5.10)$$

5.3 The boundary conditions

The chiral boundary condition is given by

$$-i\vec{\gamma}\cdot\vec{r} = \exp(-i\vec{\gamma}\cdot\vec{r}_0)\gamma \quad r = R_0, \quad (5.11)$$

which guarantees conservation of the baryon current, continuity of the axial vector current is given by

$$N_c \frac{d\vec{q}_0^{3+3}}{dt} = 4\pi \left[\frac{f_\pi}{R_0} t \right]^2 \left[\frac{d\vec{u}}{dt} + \vec{N} \frac{\sin^2 \vec{u}}{r} \vec{u} \right] \quad t = R_0 R_b, \quad (5.12)$$

where the form for the meson sector is derived in Appendix 4D, and the continuity of the baryon density is given by

$$q_0^{3+3}(s(R_b)) = -\frac{3}{N} t \sin^2 \vec{u} \frac{d\vec{u}}{dt} \quad t = R_0 R_b. \quad (5.13)$$

In both cases the contribution from the quark sector is identical to that calculated in the hybrid model with pions only.

For finite energy solutions one also requires

$$s(\infty) = 0 \quad (5.14)$$

and

$$\vec{u}(\infty) = 0.$$

For the meson fields one now observes that one has four boundary conditions

for the two second order differential equations. Thus, for any chosen value of β , or equivalently $\bar{\beta}$, there is a unique solution.

5.4 Details of the numerical solution

The long-range behavior of the meson fields can be derived from their equation of motion (XI.64). This yields

$$\phi(r) = \frac{G_0}{m_\pi r} \left[1 + \frac{1}{m_\pi r} \right] \quad r \rightarrow \infty \quad (5.16)$$

$$\omega(r) = \frac{D^2 a}{(m_\pi r)^2} \quad r \rightarrow \infty,$$

or in dimensionless units,

$$\phi(r) = \frac{G_0}{m_\pi r} \left[1 + \frac{1}{m_\pi r} \right] \quad r \rightarrow \infty \quad (5.15)$$

$$\bar{\omega} = \frac{D_0}{(m_\pi r)^2} \quad r \rightarrow \infty,$$

$$a_\pi = \frac{m_\pi}{m_\rho}.$$

As stated above, given $\bar{\beta}$, ϕ and $\bar{\omega}$ are completely specified, and therefore so must be G and D . Alternatively, if one chooses G , then $\bar{\beta}$ and D are uniquely determined. In the present work the results are presented as a function of G rather than of $\bar{\beta}$, because G is related to $g_{\pi NN}^2$, the pion-nucleon coupling constant.

for the two second order differential equations. Thus, for any chosen value of β , or equivalently $\bar{\beta}$, there is a unique solution.

5.4 Details of the numerical solution

The long-range behaviour of the meson fields can be derived from their equation of motion [1186]. This yields

$$\begin{aligned} \phi(r) &= \frac{G_0}{\mu_\pi^2} \left[1 + \frac{1}{\mu_\pi^2 r} \right] \quad r \rightarrow \infty \\ \psi(r) &= \frac{3^2 a}{(\mu_\pi^2)^2} \frac{-2\mu_\pi^2 r}{r^2} \quad r \rightarrow \infty, \end{aligned} \quad (5.16)$$

or in dimensionless units,

$$\begin{aligned} \phi(r) &= \frac{G_0}{\mu_\pi^2} \left[1 + \frac{1}{\mu_\pi^2 r} \right] \quad r \rightarrow \infty \\ \psi(r) &= \frac{3^2 a}{(\mu_\pi^2)^2} \frac{-2\mu_\pi^2 r}{r^2} \quad r \rightarrow \infty, \\ \mu_\pi &= \frac{m_\pi}{\hbar}. \end{aligned} \quad (5.16)$$

As stated above, given \bar{M} , a and \bar{G} are completely specified, and therefore so must be G and θ . Alternatively, if one chooses G , then $\bar{\beta}$ and \bar{E} are uniquely determined. In the present work the results are presented as a function of G rather than of $\bar{\beta}$, because G is related to $g_{\pi NN}^2$, the pion-nucleon coupling constant.

Given the asymptotic form

$$s(r) = \frac{G_0 \kappa^2 r^2}{4\pi} \left(1 + \frac{1}{\kappa^2 r^2} \right), \quad (5.17)$$

one can, as for massless pions (section 3.3), deduce the asymptotic form of the pion field for the nucleus as

$$\phi_{\pi} = \frac{1}{r} \kappa_{\pi} \frac{G_0 \kappa^2 r^2}{4\pi} 2(\vec{\sigma} \cdot \vec{r}) \mathcal{Y}. \quad (5.18)$$

Again, the factor κ_{π} arises because of the conversion from baryons to nucleon states and is known to be $-G_0/5$, as before. Comparing this with the form deduced from classical pion theory (3.18)

$$\phi_{\pi} = -\frac{G_0 \kappa^2 r^2}{4\pi} \kappa_{\pi} \frac{\kappa^2 r^2}{r} 2(\vec{\sigma} \cdot \vec{r}) \mathcal{Y}, \quad (5.19)$$

one obtains

$$\kappa_{\pi} = \frac{1}{5} \kappa \left[\frac{G_0}{4\pi} \right] \left[\frac{G_0}{4\pi} \right]^{-1}. \quad (5.20)$$

For the numerical solution for a given value of G_0 , β and $\bar{\beta}$ were determined using a method due to Kluwe and Kluwe (1964). One simply integrates in from large t , where the fields are given by equation (5.16), and minimizes the function

$$\left[\frac{d}{dt} \left(\frac{1}{t} \frac{d}{dt} \right) \right]^2 + \left[\frac{d}{dt} \left(\frac{1}{t} \frac{d}{dt} \right) \right]^2 \left[\frac{d}{dt} + \beta \frac{d}{dt} \right]^2 \quad (5.21)$$

to find its zero as a function of β and $\bar{\beta}$.

The energy in the mean sector is then given as

$$\begin{aligned}
 E_m &= - \int_{R_0}^{R_1} \gamma \rho_0 \, r \, dr \\
 &= \frac{2\pi r^2}{\gamma \rho_0} \int_{R_0}^{R_1} dr \, r^2 \left[\frac{1}{2} \dot{\theta}^2 + \frac{2\pi \sin^2 \theta}{r^2} + 2 \left(\frac{R_0}{r} \right)^2 (1 - \cos \theta) \right. \\
 &\quad \left. - \frac{1}{2} \dot{\theta}^2 - \frac{1}{2} \dot{\theta}^2 + 2\pi \frac{\sin^2 \theta}{r^2} \right]. \quad (5.28)
 \end{aligned}$$

To this must be added the energy in the spark sector

$$E_{\text{spark}} = 2\pi \theta \left(\frac{R_0}{2} - s(R_0) \right) + 2\pi \rho_0 (s(R_0)) / R_0, \quad (5.29)$$

where $s(R_0)$ is given by equation (4.42).

In figures 5.1 and 5.2 the values of \bar{F} and the total energy E are respectively displayed as a function of R_0 for different values of C . The behaviour of E as a function of R_0 and C is particularly interesting, showing a bifurcation point. No independent physical interpretation has been given to this bifurcation diagram. Within the confines of the model one however makes the physically reasonable assumption that the energy be stable and slowly varying as a function of R_0 , restricting one to the curves in sector IV. If one simply searches for the minimal energy subject to this proviso, one obtains an accurate and unique prediction for C , namely its value just below the bifurcation point $C = 0.194$. The corresponding value of R_{min} from equation (5.28) is

$$R_{\text{min}} = 12.4. \quad (5.34)$$

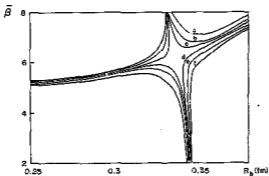


Figure 5.1 The coupling constant, $\bar{\beta}$ as a function of C , the asymptotic constant, and R_b , the bag radius. The letters a to e denote $C = 0.1025, 0.194, 0.19435, 0.1949, 0.19475$ and 0.195 respectively

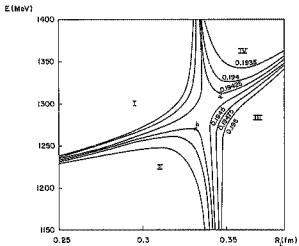


Figure 5.2 The energy E (MeV) as a function of C , the asymptotic constant, and R_0 , the bag radius

This is in remarkable agreement with the experimental value of $\epsilon_{\text{NOM}} = 13.5$. Intriguingly, the Goldberger-Treiman relation applied to $\epsilon_{\text{NOM}} = 12.4$ predicts $g_A = 1.23$, which is even closer to its experimental value. This result is particularly satisfying in view of the fact that there are no free parameters in the model [GMS7a].

One should notice that in the above prediction, the physical nucleon mass, $M_N = 938.9$ MeV, has been used and not the energy of the hybrid chiral soliton. This has been done for three principal reasons. The first and most important is that one should then reproduce the Goldberger-Treiman relation for the case of massless pions. Secondly, one notes that the energy of the hybrid chiral soliton does not represent the nucleon mass since no projection has been performed, and in fact, it must be regarded as an average nucleon-delta mass [HW7]. Thirdly, this energy is expected to be too large because of the inclusion of spurious centre of mass excitation energy.

Turning to the values of other observables predicted near the bifurcation point and summarized in Table 5.1, one sees reasonable overall agreement with experiment. As expected, the energy is somewhat higher than the average nucleon-delta mass. Using the estimate of $\frac{1}{3}$ of the bag energy, [TW82] the centre-of-mass effects contribute approximately 100 MeV or $\frac{1}{3}$ of this discrepancy. The isoscalar radius is again too small, but the inclusion of the correction factor of $(5/n_0^2)$ [AM84b], discussed in Chapter 4, yields $\langle r^2 \rangle_{\text{Isg}}^{1/2} = 0.73$ fm which is in far better agreement with experiment. If one assumes β to take on its experimental value, one sees that its predicted value is 36% too high. Since β has been regarded as a free parameter in the same manner as λ^2 , this discrepancy is not considered to be overly important. The bag radius corresponding to this bifurcation point is $R_b = 0.33$ fm. This is very similar to the values used in the original chiral bag [S79] and has been more recently used in chiral bags [D88].

Table 8.1

The static nucleon properties for the present model [QMSVa,c] compared with their experimental values

Observable	Experimental value	Prediction
E_{NMS}	13.8	12.9
$\frac{1}{2}(M_{\text{N}} + M_{\text{P}})$ (MeV)	1006	1294
β	11	15
$\langle r_{\text{ch}}^2 \rangle^{1/2}$ (fm)	0.72	0.68

One should note that the values above have been obtained by averaging over the minima and maxima on either side of the critical value. The curves for s and \bar{u} as a function of the radial variable r are practically identical and are displayed in figures 5.3 and 5.4 respectively. The baryon density, which is particularly relevant in this model, is displayed in figures 5.8 and 5.5. One notes that although it is continuous (by construction), it is not differentiable. Such remaining discontinuities induced by the bag radius will prove important in the calculation of the form factors.

5.5 Comparison with other models

As in the case of the hybrid model with pions only, the basic differences between the models lie in the σ -sector of the free parameters. In the present work these free parameters may be chosen as \bar{Y} , the coupling constant, G , the asymptotic constant of the pion field; or equivalently $g_{\text{NN}\pi}$, the pion-nucleon coupling constant; and $w^2(R_0)$.

In the present work two boundary conditions have been enforced, namely axial vector current continuity and baryon density continuity, given as

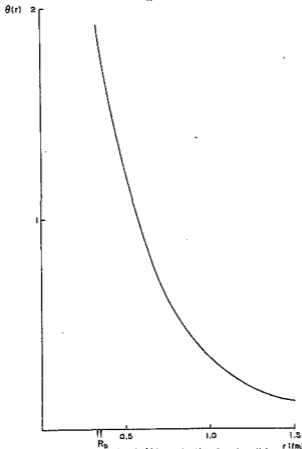


Figure 5.2 The orbital angle $\theta(r)$ as a function of r , the radial variable, for two points close to the bifurcation point (see Figure 5.1)

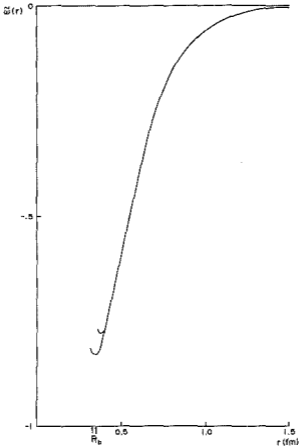


Figure 5.4 The Omega field, $\Omega(r)$, as a function of the radial variable r for two points close to the bifurcation value (see Figure 5.2)

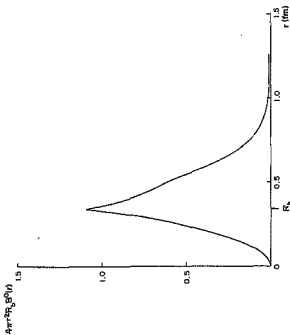


Figure 5.2 The product $4\pi r^2 \rho_0 S^2(r)$ of the beryllium density in a spherical shell with the bag radius R_0 , for the point (a) close to the bifurcation point (see Figure 5.2)

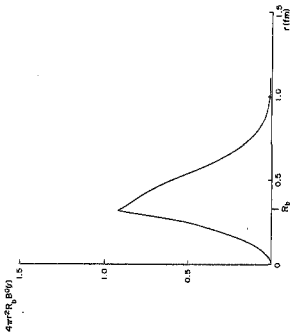


Figure 5.6 The product $4\pi r^2 R_b \rho^0(r)$ of the baryon density in a spherical shell with the bag radius R_b , for the point (b) close to the bifurcation point (see Figure 5.2)

$$D_0^{3/2}(\psi(R_b)) = -\frac{2}{W} \epsilon \sin^2 \theta \left. \frac{d\psi}{dR} \right|_{R=R_b} \quad (6.26)$$

Therefore, as stated previously, for any given value of C and R_b the model is uniquely specified. In line with previous work with pions only [CMM76], the conditions appear to be not only physically meaningful but to give reasonable numerical results.

In contrast, in the model of Hildner and Brown [HBB] the boundary condition on the baryon density has been replaced by the constraint

$$w'(R_b) = 0. \quad (6.28)$$

This condition has in fact been obtained from a Lagrange density of the form

$$W \exp(-i\vec{r} \cdot \vec{\sigma}) \delta_{\mu\nu} \quad (6.27)$$

where δ_{μ} is the surface delta function. Minimizing the Lagrangian with respect to the w field then yields equation (6.28). If, however, one enforces baryon density continuity, and applies a naive minimization argument one selects the minima in the energy surface (Fig. 5.2) which do not in general correspond to $w'(R_b) = 0$. Indeed, even if the minima did represent points at which $w'(R_b)$ equaled zero, they could readily be shifted by including a bag energy of the form $\frac{4\pi}{3} R_b^3$. For this reason, and given the physical motivation for baryon density continuity, the boundary condition (6.28) has not been applied in the present work.

In addition, in the work of Hildner and Brown [HBB], β has been fitted to

the experimental α coupling constant. In the present work this has not been done because, as has been argued, the omega field represents an auxiliary field and not the physical mass. As such, β merely represents the coefficient of a stabilizing term. As in the case of ϵ^2 , the coefficient of the fourth order term in the model with pions only, β has been treated as a free parameter.

Unlike the pure Skyrmeon, neither of these hybrid models is straightforwardly related to a sixth order model with pions only, even in the limit $m_\omega \rightarrow \infty$, $\frac{m_\omega}{m_\pi}$ fixed. As can be seen, the solution for the pure Skyrmeon

$$u(r) = \int_0^r dr' G(r, r') \{-2\epsilon^2 \frac{d^2}{dr'^2} u(r')\},$$

where

$$G(r, r') = (2m_\omega r r')^{-1} \{\exp(-m_\omega |r-r'|) - \exp(-m_\omega (r+r'))\}.$$

Incorporates the knowledge of both the boundary conditions $u'(0) = 0$ and $u(\infty) = 0$ [ANMMS]. As such, any sixth order model that might be constructed for the hybrid model is in principle expected to depend on, and be different for, each value of H_0 and $u'(R_0)$. Nonetheless, one can select the coefficient of the sixth order term ϵ_0^2 roughly to reproduce the omega stabilized model of Kluber and Brown [K185]. In the present work, however, such a simple comparison is not expected since, unlike the work of Kluber and Brown, β the coupling constant (and therefore most probably ϵ_0^2) is a function of H_0 , the bag radius for any given value of G .

6. NUCLEON FORM FACTORS

In the previous chapters it has been shown that hybrid models produce good results for the nucleon static properties. This is not surprising, given the good results for the Skyrme model, since these properties are mainly determined by the pion tail. At higher values of q^2 , the square of the momentum transferred, one expects the quark bag, giving the short range behavior, to play an increasingly important role. Indeed one then expects an improvement over the results for the pure Skyrme model, simply because the quark core incorporates the idea of asymptotic freedom. For this reason the form factors for hybrid chiral solitons are calculated here for the first time.

Only three form factors are calculated in this chapter. These are the isoscalar charge, the isovector magnetic and the axial vector form factors, which are non-zero for the quark core in a hedgehog state. The reasons for this are twofold. Firstly, their true values in a nucleon state are expected to be proportional to their values in the hedgehog state. Despite the fact that the constant of proportionality depends on the projection scheme used, the ratio $F(q^2)/F(0)$ should be independent for any form factor $F(q^2)$. Secondly, the present work has centered on the improvement of the hedgehog state, rather than the details of projection.

Nonetheless, in the next section a brief discussion of projection is presented. There it is shown that one can quantify the relations of the hybrid chiral soliton [Pae83] in the same manner as one quantifies the relations of the pure Skyrme [JMW83]. If one, however, then takes the

limit $R_0 \rightarrow \infty$, the resulting isovector magnetic moment $\mu_{2\omega 1}$ and axial vector coupling constant g_A' will then be shown to differ from those of the MIT bag, with weakly interacting pions by a factor of $\frac{5}{3}$. This will then be discussed in light of the work of Tokyo group [IN97,MY98].

Nonetheless, for reasons to be given, the spin and isospin projection method for the MIT bag has been taken as a guide in present work. As such, the results for g_A and $\mu_{2\omega 1}$ obtained for the quark core and Skyrmin tail differ by a global factor of $\frac{5}{3}$ from the respective results of Pausler [Pau85] and Adkins, Nappi and Witten [ANW83].

In sections 6.2 the form factors are formally defined while the calculational details for the skyrmin tail and the quark core are given in sections 6.3 and 6.4 respectively. Numerical results including a comparison with the dipole fit are presented in section 6.5.

6.1 The projection of the hybrid chiral soliton

The projection method of V Pausler [Pau85] for the hybrid chiral soliton is presented below. Let the total hedgehog state be denoted by

$$|h\rangle = |h_q\rangle \times |h_\omega\rangle, \quad (6.1)$$

where $|h_q\rangle$ denotes the quark bag hedgehog and $|h_\omega\rangle$ the hedgehog Skyrmin. Then

$$(T + \frac{1}{2})|h\rangle = 0, \quad (6.2)$$

but $|A\rangle$ has neither good spin nor isospin. If

$$|A\rangle = |A_s\rangle \times |A_i\rangle \quad (5.3)$$

denotes the state rotated from $|h\rangle$ through Euler angles A , one can construct a state of good spin and isospin as

$$|h\rangle = \int [dA] \hat{q}_a(A) |A\rangle, \quad (5.4)$$

where a denotes the spin and isospin quantum numbers and $\hat{q}_a(A)$ are the wave functions given explicitly in equation (2.51).

Thus any matrix element of the form $\langle \alpha | \hat{O}_q | \beta \rangle$ where \hat{O}_q is a quark operator and α and β are projected states involves a factor $\langle A | A' \rangle = \delta(A-A')$. It is this factor, entirely produced by the exterior pion field, that is responsible for the difference between the result for the chiral bag in the limit $\epsilon(\hat{S}_q) = 0$ and those for the MIT bag model.

Turning to the explicit case of the isovector magnetic moment one can verify that

$$\langle \alpha | \mu_{z=1} | \beta \rangle = I_q^{2n+2} \int [dA] \hat{q}_a^{\alpha}(A) \hat{q}_b^{\beta}(A) \left(-\frac{2}{3} \text{Tr}(G^2 A^{-1} \tau^3 A) \right), \quad (5.5)$$

where I_q^{2n+2} is the expectation value in the unprojected hadronic state

$$I_q^{2n+2} = \langle \alpha | \int_{V_q} d^3x \left[-\frac{1}{18} \sum_r^3 \epsilon^r \epsilon^r \right] | h \rangle_q. \quad (5.6)$$

but $|\lambda\rangle$ has neither good spin nor isospin. If

$$|\lambda\rangle = |\lambda_s\rangle \times |\lambda_n\rangle \quad (6.3)$$

denote the state rotated from $|\lambda\rangle$ through Euler angles A , one can construct a state of good spin and isospin as

$$|a\rangle = \int [dA] \phi_a(A) |a\rangle, \quad (6.4)$$

where a denotes the spin and isospin quantum numbers and $\phi_a(A)$ are the wave functions given explicitly in equation (2.11).

Then any matrix element of the form $\langle a | O_q | \beta \rangle$ where O_q is a quark operator and a and β are projected states involves a factor $\langle A | A' \rangle_a = \langle A, A' \rangle$. It is this factor, entirely produced by the exterior pion field, that is responsible for the difference between the result for the chiral bag in the limit $\epsilon(\mu_q) = 0$ and those for the MIT bag model.

Turning to the explicit case of the isovector magnetic moment one can verify that

$$\langle a | \mu_{z=1} | \beta \rangle = \frac{1}{q} \int [dA] \phi_a^*(A) \phi_\beta(A) \left(-\frac{3}{2} \text{Tr}(\tau^3 A^{-1} \tau^3 A) \right), \quad (6.5)$$

where $\int_q^{I=1}$ is the expectation value in the unproj. ... nucleon state

$$\int_q^{I=1} = \langle a | \int [dA] d^3x \left(-\frac{1}{16} \text{Tr} \dot{A}^2 + \bar{\psi} \not{D} \psi \right) | \beta \rangle_q. \quad (6.6)$$

For spin and isospin $\frac{1}{2}$ states one knows that

$$\int [d\lambda] \hat{q}_a^T(\lambda) \hat{q}_b(\lambda) (-\frac{i}{2} \text{Tr}(\tau^3 \lambda^{-1} \lambda)) = \langle \alpha | \sigma^3 \alpha \rangle | \beta \rangle. \quad (8.7)$$

Thus the quark isovector magnetic moment becomes

$$\mu_{I=1} = \frac{N_c}{3} \frac{1}{\alpha} \quad (8.8)$$

In contrast, the MIT bag, for which $s(N_c) = 0$, yields

$$\mu_{I=1} = \frac{N_c + 2}{3} \frac{1}{\alpha} \quad (8.9)$$

Defining g_A^2 by the relation

$$\frac{3}{2} \langle \alpha | A_3^{I=1}(0) | \beta \rangle = g_A^2 \langle \alpha | \sigma^3 \frac{1}{2} | \beta \rangle, \quad (8.10)$$

with

$$A_3^{I=1}(0) = \int_{V_0} d^3x \bar{\psi} \tau^3 \frac{\partial}{\partial x^3} \psi(r), \quad (8.11)$$

and proceeding as for the isovector magnetic moment, one calculates

$$g_A^2 = -\frac{1}{\alpha} \langle \alpha | \int_{V_0} d^3x \bar{\psi}(r) \tau^3 \gamma_3 \psi(r) | \beta \rangle. \quad (8.12)$$

Comparing this, in the limit $s(N_c) \rightarrow 0$, with the result derived from the MIT bag model, one obtains

$$g_A^2 = \frac{3}{2} \frac{N_c}{N_c^2 - 2} g_A^{\text{NIT}}, \quad (6.13)$$

where the factor $\frac{3}{2}$ arises from axial vector current conservation.

In both cases therefore one sees the expected relative factor of $\frac{5}{3}$ which is a direct result of the different projection methods applied to the hadrons [7a,8]. As such, the same correction factors should be applied to the meson and quark sector.

This proposition can be further supported by the recent work of the Tokyo group [8a,8b,8c] in which the projection method used is the generator coordinate method (GCM). If $\vec{\pi}$ denotes the quantized pion field, and \vec{P} its canonically conjugate momenta, then the pion hadronic state is given as a coherent GCM state

$$|h_q\rangle = \exp(i\vec{P} \cdot \int d^3x \vec{r}_q \cdot \vec{\pi}(x)) |0\rangle.$$

One can recover the classical hadronic field using the relation

$$\vec{P}_c = \vec{r} \cdot \vec{P}(r) = G_q(\vec{r}) |h_q\rangle.$$

States of good spin and isospin can be constructed as

$$|(L, S, M, I)\rangle = \int d(\alpha) d(\beta) d(\gamma) d(\delta) |L, S, M, I\rangle |h_q\rangle |h_q\rangle.$$

where g is an element of $SO(3)$ and $R(g)$ is the rotational operator in isospin space. If one then calculates the axial vector constant g_A , one can draw the following conclusions. Firstly, as $R_D \rightarrow 0$, one does not recover the results from a Skyrme projection, but secondly, as $R_D \rightarrow \infty$, one does recover the results from the MIT bag projection. Furthermore, their results indicate that for radii about 0.3 fm, the factor $\frac{5}{3}$ does not differ much from the true correction factor.

Unfortunately to obtain these results two approximations had to be introduced [HST7]. The first involves the replacement of the vacuum by an anti-soliton, and the second is the smoothing of θ the chiral angle at the bag radius. Until total clarity is reached, the factor $\frac{5}{3}$ is assumed in the present work. This is certainly the most reasonable choice, given the results of the present calculations.

Furthermore, such correction factors to chiral bag models are not new [Ver82]. Its inclusion is also essential to give simultaneously the correct value of g_A and a reasonable estimate for the soliton mass M_B , in the original description of the nucleon as a pure Skyrme soliton [J82].

6.2 Definition of the nucleon form factors [J82, Lee81]

The electric and magnetic form factors are defined in terms of the electromagnetic current operator between nucleon states. Firstly, one can consider the related problem of the electromagnetic current $J_\mu(x)$ of a free Dirac theory for a single particle with initial and final momenta p and p' and initial and final polarizations ϵ and ϵ' . Then

$$\langle p', p | J^\mu(x) | p \rangle = e^{-i(p-p')x} \langle p', p | J^\mu(0) | p \rangle, \quad (6.14)$$

where

$$J^\mu(0) = \bar{\psi}(0) \gamma^\mu \psi(0),$$

which can be expanded as

$$J^\mu(0) = \int d^3k_1 d^3k_2 \sum_{\tau, \sigma} \bar{u}^\tau(k_1) \gamma^\mu u^\sigma(k_2) b_1^\dagger(k_1) b_2(k_2) + \dots, \quad (6.15)$$

From this it follows that

$$\langle p', p | J^\mu(0) | p \rangle = \bar{u}^\tau(p') \gamma^\mu u^\sigma(p), \quad (6.16)$$

which is the standard expression for the Dirac single particle current.

More generally, the nucleon single-particle electromagnetic current with initial and final states as before, is given by

$$\langle p', p | J^\mu(x) | p \rangle = e^{-i(p-p')x} \bar{u}^\tau(p') \gamma^\mu u^\sigma(p) U^\tau_\sigma(p), \quad (6.17)$$

From Lorentz covariance one predicts

$$U(A) U^\tau(p', p) U(A) = (A^{-1})^\tau_\sigma U^\sigma(p', p), \quad (6.18)$$

where A is an arbitrary element of the Lorentz group, $SO(3,1)$, while from hermiticity one derives

$$\sqrt{0} \psi^{\mu}(p', p) \gamma^0 = \psi^{\mu}(p', p). \quad (6.19)$$

Requiring invariance under parity transformations yields

$$\langle p', \beta | \mathcal{J}^{\mu}(x) | \alpha \rangle = \langle \bar{p}', \beta | \mathcal{J}^{\mu}(\bar{x}) | \bar{\alpha} \rangle, \quad (6.20)$$

where $\bar{x}^{\mu} = x_{\mu}$ and $\bar{p}^{\mu} = p_{\mu}$.

Combining equations (6.18) to (6.20), one obtains the most general form for the current as

$$\mathcal{J}^{\mu}(p') \mathcal{O}^{\mu}(p', p) u^{\mu}(p) = \mathcal{J}^{\mu}(p') \{ \gamma^{\mu} \gamma_1(\alpha^2) + \frac{(p^{\mu} - p^{\mu})}{2M_N} F_2(\alpha^2) + \frac{(p^{\mu} - p^{\mu})}{2M_N} F_3(\alpha^2) \}, \quad (6.21)$$

where M_N denotes the nucleon mass. One can then use the Dirac equation to make the substitution

$$\mathcal{J}^{\mu}(p', p) \rightarrow \frac{\gamma^{\mu} \gamma_1 \alpha_1}{2M_N} \mathcal{J}^{\mu}(p', p) \frac{\gamma^{\mu} \gamma_2 \alpha_2}{2M_N}, \quad (6.22)$$

and more specifically the substitution

$$\mathcal{J}^{\mu} = \frac{1}{2M_N} \{ (p'+p)^{\mu} + i\sigma^{\mu\nu}(p'-p)_{\nu} \}. \quad (6.23)$$

This then yields the equivalent form

$$\mathcal{J}^{\mu}(p') \mathcal{O}^{\mu}(p', p) u^{\mu}(p) = \mathcal{J}^{\mu}(p') \{ \gamma^{\mu} \gamma_1(\alpha^2) + \frac{i\sigma^{\mu\nu} \gamma_2}{2M_N} F_2(\alpha^2) + \frac{\gamma_2}{2M_N} F_3(\alpha^2) \} u^{\mu}(p), \quad (6.24)$$

where q_μ denotes the transferred momentum $q_\mu = p'_\mu - p_\mu$ and q^2 is the invariant scalar

$$q^2 = (p' - p)^2. \quad (8.25)$$

If one now imposes current conservation, that is

$$0 = \langle p' | \partial_\mu j^\mu(x) | p \rangle = i(p' - p)_\mu \langle p' | j^\mu(x) | p \rangle, \quad (8.26)$$

which implies that

$$(p' - p)_\mu \mathcal{G}^\mu(p', p) = 0 \quad \text{or} \quad F_3(q^2) = 0, \quad (8.27)$$

one obtains the final form as

$$\mathcal{G}^\mu(p') \mathcal{G}^\nu(p', p) \mathcal{U}^\mu(p) = \mathcal{V}^\mu(p') \{ \gamma^\nu F_1(q^2) + \frac{i\sigma^{\mu\nu} q_\lambda}{2M} F_2(q^2) \} \mathcal{U}^\nu(p). \quad (8.28)$$

It proves convenient to introduce the nucleon electric and magnetic form factors

$$G_E = F_1 + \frac{q^2}{4M^2} F_2 \quad (8.29)$$

and

$$G_M = F_1 + F_2. \quad (8.30)$$

These have been selected so that the $q^2 \rightarrow 0$ limit of the charge form factor yields the charge and that of the magnetic form factor yields the magnetic moment. Thus

$$G_{\mu}^{\nu}(0) = 1, \quad G_{\mu}^{\mu}(0) = 0, \quad (5.31)$$

and

$$\frac{\partial}{\partial K} G_{\mu}^{\nu}(0) = 2.79, \quad \frac{\partial}{\partial K} G_{\mu}^{\mu}(0) = -1.81. \quad (5.32)$$

In terms of the above form factors, (5.17) becomes

$$\begin{aligned} & \langle p' s_3 | J^{\mu}(0) | p s_3 \rangle \\ &= \bar{u}(p', s_3) \left[\frac{G_{\mu}^{\nu} + G_{\mu}^{\lambda}}{2M} \gamma^{\nu} + \frac{G_{\mu}^{\nu} - G_{\mu}^{\lambda}}{2M} \frac{1}{2M} \sigma^{\nu\lambda} \gamma^{\mu} \right] u(p, s_3), \end{aligned}$$

where

$$r = \frac{q^2}{4M^2}. \quad (5.33)$$

Here the polarizations α and β have been replaced by the spin quantum numbers s_3 and s_3' appropriate to nucleon states.To calculate the above matrix element one moves to the Breit frame where $\vec{p}' = -\vec{p} = \vec{q}/2$, $q_0 = 0$ in which

$$\langle p' s_3 | J^0(0) | p s_3 \rangle = G_0(-q^2) \langle s_3 | s_3 \rangle, \quad (5.34)$$

and

$$\langle p' s_3 | J^1(0) | p s_3 \rangle = -\frac{i}{2M} G_1(-q^2) \epsilon^{123} \langle s_3 | \sigma^3 | s_3 \rangle. \quad (5.35)$$

Concentrating now on the axial vector form factors one sees that they are defined by the matrix elements of the charged current between a neutron state $|n\rangle$ and a proton state $|p\rangle$. Again, one imposes the conditions (5.18) to (5.20), and one can write the most general form (5.25) as

$$\langle p | \frac{1}{2} [A_1^0(0) + iA_2^0(0)] | n \rangle = \bar{u}(p', n_2) \left[g_A \gamma^0 + \frac{1}{2M_N} g_p \gamma^0 + (p_\mu \gamma^\mu) g_N \right] \gamma_5 u(p, n_1) \quad (8.36)$$

If, in addition, one assumes isospin symmetry, that is the neutron and proton have identical masses, then $g_N = G$. Finally therefore,

$$\langle p | \frac{1}{2} [A_1^0(0) + iA_2^0(0)] | n \rangle = \bar{u}(p', n_2) \left[g_A \gamma^0 + \frac{1}{2M_N} g_p \gamma^0 \right] \gamma_5 u(p, n_1) \quad (8.37)$$

For the case of massless pions the axial vector current is conserved, and one derives

$$q_\lambda (q^2) + \frac{q^2}{2M_N} g_p (q^2) = 0.$$

If one now works in the Breit frame and takes the non-relativistic limit $q^2 \ll 4M_N^2$ the matrix element now becomes

$$\langle p | \frac{1}{2} [A_1^0(0) + iA_2^0(0)] | n \rangle = 0 \quad (8.38)$$

$$\langle p | \frac{1}{2} [A_1^3(0) + iA_2^3(0)] | n \rangle = \left[g_A (-q^2) \delta^{3j} - \frac{1}{2M_N} g_p (-q^2) \gamma^j \gamma^0 \right] \langle n_2 | n^j | n_1 \rangle \quad (8.39)$$

For the case of a conserved axial vector current the second expression becomes

$$\langle p | \frac{1}{2} [A_1^3(0) + iA_2^3(0)] | n \rangle = g_A (-q^2) \left[\delta^{3j} - \frac{q^j q^0}{q^2} \right] \langle n_2 | n^j | n_1 \rangle \quad (8.40)$$

This completes the definition of the form factors, and one can now proceed to calculate them for both the Skyrme ball and the chiral quark bag.

6.3 The nucleon form factors for the Skyrme ball (BYNET)

Here the calculations are based on the work of Brooker et al [BYNET] for the pure Skyrme, the principal difference lying in the fact that the expressions will be integrated only outside the bag radius R_0 . The calculations detailed above are correct to leading order in $\frac{1}{R_0}$. In the present work, the same finite M_0 corrections are applied in the meson sector as in the quark sector. In particular, the expressions for the axial form factor and the isovector magnetic form factors are multiplied by the factor $\frac{M_0 + 2}{M_0}$. That this procedure is indeed consistent is demonstrated in section 5.5.

We now proceed to define the operators needed to specify the currents in the Skyrme model. Starting with a static Skyrme soliton $U_0(\vec{r})$, one assumes the time dependence to be given by

$$U(\vec{r}, t) = A(t)U_0(r - R(t))A^\dagger(t) \quad (6.41)$$

Substituting this into the Lagrangian, one obtains

$$L = -M_0 + \frac{1}{2} \dot{R}^2 + A_0 \text{Tr}[\dot{A}^\dagger \dot{A}] \quad (6.42)$$

where M_0 is the mass of the soliton, A_0 is its moment of inertia and the dot indicates differentiation with respect to time. The canonical momentum of the soliton is

$$p^i = \frac{\partial L}{\partial \dot{x}_i} \quad (6.43)$$

where

$$(x^i, p^j) = \delta_{ij} \quad (6.44)$$

The relations are to be quantized as given in Chapter 2, and one should recall the definition for the spin and isospin operators

$$S = \frac{1}{2} i \left[\frac{\partial}{\partial \alpha_0} - \alpha_0 \frac{\partial}{\partial \Omega} - \vec{\alpha} \times \frac{\partial}{\partial \vec{\Omega}} \right] = -i \tau_3 \tau_2 (r^{-1} \dot{a}^1 \dot{a}^2) \quad (6.45)$$

and

$$I = \frac{1}{2} i \left[\alpha_0 \frac{\partial}{\partial \vec{\alpha}} - \vec{\alpha} \frac{\partial}{\partial \alpha_0} - \vec{\alpha} \times \frac{\partial}{\partial \vec{\Omega}} \right] = -i \alpha_1 \dot{a}^1 \quad (6.46)$$

where R_{a1} is the $O(3)$ rotation matrix given by

$$R_{a1} = \frac{1}{2} \tau_2 (r^{-2} \dot{a}^1 \dot{a}^2) \quad (6.47)$$

The current operators $J^{\mu}(0)$ are then to be constructed from the operators x^i , p^i , R_{a1} and S^i to have the correct symmetries under rotations, isospin transformations and parity transformations. The most general forms are then given as

$$J_0^1(0) = -a^{1/2} \tau_3 (x^2) x^1 \dot{a}_1 \quad (6.48)$$

$$J_0^2(0) = -\frac{i}{2\alpha_0} [t_1 (x^2) x^2 \dot{a}^1 - t_2 (x^2) x^1 \dot{a}^2] (S^2, R_{a1}) \\ - \frac{1}{2\alpha_0} a^{1/2} (t_1^2 + t_2^2) x^1 \dot{a}_1 \quad (6.49)$$

for the isospin current,

$$S^0(0) = b_0(x^2) \quad (8.60)$$

$$S^i(0) = \frac{1}{2} \epsilon^{ijk} b_1(x^2) x^j x^k + \frac{1}{24} (P^j b_2(x^2) \delta^{ij} + b_3(x^2) x^i x^j / x^2) \quad (8.61)$$

for the baryon current, and

$$A_0^i(0) = (w_0(x^2) (\delta^{ij} - x^i x^j / x^2) - w_1(x^2) x^i x^j / x^2) R_{0j} \quad (8.62)$$

$$A_a^i(0) = \frac{1}{24} \epsilon^{ijk} w_2(x^2) x^j x^k R_{0i} + \frac{1}{24} (P^j w_3(x^2) (\delta^{ij} - x^i x^j / x^2) - w_4(x^2) x^i x^j / x^2) R_{aj} \quad (8.63)$$

for the axial current.

The matrix elements of these currents are then to be evaluated in the Breit frame (see Appendix SA, [SW67]) where terms containing an anticommutator of p^3 vanish. Thus

$$\langle N | S_0^i(0) | N \rangle = \mp \frac{1}{2} \frac{1}{3} \frac{1}{(q^2)} \epsilon^{ijk} \langle N | b_1^k | N \rangle \quad (8.64)$$

$$\langle N | S_a^i(0) | N \rangle = \frac{1}{24} (w_1^{22}(q^2) - \frac{1}{2} w_2^{22}(q^2)) \langle N | R_{0j} | N \rangle \quad (8.65)$$

$$\langle \alpha | \eta^0(\alpha) | \alpha \rangle = \alpha_0^{00}(\alpha^2) \langle \alpha_2 | \alpha_2 \rangle \quad (8.58)$$

$$\langle \alpha | \eta^1(\alpha) | \alpha \rangle = -\frac{1}{2M} \alpha_1^{11}(\alpha^2) \alpha^{12} \alpha^2 \langle \alpha_2 | \alpha_2 \rangle \quad (8.57)$$

$$\langle \alpha | \frac{1}{2} (\alpha_1^0(\alpha) + \alpha_2^0(\alpha)) | \alpha \rangle = 0 \quad (8.60)$$

$$\langle \alpha | \frac{1}{2} (\alpha_1^1(\alpha) + \alpha_2^1(\alpha)) | \alpha \rangle = \left\{ -\frac{1}{2M} [2\alpha_0^{00}(\alpha^2) - \alpha_1^{00}(\alpha^2)] \alpha^{12} \right. \quad (8.59)$$

$$\left. + \frac{1}{2} \alpha^2 [\alpha_0^{20}(\alpha^2) + \alpha_1^{20}(\alpha^2)] \left[\frac{1}{2} \alpha^{12} - \frac{\alpha^{12}}{\alpha^2} \right] \right\} \langle \alpha_2 | \alpha_2 \rangle$$

where the labelling α^{ab} indicates the integral

$$\alpha^{ab}(\alpha^2) = \langle \alpha | \rangle^{-2} \int_0^\infty dr 4\pi r^2 \int_{\mathbb{R}^3} d^3r (\vec{r} | r) r^a f(r^2) \quad (8.60)$$

and the α signs refer to the proton and neutron states respectively.

Comparing these expressions with the definitions for the desired form factors, one obtains

$$\alpha_0^{120}(-\alpha^2) = \frac{1}{2} (\alpha_0^2(-\alpha^2) + \alpha_1^2(-\alpha^2)) + \frac{1}{2} \alpha_0^{20}(\alpha^2) \quad (8.61)$$

$$\frac{1}{2M} \alpha_1^{121}(-\alpha^2) = \frac{1}{2M} (\alpha_0^2(-\alpha^2) - \alpha_1^2(-\alpha^2)) + \frac{1}{2} \alpha_0^{11}(\alpha^2) \quad (8.62)$$

$$\alpha_1^2(-\alpha^2) = -\frac{1}{2M} [2\alpha_0^{00}(\alpha^2) - \alpha_1^{00}(\alpha^2)] + \frac{1}{2} \alpha^2 [\alpha_0^{20}(\alpha^2) + \alpha_1^{20}(\alpha^2)] \quad (8.63)$$

$$\frac{\alpha_2^2}{2M} \alpha_2^2(-\alpha^2) = \frac{1}{2} \alpha^2 [\alpha_0^{20}(\alpha^2) + \alpha_1^{20}(\alpha^2)] \quad (8.64)$$

For the case of a conserved axial vector current one may rewrite

$$j_A^0(\vec{q}^2) = -\frac{1}{2} w_0^0(\vec{q}^2) + \frac{1}{2} w_1^0(\vec{q}^2). \quad (6.55)$$

The functions b_0 , t_0 , w_0 and w_1 are to be determined from the actual expression for the currents in the gauged Skyrme model with pions only [21907]. For the baryon density one obtains

$$b_0(r^2) = -\frac{1}{2m^2} \frac{\sin^2 \theta}{r^2} \frac{d\theta}{dr}, \quad (6.60)$$

from the isospin current

$$t_0(r^2) = r^2 \frac{\sin^2 \theta}{r^2} + m^2 \frac{\sin^2 \theta}{r^2} \left[\left(\frac{d\theta}{dr} \right)^2 + \frac{2 \sin^2 \theta}{r^2} \right], \quad (6.67)$$

and from the axial vector current

$$w_0(r^2) = r^2 \frac{\sin \theta}{r} + 6a^2 \frac{\sin \theta}{r} \left[\left(\frac{d\theta}{dr} \right)^2 + \frac{\sin^2 \theta}{r^2} \right] \quad (6.68)$$

$$w_1(r^2) = -2r^2 \frac{d\theta}{dr} - 16a^2 \frac{2 \sin^2 \theta}{r} \frac{d\theta}{dr}. \quad (6.69)$$

If one introduces the dimensionless variable of Chapter 4, $\tau = r(r/r_0)$, then one may write, to leading order in H_c , the form factors for the Skyrme cell in the hybrid soliton as

$$G_N^{I=0, S=0}(\vec{q}^2) = -\frac{1}{\pi} \int_{r_b}^{\infty} dr \int_0^{\pi} d\theta (\vec{q}|r_0\sigma^r) \sin^2\theta \quad (6.70)$$

$$G_N^{I=1, S=0}(\vec{q}^2) = \frac{2\pi N}{3} \frac{1}{|Q|} (r_0/r_b)^2 \int_{r_b}^{\infty} dr \int_0^{\pi} d\theta (\vec{q}|r_0\sigma^r) \left(e^{2i\theta} \sin^2\theta + \frac{1}{2} A_0 \sin^2\theta (\delta^2 + \sin^2\theta) \right) \quad (6.71)$$

$$G_N^0(\vec{q}^2) = -\frac{2\pi}{3} (r_0/r_b)^2 \int_{r_b}^{\infty} dr \int_0^{\pi} d\theta \left\{ j_0(\vec{q}|r_0\sigma^r) \left[e^{2i\theta} (\delta + \sin 2\theta) \right. \right. \\ \left. \left. + j_0(\sin^2\theta \delta + \frac{1}{2} \sin 2\theta (\delta^2 + \sin^2\theta)) \right] \right\} \quad (6.72)$$

$$j_0(\vec{q}|r_0\sigma^r) \left[e^{2i\theta} \left(\delta - \frac{1}{2} \sin \theta \right) + A_0 (\sin^2\theta - \frac{1}{4} \sin 2\theta (\delta^2 + \sin^2\theta)) \right],$$

where $r_b = r_0(3\mu_0/r_0)$.

6.4 The nucleon form factors for the quark chiral bag

Here the calculations are based on the fact that the core, including both valence and vacuum quarks, forms a hedgehog state. This point is essential in the description of the rotations of the core, which moves as a whole, and thus any projection scheme. Since the valence quarks are also in a hedgehog state, one might well expect the nucleon form factors to have the same form as those calculated from the valence quarks only, but incorporating the radial densities appropriate to the complete system. This then forms the central idea behind any further discussion. Again, the results are given in the next frame.

The isovector charge form factor is, without doubt, the simplest case since it is derived from the seventh component of the baryon current, or the baryon density, which is a rotational, spin and isospin scalar. As such, it is identical for the hedgehog and the nucleon, and one can write

$$G_E^{I=0, Q^{NV}}(-Q^2) = \frac{1}{2} \int_0^{R_b} dr 4\pi r^2 J_0(\frac{3}{2} |r|) \rho^0(r). \quad (6.72)$$

Introducing the variables $y = \frac{r}{R_b}$ and $\rho_0^{NV}(y) = 4\pi R_b^3 \rho^0(R_b y)$, the above expression may be written as

$$G_E^{I=0, Q^{NV}}(-Q^2) = \frac{1}{2} \int_0^1 dy J_0(\frac{3}{2} |R_b y|) \rho_0^{NV}(y). \quad (6.74)$$

The calculation of the isovector magnetic form factor parallels that for the chiral bag. If the nucleon is taken to consist of three valence quarks only, then the electromagnetic current is given by

$$j^\mu = \sum_{i=1}^3 \tau_{i3}^+ \gamma_i^\mu \psi_i. \quad (6.75)$$

The matrix element of the vector component should then be calculated between nucleon states in the Breit frame where

$$\langle N_2 | j^3(0) | N_1 \rangle = -\frac{1}{2} \langle N_2 | \sum_{i=1}^3 \tau_{i3}^+ \psi_i \psi_i^\dagger | N_1 \rangle. \quad (6.76)$$

If one constructs states of good spin and isospin and performs this calculation, [TH02] one obtains

$$q_M^{I=1, q_c=2} = -\frac{5}{3} \frac{2m}{\sqrt{3}} H_0 \int dr 4\pi r^2 J_1(\sqrt{3}r) \mu_0^{I=1}(r). \quad (6.79)$$

Here $\mu_0^{I=1}$ represents the isovector magnetic moment density for a single hadronic valence quark state

$$\mu_0^{I=1}(r) = \frac{1}{2} \vec{\sigma}_0(\vec{m}^2)_3 \vec{r}_3 \cdot \vec{\sigma}_0. \quad (6.80)$$

That this must indeed be the case can be seen by looking at the $q^2 \rightarrow 0$ limit of the form factor since

$$\mu^{I=1, q} = \frac{q}{2m} q_M^{I=1, q_c=2} = \frac{q}{2m} \frac{2m}{\sqrt{3}} H_0 \int dr 4\pi r^2 \mu_0^{I=1}(r). \quad (6.81)$$

If the valence quark spinor is written as

$$\vec{\sigma}_0 = \begin{bmatrix} J_0(\vec{k}_0 r) \{ (1/2 \ 0) \ 1/2 \ 0 \ 0 \} \\ -J_1(\vec{k}_0 r) \{ (1/2 \ 1) \ 1/2 \ 0 \ 0 \} \end{bmatrix}, \quad (6.82)$$

then one has the familiar form [TH02]

$$\mu_{I=1}^0 = -\frac{5}{3} \int dr r^3 J_0(\vec{k}_0 r) J_1(\vec{k}_0 r). \quad (6.83)$$

For the vacuum therefore one expects [TH02]

$$\rho_v^{I=1, \nu}(q^2) = -\frac{6}{3} \frac{2\pi^2}{|q|} \mu_0 \int dr dr^2 J_1(|q|r) \rho_v^{I=1}(r), \quad (6.04)$$

where $\rho_v^{I=1}$ is now the vacuum isovector magnetic moment density. For each state one can define

$$\mu_n^{I=1} = \frac{1}{2} \int d\mathbf{r} \bar{\psi}_n(\mathbf{r}) \boldsymbol{\sigma} \cdot \frac{\mathbf{r}}{r} \psi_n. \quad (6.05)$$

The total density for the vacuum should then be given by the infinite sum

$$\rho_v^{I=1} = -\frac{1}{2} \lim_{\eta \rightarrow 0} \sum_n \text{sgn}(E_n) \mu_n^{I=1} e^{-(\eta E_n)^2}. \quad (6.06)$$

Unfortunately, as for the sum for the isovector magnetic moment, this sum is divergent. It can, however, be renormalized by taking the combination (Appendix 4C, [WJBS])

$$\mu_v^{I=1} = \lim_{\eta \rightarrow 0} \left[\mu_v^{I=1}(\eta, \epsilon) - \frac{1}{2} \sin^2 \epsilon \frac{d^2 \mu_v^{I=1}}{d\epsilon^2}(\eta, \epsilon) \Big|_{\epsilon=0} \right], \quad (6.07)$$

where

$$\mu_v^{I=1}(\eta, \epsilon) = -\frac{1}{2} \sum_n \text{sgn}(E_n) \mu_n^{I=1} e^{-\eta(E_n)^2}.$$

Comparing the expression derived for the isovector magnetic moment with that of V Pasquier [Pas82] and Hual et al [WJBS], one sees the expected relative factor of $\frac{6}{3}$.

To the contributions of the valence (6.73) and vacuum (6.06) quarks must be

added that from the Skyrme infl. This is given as

$$\begin{aligned}
 \bar{q}_N^{I=1,2} &= \frac{5}{3} \frac{8\pi^2 N}{3} \frac{1}{|q|} (\xi_N r_0)^2 \int_{\epsilon_0(R_0/r_0)}^{\epsilon} dr J_1(|z| r_0 \epsilon^2) [e^{2r} \sin^2 \epsilon + \\
 &\frac{1}{2} A_0 \sin^2 \epsilon (2^2 \sin^2 \epsilon)]. \quad (5.98)
 \end{aligned}$$

Here one should note the correction factor of $\frac{5}{3}$ applied to the previous result given in equation (5.71).

Turning now to the axial vector form factor $G_A^2(q^2)$ in chiral bag models, which for $q^2 \ll 4M_N^2$ is given by

$$G_A^2(q^2) \ll \alpha_N \frac{1}{2} \frac{G_A^2}{2} = \langle N | \int d^3x \epsilon^{ijk} A^{kl}(x) | N \rangle, \quad (5.99)$$

where the α_N and r_0 refer to the nucleon spin and isospin and A_k^l denotes the axial vector current for the valence quarks given by

$$A^{kl} = \sum_{j=1}^3 \bar{\psi}_j^k \gamma_5 \psi_j^l(r^3/2) \tau_j. \quad (5.10)$$

Calculating for states of good spin and isospin constructed from the valence quarks, one obtains

$$G_A^2(q^2) = -\frac{6}{3} N_0 \left[\int_0^{R_0} dr 4\pi r^2 J_0(\pi r) u(r) + \int_0^{R_0} dr 4\pi r^2 J_0(\pi r) b(r) \right], \quad (5.11)$$

and

$$\frac{d}{dq^2} \langle \bar{\psi} \psi \rangle(q^2) = -\frac{6}{\pi} N_c \frac{3}{2} \int_0^{q^2} dr \, 4\pi r^2 \mathcal{J}_0^2(qr) b(r) . \quad (6.92)$$

At this stage one should apply the conservation of the total axial vector current. Now

$$Q_A(q^2) = Q_A^2(q^2) + Q_A^3(q^2) , \quad (6.93)$$

but

$$\frac{d}{dq^2} Q_A(q^2) = \frac{d}{dq^2} [(Q_A^2(q^2) + Q_A^3(q^2))] = Q_A(q^2) , \quad (6.94)$$

and thus

$$Q_A(q^2) = -\frac{6}{\pi} N_c \frac{3}{2} \int_0^{q^2} dr \, 4\pi r^2 \mathcal{J}_0^2(qr) a(r) + \text{Skyrme contribution} . \quad (6.95)$$

As the same argument applies when one includes the vacuum contribution, the interest lies in the function $a(r)$.

For the valence quarks this function is given by

$$a(r) = \bar{\psi}_0^2 \frac{r^2}{2} \nabla_0^2 + \frac{1}{3} \bar{\psi}_0^i \nabla_0^i \bar{\psi}_0^j \nabla_0^j , \quad (6.96)$$

representing twice the quark axial vector current density for the hedgehog state. Explicitly calculating the form factor for the valence quarks then gives

$$a_h(q^2) = \frac{2}{3} \int_0^1 dx x^2 j_0(qr) (L_0^2(k_0 r) - \frac{1}{2} J_1^2(k_0 r)) , \quad (8.97)$$

which is in line with MY bag result with weakly interacting pions [Fm86].

It is interesting at this stage to consider the $q^2 \rightarrow 0$ limit of the quark contribution to the axial form factor. If one compares it with the expression given by V. Pasquier [8.12], one again sees the expected relative factor of $\frac{2}{3}$.

To obtain the corresponding density distribution for the vacuum one writes for each quark state n

$$a_n = \frac{1}{3} \bar{\psi}_n \gamma_5 \psi_n . \quad (8.98)$$

Thus one can show, using the axial vector conservation for massless quarks, that

$$\begin{aligned} \int_{V_b} d^3x a_n(r) &= \frac{2}{3} \int_{V_b} d^3x A_n^{50}(T) = \frac{2}{3} \int_{V_b} A_{10}^{50} \\ &= + \frac{2}{3} (m_b^2) \bar{\psi}_n \gamma_5 \psi_n . \end{aligned} \quad (8.99)$$

This last expression can then be related to the derivative of the Casimir energy, as before (4.21). One thus obtains

$$\int_{V_b} d^3x a_n(r) = \frac{2}{3} \frac{dE_n}{dV} . \quad (8.100)$$

One should therefore renormalize the vacuum density $a^V(r)$ in the same way as $\frac{da_V}{dV}$ (see Appendix 4C, (NAGM)).

Defining

$$a^V(r, \theta, \eta) = -\frac{1}{2} \sum_{\alpha} \text{sign}(n_{\alpha}) n_{\alpha} e^{(-\eta \alpha) h^2}, \quad (6.101)$$

then the vacuum axial vector current density $a^V(r, \theta)$ should be given by

$$a^V(r, \theta) = \lim_{\theta \rightarrow 0} \left[a^V(r, \theta, \eta) - \frac{1}{2} \sin 2\theta \frac{da^V(r, \theta, \eta)}{d\theta} \Big|_{\theta=0} \right], \quad (6.102)$$

and the form factor from the vacuum is given by

$$G_A^V(q^2) = -\frac{6}{5} \frac{3}{2} \frac{3}{2} \int_0^{R_0} dr \sin^2 \theta_0 (qr) a^V(r, \theta). \quad (6.103)$$

In total therefore, the axial form factor is given as the sum of three terms, one from the valence quarks (B.37), one from the vacuum (B.103) and one from the Skyrme. Given axial vector continuity (B.62) - (B.63), the Skyrme contribution is given as

$$G_A^S(q^2) = \frac{6}{5} \frac{3}{2} \frac{3}{2} (f_{\pi} r_0)^2 \int_{r_0}^R dr \int_0^{\theta_0} d\theta (|\nabla| r_0 a^S) (r_0)^2 (\delta + \sin 2\theta) - \\ f_0 (\sin 2\theta \delta + \frac{1}{2} \sin 2\theta (\delta^2 + \sin 2\theta)). \quad (6.104)$$

The $q^2 \rightarrow 0$ limit of $G_A(q^2)$, namely the axial vector constant g_A , should in fact be the same as that calculated from the asymptotic behaviour of the pion field (4.50). This proves to be the case *ii* and only if the expression 5.104 includes the factor $\frac{5}{3}$. In short, the correction factor $\frac{5}{3}$ applied in the quark sector should be applied also in the meson sector. One also sees that the correction factor suggested by Jackson and Ito [JMI2] for the pure Skyrme is indeed equivalent to the correction factor in chiral bag models.

5.5 Numerical results

These will be presented for two different models, namely the model discussed in Chapter 3 incorporating pions only and the original model of Brown et al [BJW84] in which g_A is fixed. In both cases, the pions and the quarks are taken to be massless, and one can therefore apply conservation of the axial vector current.

The resulting curves are shown in figures 5.1 to 5.3. The triangles and squares denote the present model with $R_0 = 0.305$ fm and 0.425 fm respectively. The stars denote the model of Brown et al [BJW84] with $R_0 = 0.425$ fm.

For the purposes of comparison with the experimental data, the results for the standard dipole fit are indicated by the solid circles. The specific fits used are [BY87]

$$G_E^{1-0}(q^2) = \frac{1}{2} (G_E^p(q^2) + G_E^n(q^2)) , \quad (5.105)$$

$$G_M^{1-1}(q^2) = \frac{1}{2} (G_M^p(q^2) - G_M^n(q^2)) , \quad (5.106)$$

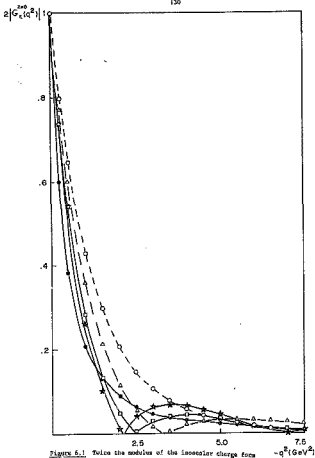


Figure 5.1 Twice the modulus of the isoscalar charge form factor, $2|G_e^{z=0}(q^2)|$ as a function of q^2 (GeV²)

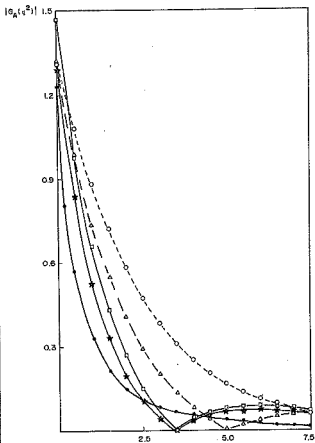
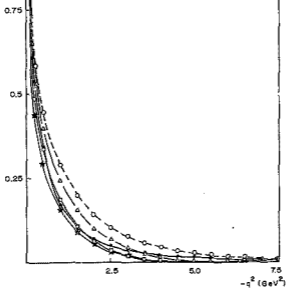


Figure 3.2 The modulus of the axial vector form factor, $|G_A(q^2)|$ as a function of q^2 (GeV^2).

$$\left| \frac{G_M^{\text{iso}}(q^2)}{G_M^{\text{iso}}(0)} \right|$$

Figure 8.2 The modulus of the ratio of the isovector magnetic form factor to its value at $q^2 = 0 \text{ GeV}^2$, $\left| \frac{G_M^{\text{iso}}(q^2)}{G_M^{\text{iso}}(0)} \right|$, as a function of $q^2 (\text{GeV}^2)$.



where

$$a_2^D(q^2) = \frac{1}{(1-q^2/M_D^2)^2}, \quad (6.107)$$

$$a_2^P(q^2) = \frac{\mu_P}{(1-q^2/M_D^2)^2}, \quad (6.108)$$

$$a_2^N(q^2) = \frac{\mu_N}{(1-q^2/M_D^2)^2}, \quad (6.109)$$

$$a_2^H(q^2) = \frac{0.20g^2}{1-1.13q^2/M_D^2} a_2^D(q^2), \quad (6.110)$$

with $M_D = 0.64$ GeV (the parameterization for $a_2^D(q^2)$ is that used by S. Galster et al. [Gal71]) and

$$a_A(q^2) = \frac{g_A}{(1-q^2/M_A^2)^2}, \quad (6.111)$$

where $M_A = 1.03$ GeV and g_A is the experimentally measured value for the axial vector constant, that is $g_A = 1.23$.

It is also interesting to compare the results for the pure Skyrme with $f_\pi = 93$ MeV and $g_A = 1.31$ ($g_A^2 = 0.1694$). These curves are indicated by open circles on the figures. One expects the results for the hybrid models to display more higher momentum components. This indeed proves to be the case, but unfortunately, they appear as diffraction minima (one should note that the modulus of the form factor has been plotted in each case). Such minima are not experimentally observed, and although zeros have been predicted theoretically in the nucleon form factors [GEM, IN207], in no

model do they occur for $q^2 < 7.5 \text{ GeV}^2$. In fact, the movement of the positions of these minima with R_0 , the arbitrary bag radius, suggests that they are an artifact of the sharpness of the boundary condition and not a physical effect. They merely display the discontinuities induced in the radial dependence of the variables by the sharp bag boundary, see figures 4.2 and 4.4. Here one sees the confirmation of the supposition that form factors, which probe densities, are more sensitive to the details of the model than the static properties, which involve integrals over all space.

Corresponding to the appearance of these diffraction minima, however, is a reduction in the low momentum components of the form factors from the Skyrme model results. In all three cases, this provides better agreement with the experimental dipole fit for $q^2 < 28\text{GeV}^2$.

These results suggest that the introduction of quarks is indeed valid, but that one should soften the bag surface. If one very crudely considers the effect of a diffuse surface to be given as an "average" over different bag radii, one would obtain overall a very encouraging picture. The diffraction minima disappear, and the fit appears far better than that for the pure Skyrme. Although such an argument is certainly not correct, one hopes that it gives at least a schematic picture of the results of softening the bag.

The above results do not appear accurate enough, particularly in light of the diffraction minima, to make a meaningful distinction between the models. In the case where ω mesons are included, the results are not expected to differ much in overall behaviour. Here too, one predicts the appearance of diffraction minima, caused by discontinuities at the bag surface, most clearly in fig. 5.6 and 5.8 for the baryon density.

APPENDIX GA THE CALCULATION OF THE MATRIX ELEMENTS OF THE
ELECTROMAGNETIC CURRENT OPERATOR FOR THE PION NUCLEON

Let the initial and final baryon states be given as $|\beta\rangle = |1, \frac{1}{2}, n_3\rangle$ and $|\beta'\rangle = |1', \frac{1}{2}, n_3'\rangle$. Then the matrix element factor into a momentum and isospin piece.

(1) Momentum factor

These factors all reduce to the matrix element of a function of the centre of mass operator \vec{X} between the states $|\beta\rangle$ and $|\beta'\rangle$. The wave function of $|\beta\rangle$ is

$$\langle \beta | \vec{X} | \beta \rangle = \exp(i\vec{p} \cdot \vec{X}) . \quad (8A.1)$$

The matrix elements are thus Fourier transforms, which can be rewritten as Fourier-Bessel integrals, using the relation

$$\exp(i\vec{q} \cdot \vec{X}) = 4\pi \sum_{\ell} i^{\ell} J_{\ell}(|\vec{q}|r) Y_{\ell m}^{\ell}(\hat{q}) Y_{\ell m}^{\ell}(\hat{X}) . \quad (8A.2)$$

In particular,

$$\langle \beta | r(X^2) | \beta \rangle = \int d^3r J_0(|\vec{q}|r) r(r^2) , \quad (8A.3)$$

$$\langle \beta | r(X^2) X^j | \beta \rangle = -\frac{1}{|\vec{q}|} q^j \int d^3r J_1(|\vec{q}|r) r(r^2) , \quad (8A.4)$$

$$\langle \beta | \langle r, r^2 | (x^4 y^4 - \frac{1}{2} y^2 x^2 y^2) | \beta \rangle = -\frac{1}{|\beta|^4} \langle x^4 y^4 - \frac{1}{2} y^2 x^2 y^2 \rangle \int d^3 r \frac{1}{r^2} \langle \beta | r \rangle r^2 | r^2 \rangle. \quad (6a.5)$$

where $\beta = \beta' - \beta$.

(4) Isospin factor

Here one need only consider the operators I , R_{21} , S^k and (S^k, R_{21}) . The initial and final states are $|\frac{1}{2}, l_3, a_3\rangle$ and $|\frac{1}{2}, l_3', a_3'\rangle$ and the wave-functions are given by

$$\langle A | l_3, a_3 \rangle = (-)^{l_3 + \frac{1}{2}} \int \frac{d^3 r}{r^2} R_{l_3 - \frac{1}{2}}^k(A). \quad (6a.6)$$

The rotation matrix, R_{21} , can be given as

$$R_{21} = R_{21}^k(A), \quad (6a.7)$$

while the spin operator, S^k , is specified by

$$S^k | \frac{1}{2}, l_3, a_3 \rangle = \sum_{a_3'} C(l_3 \frac{1}{2} a_3 | \frac{1}{2} a_3') | \frac{1}{2}, l_3, a_3' \rangle. \quad (6a.8)$$

Thus one knows that

$$\langle \frac{1}{2}, l_3', a_3' | 1 | \frac{1}{2}, l_3, a_3 \rangle = \langle a_3' | a_3 \rangle \langle l_3' | l_3 \rangle, \quad (6a.9)$$

$$\langle \frac{1}{2}, l_3', a_3' | S^k | \frac{1}{2}, l_3, a_3 \rangle = \frac{1}{2} \langle l_3' | l_3 \rangle \langle a_3' | a_3 \rangle S^k | a_3 \rangle.$$

Furthermore, applying the identities

$$\begin{aligned}
 \langle \frac{1}{2}, l_3, m_3 | R_{z1} | \frac{1}{2}, l_3, m_3 \rangle &= \int d\Omega \langle \frac{1}{2}, l_3, m_3 | A \rangle R_{z1} \langle A | \frac{1}{2}, l_3, m_3 \rangle \\
 &= \frac{2}{2\pi} \int d\Omega a_{\frac{1}{2}, l_3}^{1/2} (A) D_{z1}^1 (A) b_{\frac{1}{2}, l_3}^{1/2} (A) \quad (6A.11)
 \end{aligned}$$

and

$$\begin{aligned}
 \frac{2J_3+1}{2\pi} \int d\Omega b_{\frac{1}{2}, l_3}^1 (A) a_{\frac{1}{2}, l_3}^1 (A) b_{\frac{1}{2}, l_3}^1 (A) &= O(J_3, m_3, l_3 | J_3, m_3) \\
 O(J_3, m_3, l_3 | J_3, m_3) & \quad (6A.12)
 \end{aligned}$$

one obtains

$$\langle \frac{1}{2}, l_3, m_3 | R_{z1} | \frac{1}{2}, l_3, m_3 \rangle = -\frac{1}{2} \langle l_3 | r^{-2} | l_3 \rangle \langle m_3 | p^1 | m_3 \rangle. \quad (6A.13)$$

Finally, using (6A.10) and (6A.13)

$$\langle \frac{1}{2}, l_3, m_3 | (S^1 \cdot p_{z1}) | \frac{1}{2}, l_3, m_3 \rangle = -\frac{1}{2} a^{1/2} \langle l_3 | r^{-2} | l_3 \rangle \langle m_3 | m_3 \rangle. \quad (6A.14)$$

7. CONCLUDING REMARKS

An in-depth review of possible models for the nucleus has been presented. It has been shown that both chiral bag models and the Skyrmin provide a good description of nuclear static properties. The Skyrmin provide a complete description of low-energy pion theory, including the chiral anomaly. It cannot, however, predict the appearance of Bjorken scaling, so simply described in all bag models. It therefore appears natural to introduce the idea of a hybrid chiral soliton with a quark core surrounded by a Skyrmin tail, the hope being that such a model will contain the physical content of both the Skyrmin and the chiral bag.

Central in the discussion of the hybrid soliton is its baryon number. This has been shown to be unity, independently of the bag radius (QWR), a truly remarkable result. In the present work the behaviour of the baryon density has been investigated. In particular, the continuity of the baryon density at the bag surface has been enforced.

This constraint is not only physically meaningful but greatly increases the predictive power of the hybrid model. Two cases have been presented here. The first is the model involving pions only. Here the axial vector coupling constant g_A is now given as a smooth function of R_b . The agreement with the value predicted from the Goldberger-Treiman relation $g_A = 1.33$ is particularly encouraging. Good results are also obtained for the other static properties.

More promising is the second case where both pions and sigma mesons have been incorporated. Here the continuity condition produces a bifurcation

diagram for the energy as a function of g_{eff} and the bag radius R_b . Although such a diagram may well prove to be an artifact of the model, it can be used, in the context of the model, to make a precise and unique prediction for g_{eff} , namely $g_{\text{eff}} = 12.7$. Again, the agreement for the other static properties with their experimental values is perfectly acceptable. A number of points should however be considered.

Firstly, the energies predicted should in principle be corrected for centre of mass effects in the chiral bag. Since such corrections should lie within the error bars, and in the absence of any reliable estimates, they can and have been neglected in the present work.

Secondly, the appearance of the sharp bag boundary proves problematic. Indeed, enforcing baryon density continuity at the bag surface can be viewed as an additional source to reduce sensitivity to its particular position. This problem is most noticeable in the calculation of the form factors. Unfortunately, any attempt to soften the surface would involve completely reworking the model. Fortunately, despite the existence of the sharp surface, one still obtains good predictions for the static properties and the general behaviour of the form factors. As such, the model proves useful, even if not entirely consistent.

Thirdly, further clarification is needed on the factor $\frac{5}{3}$ appearing in the axial form factor $G_A(q^2)$ and the isovector magnetic form factor $G_M^{I=1}(q^2)$. This factor, or one similar in magnitude, is essential, both in the para Skyrmeon and in the present hybrid chiral soliton, to produce a realistic fit value for M_p and g_A respectively. That such a factor arises in the limit

$R_0 \rightarrow \infty$ ($\phi(R_0) \rightarrow 0$) argues strongly in favour of its use. Its assumption in the present work leads to meaningful results for both the models considered.

Lastly, but most importantly, one should note that it is possible to add an additional term to the definition of the baryon density. This was first noted for the pure Skyrmeon with pions and sigma mesons by Adkins and Suppi [ABS94]. In this case the term takes the form

$$\Lambda_2 \mu^{2\alpha} \quad (7.1)$$

Under certain assumptions it is this term that gives rise to the correction factor of $\frac{2}{3}$ to the isoscalar radius for the pure Skyrmeon. As expected, its contribution to the baryon number for the pure Skyrmeon is zero. In the hybrid model this is not necessarily the case. The additional contribution may be given explicitly as

$$\Lambda_2 \mu^{2\alpha} (R_0) \quad (7.2)$$

In general, this will be non-zero, unless, as in the work of Einbecker and Brown [EB95], one imposes the boundary condition $\psi'(R_0) = 0$. This constraint in fact increases the total energy of the system, since the energy minima do not correspond to $\psi'(R_0) = 0$. Furthermore, the introduction of such a term automatically increases the size of the parameter space. Despite its importance for the isoscalar radius, one might well choose to omit such a term in the interest of simplicity, as has been done in the present work.

This relation finds further support when one considers the case of massless pions only. Here one can construct an analogous term, assumed to be given by elimination of the π meson, of the form

$$\Lambda^2 \mu^2 (\partial_\nu \eta^\mu - \partial_\mu \eta^\nu), \quad (7.2)$$

where η^μ is the baryon current. It too will contribute a term to the baryon number, now given by

$$\Lambda^2 \frac{4\pi^2}{3} \int d^3x (\eta_0) = - \frac{2\Lambda^2}{3} \left[\sin^2 \theta \frac{d^2 \phi}{dx^2} + \sin \theta \partial_0 \left(\frac{d\phi}{dt} \right)^2 - \frac{1}{3} \sin^2 \theta \left(\frac{d\phi}{dt} \right)_{r=R_0} \right]. \quad (7.4)$$

Again, this term is not necessarily zero, and again, it must in general be omitted from the hybrid models with pions only.

Having explored the two bag models proposed, focusing on the approximations and assumptions that have been incorporated, it is appropriate to ask whether introducing a hybrid model has indeed provided more information.

One observes immediately that f_A and $f_{\pi NN}$ are now predicted. The most noticeable differences do not, however, lie in the static properties but in the behaviour of the nucleon form factors that have been calculated in the hybrid model for the first time. Apart from the appearance of unphysical diffraction minima, one sees here better overall agreement with the experimental dipole fit, particularly if one were to "average" over several different bag radii. They provide a far more stringent test of any model than do the static properties. As such, the agreement achieved, while not

overwhelming, certainly encourages the introduction of quarks into the model.

In summary, two new hybrid chiral soliton models have been proposed in which the continuity of the baryon density is the pertinent new feature. This enables one to predict $g_A(N_p)$ for the model with pions only and $g_{A,HN}$ for the model also incorporating omega mesons. Agreement with the experiment for these and other static properties is good. To test the models further the isoscalar charge, isovector magnetic and axial vector form factors have been calculated. The results here provide overall better agreement with the experimental dipole fits, supporting the idea of a hybrid model, albeit with a softened surface to remove the appearance of unphysical diffraction minima.

REFERENCES

- Ad155a S.L. Adler, Phys. Rev. Lett. 34 (1965) 1061.
- Ad155b S.L. Adler, Phys. Rev. 140B (1965) 736.
- Ad54a G.S. Adkins and C.R. Nappi, Nucl. Phys. B232 (1984) 169.
- Ad54b G.S. Adkins and C.R. Nappi, Phys. Lett. 137B (1984) 251.
- Ad55 G.S. Adkins and C.R. Nappi, Nucl. Phys. B245 (1985) 507.
- Ad593 G.S. Adkins, C.R. Nappi and E. Witten, Nucl. Phys. B233 (1983) 552.
- Bj64 J.D. Bjorken and S.D. Drell, Relativistic Quantum Mechanics (McGraw-Hill, New York, 1964).
- Di54 L.C. Nienhuysen, T. Dothan and S. Stern, Phys. Lett. 44B (1964) 289.
- Dj68 J.E. Djonkic, Phys. Rev. 179 (1969) 1567.
- EJ594 G.H. Eichen, A.D. Jackson, M. Ito and V. Vento, Phys. Lett. 140B (1984) 285.
- Er78 G.E. Eron and M. Ito, Phys. Lett. 62B (1979) 177.
- Er86 E. Eron, S. Yee and C. Hillson, Phys. Rev. D34 (1986) 1482.
- GLJW74 A. Gidon, R.L. Jaffe, K. Johnson, C.R. Thorn and V.F. Weiskopf, Phys. Rev. D9 (1974) 3471.
- Cl078 F.K. Close, An Introduction to Quarks and Partons (Academic Press, London, 1979).
- Co86 T.D. Cohen, Phys. Rev. D34 (1986) 2187.
- Ch84 V.L. Chernyak and I.R. Zhitnitsky, Nucl. Phys. B245 (1984) 62.
- De87 Y. Dothan and L.C. Nienhuysen, Commun. Nucl. Part. Phys. 17 (1987) 83.
- Ed80 A.H. Eichen, Angular Momentum in Quantum Mechanics, 2nd ed. (Princeton University Press, Princeton, 1980).
- Ei87 J.M. Eisenberg, private communication.

- FM0107 M. Fiolhais, A. Nigge, K. Goebel, F. Göttsche and J.N. Urbano, Phys. Lett. 194 (1987) 167.
- Gal71 S. Galster et al, Nucl. Phys. B23 (1971) 221.
- GJ83 J. Goldstone and E.L. Jaffe, Phys. Rev. Lett. 51 (1983) 1018.
- GT58 M.L. Goldberger and S.S. Treiman, Phys. Rev. 110 (1958) 1178.
- W1985 E.J. Naylor, M. Jambor and M.A. Nowak, Z. Phys. C30 (1986) 483.
- HT786 A. Hosaka, K. Kusaka, H. Takahata and H. Toki, Prog. Theor. Phys. 75 (1985) 315.
- Y585 G. Holzwarth and B. Schwesinger, Sept. Prog. Phys. 40 (1988) 825.
- HT86 A. Hosaka and H. Toki, Phys. Lett. 167B (1986) 183.
- HT87 A. Hosaka and H. Toki, Phys. Lett. 188B (1987) 381.
- Rus82 R. Rieg, Quarks, Leptons and Gauge Fields (World Scientific, Singapore, 1982).
- IN887 K. Inari, O. Karl and J. Soffer, Phys. Rev. D36 (1987) 1865.
- IZ80 C. Itzykson and J.B. Zuber, Quantum Field Theory (McGraw-Hill, New York, 1980).
- Ja79 E.L. Jaffe, Proc. 1979 Erice Summer School "Structure of Quarks", ed. A. Eichichi (Plenum, New York, 1981).
- JJ8286 A. Jackson, A.D. Jackson, A.S. Goldhaber, G.F. Brown and L.C. Osstilla-Jo, Phys. Lett. 154B (1985) 101.
- JJ86 A. Jackson, A.D. Jackson and V. Pasquier, Nucl. Phys. A432 (1985) 887.
- JKV807 A.D. Jackson, G.E. Zahab, L. Vepstas, H. Verschelde and E. Wiat, Nucl. Phys. A482 (1987) 881.
- JH83 A.D. Jackson and M. Ho, Phys. Rev. Lett. 51 (1983) 781.
- JH85 A.D. Jackson and M. Ho, Phys. Lett. 138 (1985) 221.
- KH85 D. Klebaner and G.E. Zahab, Nucl. Phys. A454 (1986) 589.

- KJRBH B.R. Kabana, A.D. Jackson and G. Ripka, Nucl. Phys. A459 (1986) 633.
- Klu84 D. Klöbucar, Phys. Lett. 140B (1984) 31.
- Lee81 T.D. Lee, Particle Physics and Introduction to Field Theory (Dorwood, Calif, 1981).
- MOSES U.G. Meissner, H. Kaiser, A. Wirzba and W. Weise, Phys. Rev. Lett. 57 (1986) 1076.
- Mu186 F.J. Mulders, Phys. Rev. 230 (1986) 1073.
- Paas5 V. Paschos, Phys. Lett. 151B (1985) 27.
- Qa87a R.M. Quick and H.G. Miller, Phys. Rev. Lett. 59 (1987) 30.
- Qa87b R.M. Quick and H.G. Miller, to be published in Rapid Communications in Phys. Soc. D.
- Qa87c R.M. Quick and H.G. Miller, Proceedings of the 1987 Copen Town Workshop on Quarks, Gluons and Hadronic Matter, ed R.D. Viollier and S. Werner (World Scientific, Singapore, 1987).
- Qa87d R.M. Quick and H.G. Miller, submitted to Phys. Lett. B.
- Sky61 T.H.E. Skyrme, Proc. Roy. Soc. A207 (1951) 127.
- Sky62 T.H.E. Skyrme, Nucl. Phys. 31 (1962) 205.
- Tan82 E. Tegen, H. Hrodemann and W. Weise, Z. Phys. A207 (1982) 239.
- Tha71 G. 'tHooft, Nucl. Phys. B33 (1971) 173; B35 (1971) 167.
- Thom3 S. Thorge, A.W. Thomas and G.A. Miller, Phys. Rev. 222 (1980) 2892.
- Urb84 J.N. Urbana and K. Goebel, Phys. Lett. 143B (1984) 519.
- Ven80 V. Vento, Ph.D. thesis, SUNY at Stony Brook (1980), unpublished.
- Ven84 J. Vepstas, A.D. Jackson and A.S. Goldhaber, Phys. Lett. 140B (1984) 200.
- Vie84 V. Vento and M. Sho, Nucl. Phys. A122 (1984) 413.

- VEN7980 Y. Vanka, M. Ito, S.M. Ryan, J.H. Jun and G.E. Brown, Nucl. Phys. A295 (1980) 413.
- Wat44 G.N. Watson, A Treatise on the Theory of Bessel Functions (Cambridge University Press, Cambridge, 1944).
- Wei65 W.I. Weisberger, Phys. Rev. Lett. 14 (1955) 1047.
- Wit62a E. Witten, Nucl. Phys. B223 (1982) 422.
- Wit62b E. Witten, Nucl. Phys. B223 (1982) 435.
- WV308 S. West, L. Vegeton and A.S. Jackson, Phys. Lett. 192B (1985) 219.

- WIK780 V. Vento, H. Haa, E.M. Nyman, J.H. Jun and G.E. Brown, Nucl. Phys. A245 (1985) 619.
- Wat44 G.N. Watson, A Treatise on the Theory of Bessel Functions (Cambridge University Press, Cambridge, 1944).
- Wei60 H.L. Weisburger, Phys. Rev. Lett. 14 (1965) 1097.
- Wit82a E. Witten, Nucl. Phys. B228 (1983) 422.
- Wit82b E. Witten, Nucl. Phys. B223 (1983) 423.
- WJ780 H. Wot, L. Vepster and A.D. Jackson, Phys. Lett. 273B (1983) 217.

Author Carter Rachel Mary

Name of thesis Form Factors In A Hybrid Chiral Soliton Model With Continuous Baryon Density. 1987

PUBLISHER:

University of the Witwatersrand, Johannesburg

©2013

LEGAL NOTICES:

Copyright Notice: All materials on the University of the Witwatersrand, Johannesburg Library website are protected by South African copyright law and may not be distributed, transmitted, displayed, or otherwise published in any format, without the prior written permission of the copyright owner.

Disclaimer and Terms of Use: Provided that you maintain all copyright and other notices contained therein, you may download material (one machine readable copy and one print copy per page) for your personal and/or educational non-commercial use only.

The University of the Witwatersrand, Johannesburg, is not responsible for any errors or omissions and excludes any and all liability for any errors in or omissions from the information on the Library website.